UNITED STATES EXPERIMENTAL MODEL BASIN

NAVY YARD, WASHINGTON, D.C.

THE STUDY OF CAVITATION ON SCREW PROPELLERS

BY H. LERBS

APRIL 1937

TRANSLATION 46

STUDY OF CAVITATION ON SCREW PROPELLERS

(UNTERSUCHUNG DER KAVITATION AN SCHRAUBENPROPELLERN)

by

Herman Lerbs, Dr. Eng.

Report 131, HSVA

(Mitteilung 131, Hamburgische
Schiffbau-Versuchsanstalt, Hamburg, 1936)

HSVA Mitteilung 131 is the same as HSVA Bericht 311.

Translated by M.C. Roemer

U.S. Experimental Model Basin
Navy Yard, Washington, D.C.

April 1937 Translation 46

STUDY OF CAVITATION ON SCREW PROPELLERS.

Table of Contents:

I. DATA ON THE OCCURRENCE OF CAVITATION HITHERTO AVAILABLE.

a) Summary Criteria 2
b) Pressure Tests with Sections 7
c) Cavitation Tests of Sections 11

II. EXISTENT POSSIBILITIES OF DESIGNING PROPELLERS WITHIN THE CAVITATION ZONE 14

III. THE CAVITATION TANK OF THE HAMBURGISCHE SCHIFFBAU VERSUCHSANSTALT.

a) Description of the Plant 16
b) Test Methods and Test Instruments 20

IV. THE LAWS OF SIMILARITY AND THE CONCLUSIONS DRAWN FROM THEM . 35

V. RESULTS OF TESTS WITH SYSTEMATICALLY ALTERED MODEL PROPELLERS 41

a) The Cavitation Picture and the Forces 42
b) Limits of Validity of the Earlier Series Tests and Limits of Corrosion 44
c) Results of Thrust and Torque Measurements in the Cavitating Zone 46

VI. THRUST DISTRIBUTION WITH GREATEST POSSIBLE SECURITY FROM CAVITATION 53

STUDY OF CAVITATION ON SCREW PROPELLERS

by

Herman Lerbs, Dr. Eng.

By cavitation is meant a modification in the flow of a liquid due to the fact that the pressure at certain points in the field of flow decreases, causing the liquid to change into a saturated vapor and interrupting the homogeneity of flow. These points of lowest pressure which, according to Bernoulli's theorem, coincide with the points of greatest velocity in non-gravitational uniform flow, exist, according to one of Kirchhoff's laws, on the surface of a solid body, in frictionless, vortex-free flow, submerged in the liquid, for example the suction side of a blade section. According to this the flow in direct proximity to the section is interrupted on the inception of cavitation, and it is therefore to be expected that the section characteristics also will be altered as compared to those in homogeneous flow, which again leads to the fact that the characteristics of all hydraulic machines regarded as aggregates of individual blades, as for instance rotary pumps, turbines and propellers, undergo an alteration when cavitation sets in.

In the following the effects of cavitation particularly on the propeller and limited to the beginning of cavitation and the effects on the forces at the inception of this phenomenon are studied in detail, while the destruction of material connected therewith is considered only insofar as conditions exist under which an attack upon the material must be reckoned with, while the process of destruction itself and its dependence upon the various materials are not taken up [1]. Investigation of the relation between cavitation and excitation of vibration likewise is beyond the scope of this paper.

To the engineer it is of importance first to know the limits beyond which it is to be expected that the propeller will be affected, for the available design data generally are the results of model tests obtained in an open water basin and so arranged that the dynamic forces, and thus also the pressure differentials, obtained in the model will be similar to those in the full scale structure, but not the absolute pressures, which, since the surface of the water is in both cases under atmospheric pressure, are too high in the case of the model. From this it is evident that the ordinary model tests, at least within the speed limits in which it is possible to carry them out, fail to reproduce the setting in of cavitation, but that to accomplish this a reduction in air pressure is requisite. In the absence of suitable plants an attempt has been made to obtain information as to the inception of the effects of cavitation, and therewith the limit of validity of systematic propeller tests such as have been given by Taylor and

1) Schröter, Z.V.D.I. 1932, 1933 and 1934.

Schaffran, by simple summary general formulas without considering details obtained from trial run data, which will be reported in the near future.

I. DATA ON THE OCCURRENCE OF CAVITATION HITHERTO AVAILABLE.

a) Summary Criteria.

In the literature on the subject the first reports of experiences with cavitation phenomena in propellers are found since the introduction of turbine drive and the considerable increase in propeller RPM then attempted by its means; in 1895 Thornycroft and Barnaby [2] published the trial run data of the torpedo boat DARING, in 1897 Parsons published his experiences with the experimental boat TURBINIA [3]. In the case of the DARING, a speed of 24 knots at 384 RPM and an output of 3,700 IHP was attained with the first propeller installed, whose diameter was 1.88 m, the ratio of the blade area to the disc area being $F_p/F = 29.8\%$, while the ultimate propeller, the sixth, differing from the first only in a 45% increase in area ($F_p/F = 43.3\%$), used only 3,050 IHP for the same speed, the number of revolutions having fallen to 317 RPM. Barnaby interprets this conspicuous relationship between blade area and output as indicating that [4] the negative pressure on the suction side of the propeller can not become greater than the superposed static pressure of the air and water column without destroying the contact between the liquid and the propeller blade and without formation, in the water, of cavities filled with saturated vapor. As he expresses it, the water is then no longer able to follow the propeller blade. Assuming constant thrust distribution over the radius, this view leads to the concept that the mean thrust factor of the projected propeller area, which is related to the magnitude of the negative pressure, is a sufficiently accurate limit for the cavitation effect on the propeller. According to trial run data, Barnaby obtained a maximum admissible load factor S/F_p for a propeller near the surface of the water of 7,900 kg/m², which will increase with increasing submersion of the propeller, as follows naturally from the interpretation of the occurrence presented by him. According to later data [5] this value can be increased to 9,100 kg/m², on the basis of empirical values obtained in the meantime.

Barnaby's explanation, so far as the essentials of the phenomenon are concerned, remains completely tenable even now, although no explanation has been given of the decrease in performance and the considerable increase in RPM after the admissible limit has been reached. In this connection attention is directed to the fact that an explanation similar in sense to Barnaby's had already been

2) Proc. Inst. Civ. Engin., 1895
3) Inst. Nav. Arch. 1897 (38)
4) Inst. Nav. Arch. 1897 (39)
5) Inst. Nav. Arch. 1911 (53

given in Euler's paper: Theorie complete des machines qui sont mises en mouvement par la réaction de l'eau, 1754, page 42 of the translation [6], where it is said: "But if it should happen that at any place in the tube this value (absolute pressure) becomes negative, the water would separate from the wall of the tube, leaving a vacant space there. This is to be avoided with all care, since in that event there would be complete disagreement between actual conditions and theory".

The results obtained by Parsons with the TURBINIA which was originally designed as a twin-screw vessel with a propeller diameter of 0.40 m and 2,500 RPM, confirmed Barnaby's reported limit value of the thrust factor. This critical value was exceeded by the twin-screw design, and the propellers were kept within this limit only after remodelling as a triple-screw vessel, which at the same time also resulted in an increase in propeller performance. Noteworthy in the paper by Parsons cited above is the mention of model tests in which water heated to a temperature of several degrees below boiling was used in order to produce cavitation at RPM's obtainable in model testing technique. Through this expedient Parsons succeeded in producing cavitation even at low RPM's, since now a slight decrease in dynamic pressure on the blade was sufficient to bring the absolute pressure to the vapor pressure of the water which had been increased by raising the temperature. This first experimental plant, as nearly as can be learned from the literature on the subject, was not equipped for measuring output, but by observing the different cavitation formations on various propeller models, differing in blade thickness and shape of sections, Parsons arrived at the conclusion that the criterion reported by Barnaby could not be generally valid, but was greatly dependent upon the form parameters of the propeller. At the same time, due to the fact that he succeeded in producing cavitation near the boiling point, i.e. in water that was to a large extent de-aerated, Parsons was able to prove that the phenomenon is not to be attributed to air set free in the water, as had been stated in the appendix to Barnaby's paper.

In 1893 several tests of a torpedo boat with a propeller diameter of 2.03 m were published by Normand [7] on the effect of the depth of immersion of the propeller upon the resistance under test, but it is probable that the decrease in resistance with decreasing immersion observed by him should be attributed to penetration of air into the water rather than to cavitation, since at the immersion at which the reduction began the water column above the blade tip amounted to only 0.245 m. Induced thereto by these experiments and the papers by Barnaby and Parsons published in the meantime, Normand reported in 1899 [8] the result of calculations

6) Ostwalds Klassiker der exakten Wissenschaften, No. 182.

7) Bull. Assoc. Techn. Maritime 1893.

8) Bull. Assoc. Techn. Maritime 1899; see also: Comptes rendus 1902 and Proc. Inst. Civ. Eng. 1906.

in which an attempt is made, although based on highly questionable assumptions, to derive a cavitation criterion in more analytical form than that applied in the case of Barnaby's summary limit value. Starting with the slipstream theory according to which the developed thrust S is proportional to the mass of liquid passing through the propeller disc per second and the induced axial acceleration on the propeller circle, Normand assumes that the acceleration when cavitation occurs has a value constant for all propellers (while actually the relative speed and depth of immersion are the governing factors), and concludes from this that in this case the maximum obtainable thrust is proportional to the volume of water passing through the propeller. The thrust, then, he makes proportional to the product of the square of the diameter, the ship velocity v_s and a function of the projected area ratio, which, in consideration of the fact that thrust increases more slowly than the area, he sets at $(F_p/F)^{0.75}$: $S = \text{const.}\ D^2\ v_s\ (F_p/F)^{0.75}$: Further, the thrust of the x propellers is taken in proportion to the ship resistance, the product of which multiplied by v_s gives the power, so that Normand's criterion is written as $x\ D^2\ (F_p/F)^{0.75} = \text{const.}\ IHP/v_s^2$, where the constant, according to trial run data of cruisers should not be taken as smaller than 0.65 to 0.75 to avoid cavitation (D in m, v_s in knots). The statements of this equation, especially that, other conditions being equal, a propeller is endangered independently of its RPM in inverse proportion to the velocity, or better, to the $(D\ v_s)^2$, must be applied with great caution in view of the rough assumptions, and are hardly to be regarded more highly than Barnaby's and the subsequent summary criteria.

A number of summary criteria on the pattern of Barnaby's are given in the literature as averages of trial trip data on the basis of rather arbitrary viewpoints, which are intended to present the builder with a convenient means of deciding whether he must take into account the effects of cavitation or not. In this connection we must not forget that the range of the validity of a given criterion is closely limited by the type of ship and propeller with which the trial trips are carried out, and that consequently extrapolation can easily lead to errors.

Schaffran [9], from trial trips of American torpedo boats, holds the view that the magnitude of the propeller disc area rather than the projected blade area governs the cavitation effect, and that the maximum load limit of the propeller disc S/F has the value 4,650 kg/m², which is found from Barnaby's statements for $F_p/F = 0.59$ or 0.51. The average of F_p/F for the propellers analyzed by Schaffran is about 0.56, so that Schaffran's figure coincides very well with the first limit value reported by Barnaby, but is to be regarded in its given form as only a special instance of this limit value. The good agreement is to be attributed

9) Schiffbau 1916/17.

essentially to the fact that in both cases ship and propeller dimensions were of the same order of magnitude.

The criteria hitherto cited agree with each other in the concept of the occurrence of cavitation, that there is connected with it a definite load on the propeller area, deduced from the thrust or the power. In opposition to this is a number of other writers, represented primarily by D. W. Taylor, likewise with a purely empirical view that the tip velocity of the blades rather than the load over the area is the decisive factor. According to Taylor's findings the influence begins at a tip velocity of about 60 m/s[10], the only other factor affecting this figure in his opinion being the blade section. Barnaby had already proved [10] that this figure also varies considerably with the pitch of the propeller and is therefore valid only for a definite type of propeller.

To this group, in which the occurrence of a cavitation effect is attributed to one velocity, the works of W. Schmidt [11] are also to be counted, who, by means of data obtained on runs over measured miles of cruisers and torpedo boats arrives at the result that as a rule the influence of cavitation becomes noticeable with n H = 14.5, but occasionally even earlier. Here n is the revolutions per second, H the face pitch of the propeller in m, so that the critical product n H has the dimension of a velocity.

Recently Irish [12] also made an attempt by purely empirical means to combine the two views as to the decisive value inasmuch as he gives one function for the two, which it is not permissible to exceed in order to avoid the effects of cavitation; if the slight curvature of this function is neglected, which is justifiable in view of the inaccuracy of the assumptions on which it is based, then this criterion can be expressed as $SHP = v_s F_p(7.3\ DN - 18.5)$; the ship velocity is here to be given in knots, the other values in meters and seconds. As nearly as can be learned from the paper, this function is based upon mile runs with large cruisers, and for these types experience has shown the equation to be useful in making the first estimate of the required area. In this connection it is advantageous that the load per unit of area is taken from the power, thus eliminating the inaccuracy in estimating the thrust deduction included in the loads found from the thrust.

In contrast to the views hitherto represented is the concept of Gümbel [13], who was probably the first to attempt a theoretical solution of the question of the occurrence of cavitation and obtains the unfortunately untenable result that the angle of the suction side tangent at the trailing edge of the section with the

10) See the discussion of Barnaby's paper in INA, 1911.
11) Z.V.D.I. 1928 and Hydromech. Probl. d. Schiffsantr. p 301–310.
12) Amer. Soc. Nav. Eng. 1929.
13) INA 1913 and J.S.T.G. 1914.

pressure side has considerable influence and should be made as small as possible. This result of Gümbel's follows by application of Bernoulli's equation to the forward part of the propeller race, in doing which, however, there is assumed to be a tangential component in the race ahead of the plane of the propeller, and further, for unknown reasons, the angle of inclination of the resultant velocity with the plane of rotation (angle β of Fig. 33) is taken to be equal to the angle of the suction side tangent at the trailing edge with the plane of rotation. At all events, Gümbel's reasoning remains valuable inasmuch as it represents a first attempt to take into consideration quantitatively the influence of water temperature and static pressure on the blade, i.e., barometer reading and depth of immersion.

An idea of the reliability of the various reported methods can best be obtained by testing them on a concrete example, for which purpose the trial run data of the 4 S.S. BREMEN are used. The values measured on the trial run for revolutions per second n/sec, ship velocity v_S m/sec, and shaft horsepower WHP are given non-dimensionally in Fig. 1 in such form that the speed ratio $\lambda_s = v_S/nD$ was plotted over the non-dimensional moment coefficient $c_2 = 75\ WPS/\rho\ D^5\ n^3$. In this chart the inception of the cavitation effect is recognized by a sharp bend in the curve connecting the individual measured points, which is caused by the fact that the revolutions in the cavitation zone increase disproportionately and therefore lead to a retrogressive branch of the curve because of the cube in the denominator of the abscissa. This method of plotting, which was probably first introduced by Gümbel and later used by Schmidt for further conclusions as to the behavior of propellers when cavitation has formed, gives clearer evidence of the beginning of the cavitation effect than the usual method of plotting test data over the velocity. In the case of the BREMEN it is found that the power of the propellers is influenced from $v_s = 27.2$ knts on, the total output of the four shafts having been measured at SHP = $105 \cdot 10^3$ (HP) and the revolutions at 190 RPM. The propeller diameter amounted to D = 5 m, the pitch H = 5.20 m, the projected blade area $F_p = 9.33\ m^2$ and the ratio of the developed blade area to the disc area $F_a/F = 0.56$. The thrust delivered by one propeller can be computed from the resistance measured on a model and converted to the ship $Wv_S/75$, which at $v_S = 27.2$ knots = 14 m/sec is found to be equal to 61.2×10^3 (HP), and taking into consideration the thrust deduction factor t = 0.21, likewise determined by model test, results in a thrust $S = (1 + t) \times 75 \times 61.2 \times 10^3/4\ v = 99.3 \times 10^3$ kg for a single propeller. With these values we obtain the following table by listing the summary criteria:

Test Data for	Permissible Values
S/F_p = 10640 kg/m²	Less than 9100 , Barnaby [14]
const=xD^2 $(F_p/F)^{0,75}v_s^2/IPS$=0,324	More than 0,65 , Normand
S/F = 5060 kg/m²	Less than 4650 , Schaffran
πDn = 50,0 m/sec	Less than 60 , Taylor
$WPS/v_s F_p$ = 103,5 PS/Kn.m²	Less than 97,1 , Irish
nH = 16,5 m/sec	Less than 15 , Schmidt

It is to be noted that in Norman's report a turbine efficiency inclusive of the losses in the shafting, of 0.8 was assumed in calculating the IHP.

Comparison of the various values shows that the condition at 27.2 knots, according to Taylor's data, is not yet dangerous, while according to the other data the danger in some cases is very great. The values computed by the methods of Irish and Barnaby are in this case the nearest approach to reality.

b) Pressure Tests with Sections.

It is shown by comparison that the results of the summary method can not be extended with sufficient accuracy to cover the range of special types of ships and propellers, as well as draughts, upon which the various results are based. However, it was necessary to resort to this until the airfoil theory of the propeller was so far developed that it was possible reliably to calculate the flow and pressure conditions on a blade and then to make use of pressure distribution measurements on individual sections in estimating the beginning of cavitation. This naturally narrowed down the data considerably as compared to the summary method of reasoning, but the question remains open whether an effect on efficiency is connected with the cavitation thus computed, or whether this will first become noticeable after the cavitation zone has attained a certain extent. This question can not be answered when pressure measurements on single blades are used as a basis, since the relation between the extent of the zone of cavitation and the modification of the forces can hardly be defined theoretically.

A new realization resulting from pressure tests is that contrary to the data supplied by the summary criteria there are conditions which no longer admit a cavitationless propeller, while according to the statement of Irish, for example, any desired output can be absorbed without cavitation by increasing the projected blade area. That this is not true can easily be understood if we observe the beginning of cavitation on a blade section, which occurs only when

14) According to Baker (Ship Design, Resistance and Screw Propulsion, II, Liverpool 1933), S/F_p should be equal to or smaller than (7,900 + 810 h)kg/m² when h is the distance from the blade tip to the surface in meters. In the above example h is equal to 4.00 m, and therefore S/F_p = 11,140 kg/m² is arithmetically admissible, according to which the operating conditions would not yet be endangered.

the sum of the static pressure in the stream at the position of the section p and the maximum negative pressure on the section ($-p'$) is equal to the vapor pressure e, or, if the section negative pressure is referred to the dynamic pressure of the relative velocity, when $p-(p'/q_r)q_r = e$, which is the same as $(p-e) / q_r = \sigma = p'/q_r$; and can be expressed so that cavitation on the radius r begins when the non-dimensional number σ here present, which is designated as the local cavitation index [15], becomes equal to the absolute value of the maximum negative pressure on the section taken with respect to the dynamic pressure. To avoid cavitation σ must be greater than p'/q_r. Here σ is given by the propeller conditions, i.e., by the stated problem, while p'/q_r is still variable with the section parameters - thickness and camber ratio, lift coefficient. Now, however, the airfoil theory demands a definite product zc_at [16] to satisfy the present problem at the radius r under consideration, while the extreme method (Extremalbetrachtung) of considering the propeller sets no conditions for selecting individual factors: number of blades z, lift coefficient (c_a) and blade thickness t, and we are therefore justified in our case in assuming zt as very large, and correspondingly, c_a as very small. But even in the limit when $c_a = 0$, there is always a finite value p'/q_r [17], so that when σ is sufficiently small the condition for freedom from cavitation at no matter how high values of t, i.e. no matter how great the area ratio, can no longer be fulfilled. Plotting the maximum section negative pressure divided by the dynamic pressure over the lift coefficient [18] shows that in the case of thin sections this curve has a maximum at $c_a \approx 0.25$, $p'/q_r \approx -0.3$. This indicates that the possibility of a cavitationless propeller is limited by $\sigma \approx 0.3$, which is approximately confirmed by Walchner's [19] direct cavitation tests of ogival sections, insofar as the lower cavitation-free limit of the thinnest measured section still admissible from strength considerations in the endangered outer portions of the propeller lies at $\sigma = 0.2$.

Before Walchner's tests became known it was theoretically desirable in the construction of propellers to know the maximum permissible lift coefficient, particularly since at that time only isolated pressure measurements on airfoils were available in the literature on the subject. The first attempt of this kind originated with Horn [20]. On the basis of two established facts he gives the limiting value $c_a = \sigma /1.3$. These facts are that in the range of angles of

15) Introduction of the number in cavitation problems, so far as the publisher knows, is due to D. Thoma. Z.V.D.I. 1925.

16) See Helmbold WRH. 1926, No. 23 and 24.

17) See Ergebnisse der A.V.A. Göttingen II, p 43-47

18) Lerbs, WRH 1931, No. 13.

19) Hydrom. Prob. d. Schiffsantr. 1932, pp 256-267.

20) J.S.T.G. 1927.

attack found in practice the negative pressure is distributed in nearly triangular form over the width of the airfoil, and furthermore the ratio of the negative pressure area of the pressure distribution curve to the total pressure area is constant and approximately 0.65.

It has been attempted by the author to reduce the tests of Ackeret on occurrence of cavitation on ogival and airfoil sections [21] to a common denominator [22]. As is to be expected from experience, it becomes evident that p'/q_r, in the case of thin sections, in the range of higher lift coefficients at least (c_a greater than about 0.25) is independent of camber and thickness and dependent only upon c_a. Due to this fact, it is possible to use the most convenient substitute section as a basis for calculating these higher lift coefficients, thus obtaining in this range an approximately generally valid result, while for lower c_a values a satisfactory relation between c_a and p'/q_r can be obtained only by calculation with special sections. An ogival section was used as a substitute. To avoid the long calculations which, in view of the uncertainty of basic data appeared unjustified, it was assumed that the maximum velocity on the suction side of the ogival section can be replaced with sufficient accuracy by the greatest velocity on the infinitely thin crescent circumscribing the section. The resultant infinite negative pressure on the leading edge in assuming a section of infinite thinness can be obviated by using only zero as the angle of incidence in the calculation. It will still be possible to effect a change in the lift coefficient by changing the camber ratio f/t. Thus an ogival section with an angle of incidence zero whose camber is so chosen that the given and the substitute sections will have the same lift coefficient is substituted for the given section having a definite angle of incidence with respect to the greatest relative velocity v' affecting it. Then it is assumed that v on the ogival section agrees sufficiently well with v' on the circular arc bounding the suction side. By doing this the calculation can be carried out very simply. First the greatest relative velocity on the crescent having a camber ratio f/t and at an angle of attack zero is found to be [23]

$$v'/v_r = \frac{1 + 8\,(f/t)^2}{1 + 4\,(f/t)^2} + \frac{4\,(f/t)}{\sqrt{1 + 4\,(f/t)^2}}$$

where v_r is the velocity in infinity. Furthermore, the lift coefficient of the ogival section is approximately equal to the coefficient of the median line of the section, i.e. of an arc with a camber ratio of $f'/t = \frac{1}{2}\, f/t$. The lift coefficient of such an arc for $\alpha = 0$ [24] is $c_a = 4\pi f'/t = 2\pi f/t$. With this

21) Z. f. t. Mechan. u. Thermodyn. 1930, No. 1 and 2.

22) WRH. 1931, No. 13.

23) See Fuchs–Hopf–Sewald, II, p 64.

24) See Hütte, 26th edition, p 401.

v'/v_r can be expressed in terms of c_a. For this, in developing in terms of c_a/π up to higher terms that are no longer significant, we get $v'/v_r = 1 + 2c_a/\pi + (c_a/\pi)^2$, and from this, according to Bernoulli's equation, the maximum negative pressure $p'/q_r = 1 - (v'/v_r)^2 = -4(c_a/\pi) + 6(c_a/\pi)^2$. With this last equation, the condition of freedom from cavitation $\sigma \geqq p'/q_r$ leads to the admissible upper limit $c_a = \frac{\pi}{3}\left[\sqrt{1 + 1.5\sigma} - 1\right]$. This relation together with Ackeret's test points is shown in Fig. 2, in which it is seen to reproduce the test points passably well, down to the measurements of Sections D and E at an angle of incidence α_∞ of 5° taken with respect to an inverse aspect ratio zero. Here, however, to judge from the polars of these sections in the sixth edition of the A.V.A., p 39, the flow begins to separate from the surface, and therefore the principles upon which the potential flow assumed in the estimate is based are no longer satisfied. At small σ values the substitute section is no longer valid, since the given relation still permits small c_a values free from cavitation in this range, which is due to the fact that the substitute section tends towards the flat plate as c_a approaches zero, the flat plate being at zero angle and producing no resultant field of pressure.

The relation has recently been tested by Kell [25] on a series of propeller models in the water tunnel of the American Navy. It was found that, in general, cavitation sets in only at lift coefficients 15% higher than those following from the equation, while it is only in isolated cases that it is noted at values lower than those calculated. Unfortunately the paper does not describe the method according to which the propeller stream was analyzed and the angle of incidence of the blade element calculated, so that nothing is known as to the accuracy of this calculation and consequently the accuracy of c_a. At any rate, these tests appear to bear out our own experience that the relation developed is useful for estimating the admissible c_a when the limits of validity are adhered to. – It is to be noted that the critical value reported by Horn from the foregoing equations when limited to terms of the first order, is found to be $c_a = \sigma/1.27$, so that there is no contradiction between the two relations.

Walchner [26] undertook to improve the calculation by rigorously calculating the maximum velocity on the ogival section based on the Karman–Trefftz transformal function for $\alpha = 0$, by which he obtained in second approximation the critical value $c_a = -2.45 + \sqrt{5.98 + 4.70\,\sigma}$, which is also plotted in Fig. 2. This relation which approximates the estimate made above very closely and therefore tends towards Kell's measurements, represents Walchner's cavitation data for ogival sections at $\alpha_\infty = 0°$ very well.

In connection with the estimate made in the foregoing, the writer has

25) INA 1934.

26) Hydrom. Probl. d. Schiffsantr. 1932, p 267.

attempted to obtain a more accurate idea of the minimum σ or c_a, as the case may be, down to which the equation still remains valid, by calculating the pressure distribution on Youkowsky sections of varying thickness and camber ratios. Here the circulation about the section was determined from measured lift coefficients[27] by which, according to Betz [28], a pressure curve is obtained that for the leading part of the section is in good agreement with measurements, while with a circulation resulting in a smooth exit an excessively high value results for the pressure minimum. There now also results with a given σ a lower limit for the admissible c_a, caused by the increase of the maximum negative pressure on the pressure side of the section as the negative angle of incidence increases. There also results a minimum σ value dependent upon camber and thickness, below which it is impossible to avoid cavitation with the given section. This limit approaches small σ values the more closely, the thinner and less cambered the section. Above all, it becomes evident that in the proximity of this minimum σ value great care must be taken in limiting c_a in order to avoid re-entry into the cavitation zone by passing through the lower limit of the non-cavitating zone. These data which formerly yielded valuable hints for dimensioning propellers, must now be regarded as obsolete since cavitation data for sections have been published. Therefore the calculations will not be taken up in detail, especially since the methods are already familiar.

c) CAVITATION TESTS OF SECTIONS.

The first experimental investigation of cavitation phenomena on blade sections was carried out by Ackeret [29] in a small water tunnel of the K. W. Institut für Strömungsforschung in Göttingen. This tunnel permitted the cavitation index to be altered by changing pressure and velocity, and the experiments were carried out with a series of three ogival and two airfoil sections and different angles of incidence. Part of these data – c_a dependent upon at the moment when cavitation starts – is already indicated in Fig. 2. In this connection it is to be noted that the polars were determined in the wind tunnel with geometrically similar enlarged sections, since no apparatus for measuring blade forces was available in the water tunnel. The relation between static pressure and dynamic pressure at the same stage of cavitation was investigated particularly, for example at the beginning or when cavitation extended up the trailing edge of the section. It was found that this relation is linear and that the intersection on the axis of static pressure co-ordinates is equal to the vapor pressure of the water. In other words, that similar cavitation conditions are determined by the

27) Third issue of A.V.A. Göttingen.

28) Z. f. M. 1915, p 173.

29) Z. f. techn. Mech. u. Thermodyn. I, 1930, No. 1 and 2.

cavitation index of the flow $\sigma = (p-e)/q_r$, the sections being similar and the angle of incidence unaltered. This relation can easily be proven, particularly when we consider the similarity of cavitation phenomena to be discussed later, when we estimate the static pressure p which must be present in undisturbed flow of the velocity v_r, so that cavitation can begin at any desired point (a) of the section. Let p_a be the existing pressure at a, v_a the local velocity at that point. Between p_a and v_a, according to Bernoulli's equation, the relation holds, $p_a = p - \frac{\rho}{2}(v_a^2 - v_r^2)$. Since the local velocity v_a is proportional to v_r : $v_a = kv_r$, we get $p_a = p - \frac{\rho}{2} v_r^2 (k^2 - 1) = p - cq_r$, when q_r represents the dynamic pressure of the undisturbed flow and c a constant dependent only upon the position of the point a (and upon the angle of incidence). For the beginning of cavitation at a we obtain from this the linear relation $p = e + cq_r$ in agreement with measurements, and it follows further by derivation that the same relation holds for the beginning of cavitation at similar points of geometrically similar hydrofoils. This is true since in an ideal fluid (with certain limitations to be given subsequently), c is independent of the size of the hydrofoil whatever it may be. Now since under the same assumption the proportionality between v_a and v_r, essential to the development of the equation, is valid for every point in the field of flow, in general the formation of similar cavitation conditions on geometrically similar blade sections is limited only by the relation just developed. To express it briefly and synonymously, similarity is assured by the constancy of the cavitation index $\sigma = (p - e)/q_r$.

Ackeret's further investigations relate to what occurs when the cavitating zone collapses. He obtains fundamentally new information by establishing that the vanishing of the vapor bubbles and the increase in pressure connected with it, is analogous to a water hammer. This might explain mechanically the destruction of material connected with cavitation in view of the extremely brief time of compression of the bubbles. Details of these investigations are outside the scope of this paper; only, the term "water hammer" is introduced for the zone of transition downstream.

The set-up used by Ackeret was later improved by H. Mueller and supplemented by addition of a two-component balance. With this Walchner, in the paper mentioned in the foregoing, determined section polars with ogival sections as functions of σ, which yielded primarily the previously sought relation between c_a, camber ratio f/t, and σ at the moment when cavitation begins. In agreement with the calculations for Yukowsky sections mentioned on page 11 these limiting curves consist of three branches for each section; an upper, on which cavitation emanates from the leading edge of the suction side (forward impact point on the pressure side), a lower which is connected with the pressure side cavitation from the leading edge (forward impact point on the suction side), and a connecting branch which governs the minimum value of σ still admissible without cavitation

and for which cavitation begins approximately at half width of the section (shockfree entry). Helmbold has shown [30] that the curves obtained for the individual sections within a group of sections with similar ratios go over into a single curve valid for the whole group when in place of c_a and σ the expressions $\frac{c_a}{f/t}$ and $\frac{\sigma}{f/t}$ are taken as coordinates. This becomes evident when we consider two ogival sections having different cambers f/t and if/t in the scope of the theory of the first order, which will then differ by the lift coefficients c_a and ic_a, and the accelerations w/v_r and iwv_r; furthermore, the negative pressure on two corresponding points of the suction side is $(p - p_a)/q_r = 2w/v_r$ or, as the case may be, $i2w/v_r$, so that with p_a = e a cavitation index for the fundamental flow of σ or $i\sigma$ is required for equal cavitation conditions. In a chart c_a/i over σ/i, accordingly, the values relating to the same cavitation conditions will yield coinciding points. This relation is confirmed by Walchner's experiments.

The other result of these experiments important in application to propellers is that the D/L ratio $\epsilon = c_w/c_a$ after inception of cavitation generally becomes less favorable because in addition to an increase in drag, the lift decreases greatly in consequence of the negative pressure being constant in the cavitating zone and no longer decreasing as the square of the velocity. Only in the case of positive angles of incidence at which cavitation starts from the leading edge of the suction side was a partial improvement in the D/L ratio noted, due to increased lift and decreased drag. This improvement is attributable to the fact that the cavitating layer has the effect of a change in form of the section in the sense of greater camber, thus causing the greater lift, while the drag is first decreased by decreasing friction, but subsequently, as cavitation proceeds, once more increases through an increase in pressure due to extension of the dead water. The D/L ratio begins to deteriorate when the cavitation zone has advanced to about the middle of the section.

As the cavitation index continues to decrease, a flow is ultimately formed at positive angles of incidence, in which only the pressure side remains in contact with the liquid, while the suction side is completely in the vapor zone which is separated from the liquid by two sharply defined boundaries (fully developed cavitation). For this condition, in which the form of the suction side is no longer important, Betz undertook to estimate the blade characteristics using Helmholtz's and Kirchhoff's data on flow about bodies with free boundaries [31], and obtains as lift coefficient $c_a = \frac{\pi}{2} \alpha + \sigma$, where the first term signifies the lift coefficient of a plate with free flow boundaries, whose deadwater pressure is equal to the pressure of the undisturbed flow. The second term takes into account the fact that in the deadwater the vapor pressure of the liquid, and not

30) Hydrom. Probleme d. Schiffsantr. p. 338.

31) Verh. des II. intern. Kongr. f. techn. Mechan., Stockholm 1932.

the pressure of undisturbed flow exists. Walchner checked the given relation on the basis of his tests and found that as long as the assumption of fully developed cavitation is satisfied they are well borne out.

Simultaneously with Walchner, Martyrer [32] published his cavitation tests with several sections, which, however, contain nothing new so far as the purpose of this paper is concerned. The tests reported by Legras [33], on the other hand, are considerably more extensive. They were performed with a grid of ogival sections with a grid spacing (distance between blades/chord of blades) = 0.51 and an angle of stagger of 45°, corresponding approximately to the conditions of a blade section in the propeller of a fast ship at 1/3 its radius. The results of the two-component measurements indicate that cavitation sets in earlier in grid arrangement and that there is here a greater decrease in lift and increase in drag in the cavitating zone than in the case of similar values of isolated sections under similar conditions, so that according to these tests, a considerable grid effect must be counted upon in cavitation phenomena. This gives rise to a doubt as to the possibility of constructing a propeller according to theoretical conceptions in the cavitating zone based on the polars of isolated blades. This pronounced influence can be explained by the fact that the flow at the place of the section considered as removed from the grid is curved through the influence of the neighboring blades and therefore shows a lesser static pressure over the place of the section, on the average, than the flow far in advance of the grid. Therefore a lower cavitation index and consequently more extensive development of cavitation are to be expected on the section in a grid, pressure and velocity far in advance being unchanged, than in the case of the isolated section. A possible method of estimating this grid effect at least on the setting in of cavitation is given by Betz's method of using charts for calculating blade series [34], which, however, will not be taken up further here.

II. EXISTENT POSSIBILITIES OF DESIGNING PROPELLERS WITHIN THE CAVITATION ZONE.

The present data of pressure and cavitation tests with isolated blades, while permitting a series of valuable deductions as to the propeller, are not yet sufficiently complete with respect to the grid effect to permit quantitative statements as to when efficiency begins to be affected and as to the performance of propellers in the cavitation zone, to say nothing of the fact that the calculations required in every case demand a certain expenditure of time and in addition

32) Hydrom. Probl. d. Schiffsantr. 1932, p 268–286.
33) Bull. Assoc. Techn. Maritime 39, 1935.
34) Ing. Archiv 1931, pp 359–371.

it is possible to make statements only for the optimum propeller, i.e., only for a special thrust distribution.

A method of designing propellers in the cavitation zone based on trial run data, the only one to be found in literature on the subject, has been reported by R. Fresenius [35], and later independently by W. Schmidt [36]. This method is based on the chart already used on p 6 , in which the non-dimensional torque coefficient $c_2 = 75\ SHP/\rho\ D^5n^3$, measured on a trial run, is plotted over the speed ratio of the propeller, $\lambda = v/nD$. In addition to this curve, which for reasons previously given, tends towards smaller c_2 values after the efficiency begins to be affected, the open water curve obtained in model tests of the propeller concerned is plotted (Fig. 3). The vertical distance of these curves from each other, when logarithmically plotted, give the ratio of the ship's speed v_s to the speed of advance v_e, i.e. the wake factor. The cavitation effect, then, is regarded as of such form that the density of the propeller stream decreases in proportion to the efficiency, i.e. by so much, that cavitation curve 3, with the correct value of density in c_2, would coincide with the cavitationless curve 2 extrapolated according to the open-water curve 1. On this assumption, the horizontal distance of the extrapolated curve 2 from curve 3 represents the ratio of the density of the propeller stream in cavitation ρ_k to the density of the cavitationless stream ρ . For the relation between ρ_k/ρ with designed values of the propeller we write: $\rho_k/\rho = (C/nH)^x$, where as has been said C = nH amounts to about 14.5 to 15.4 m/sec when the cavitation effect begins, while x, in a manner not known, depends upon the draught and is of the order of magnitude of 1.8. In addition, the form elements of the propeller will be contained in x which indicates the steepness of efficiency drop. However, nothing is said regarding this. In designing a propeller according to systematic tests we first compute as usual with the density and with this obtain, within a series characterized by the area ratio F_a/F a definite optimum propeller with pitch H, from which the density ρ_k appropriate to this instance follows by means of the reported equation. The selection is repeated with constantly improving ρ_k values until two consecutive calculations no longer result in any appreciable difference in pitch. A propeller thus obtained, if the exponent x has been properly postulated, takes up the given power in accordance with the given test data at the prescribed RPM. On the other hand, it is questionable whether the intended speed will be attained, since no information can be given as to the decrease in performance because no thrust measurements are available. At the least, an extensive experience is required in order to apply this method correctly.

In view of the uncertainty and incompleteness of available data in their

35) See G. Bauer, Der Schiffsmaschinenbau, Vol I, 1923, p 553.
36) Z.V.D.I. 1928, pp 1713-1718.

application to propeller design, it was necessary to erect a plant that renders it possible to measure the performance of propeller models under any cavitation conditions desired. Construction of such a plant, to be described in the following, was begun about 1928 by the Hamburg Model Basin, and with means supplied by the Notgemeinschaft der deutschen Wissenschaft, completed about 1931.

III. THE CAVITATION TANK OF THE HAMBURGISCHE SCHIFFBAU VERSUCHSANSTALT.

a) Description of the Plant [37].

The viewpoints according to which such a plant should be designed follow from the condition given on pp 11 and 12 for similar cavitation patterns on similar blade elements in an ideal liquid: $\sigma = (p - e)/q_r$ = constant, from which follows the static pressure $p = e + (p' - e') q_r/q'_r$, required for a model in a liquid having the dynamic pressure q_r and vapor pressure e, the values marked with ' applying to the full-scale propeller and those without to the model. In agreement with the requirement, stated at the beginning, of a complete model test, the pressure must be decreased as long as q'_r is greater than q_r, as is the case in by far the greater number of instances. Furthermore it is evident that extremely low pressures can be avoided by increasing the vapor pressure of the experimental liquid, i.e. by heating. Parsons had already made use of this fact, as previously mentioned. On the basis of these considerations, the structure was built in the form of a closed tunnel with a free surface, which, however, was also shut off from the outer atmosphere. In this tunnel a vacuum pump was provided for the necessary pressure decreases, and a heating jacket for increasing e (Fig. 4). Due to its construction as a closed tunnel, the model testing process is the reverse of Froude's method using a towing carriage. While in that case it is towed through the water, it now is free only to carry out a rotary motion without progressing, and must therefore be given relative motion by the water being set in motion by a driving impeller. Naturally the beginning of cavitation in this impeller must be delayed as much as possible, which is accomplished most simply by setting up the tunnel in vertical position with the drive at the bottom. With the experience then at hand it appeared adequate to impose a static pressure of 0.5 atm upon the driving impeller, resulting in a height of 5 m for the tunnel. Cavitation on the propeller model without subjecting the vacuum pump to superimposed static water pressures requires that the model be placed in places of low pressure, i.e. in the upper portion. These requirements established the essential structure of the tunnel. Beginning with a circular section in the plane of the driving impeller, the cross-sections gradually and uniformly change until they assume the shape of a flattened rectangle in the section of the final bend before

37) See Lerbs, WRH, 1931, No. 11.

the testing chamber, and from there on to the jet assume a circular form. This result was found in model tests to give bends of low resistance, which, however, according to Nippert's subsequently published test data [38], can be improved by increasing the width in the crests of the bends and choosing bends of narrow rectangular section. Built-in guide vanes, as yet designed as partitions of wide surface, suppress the rotary motion imparted to the liquid by the driving force and changes in direction, the final vestiges of which are removed by a honeycomb consisting of square cells with 11.1 cm sides. According to more recent papers [39] hydrofoil grids have been found superior to the guide vanes originally used. The design of the nozzle resembled that of the Göttingen wind tunnel. At the measuring section it consists of two interchangeable parts having the cross sections indicated in Fig. 4. In the plane of the object to be studied windows of 11.0 x 20.0 cm are inserted to illuminate and observe the model. These necessitate a section flat in the horizontal and vertical. The greater length of the tunnel in comparison to its width resulted through the insertion of a portion with a large cross section between the last bend before the measuring section and the honeycomb, in which the air contained in the water is separated out as a result of the low velocity prevailing there and the longer direct connection with the pumping device at a low pressure.

The former Vulkanwerft in Hamburg undertook the construction of the tunnel and the supporting frame. To cut down the cost, the tunnel was built of 12 mm steel shipbuilding plates by electric welding. On the suggestion of this firm, the flanges, after the faying surfaces had been carefully smoothed, were packed with oiled cardboard, which, even after being in use for a considerable time, has given no difficulty. The machined parts such as the driving propeller with reduction gears and labyrinth packing were built by the firm "Weser", successor to the Vulkan Werft.

It is possible to estimate the hydraulic efficiency of a flow plant from the performance factor of the tunnel, which is defined as the ratio of the energy fed into the motor (input) to the kinetic energy of the volume of liquid passing through the measuring section per second (jet efficiency), (ξ = input from $\frac{\rho}{2} F_o v_o^2$), and comparison of geometrically similar tunnels, the one having a lower performance factor being regarded as the better. The mean velocity v_o in the measuring plane was derived from the pressure drop in the nozzle between Aperture 1 (Fig. 4) and another aperture at the same height in the measuring section as No. 1, using Bernoulli's equation and the continuity equation. It was found to be

$$v_o^2 = \frac{2(p_1 - p_0)}{\rho \left[1 - (F_0/F_1)^2\right]}$$

38) Forschungsarbeiten des VDI, No. 320.

39) Kröber, Ing. Archiv., 1932.

Using a mercury manometer, $p_1 - p_0 = 12.59\ \Delta h$ in kg/m², when Δh is writen in mm Hg. Since further $F_1 = 15,580$ cm² and F_o for the large nozzle amounts to 2,146 cm², as was found by measuring with sectional templates, $v_0 = 0.501\sqrt{\Delta h}$, which is subject to a correction by the nozzle factor which allows for the pressure drop resulting from viscosity and the non-uniformity of velocity distribution. A basis for this is given by the values for a standard nozzle reported in the "Rules for measuring flow by means of standardized nozzles and diaphragms" (VDI Verlag 1930). The coefficient of flow of this standard nozzle within the range of Reynold's numbers and at the existing aperture ratio F_0/F_1 amounts to about 0.994, making the velocity in the measuring section $v_0 = 0.496\sqrt{\Delta h}$ (m/sec, Δh in mm Hg), on the assumption that the flow coefficient of the standard nozzle also applies to the tunnel. On this assumption there results the performance curve plotted in Fig. 5, whose abrupt rise at low velocities may be attributed to the driving motor selected. This is a DC motor of 102 HP maximum output with a separately excited field of 220 V and an armature voltage of 220 V controlled by a Ward-Leonard unit. The field energy which is almost constant over the whole speed range, exceeds the energy input for the armature considerably at low speeds, which explains the rise in the performance factor which contains in its numerator the entire electrical input. In comparison with closed wind tunnels, the measured performance factor of 0.53 is not particularly high. The reason for this aside from the mentioned possibilities for improvement of the guide vanes and bend cross sections, lies in the fact that with the small cross sections of the tunnel the bearing supports installed for the model and the impellers represent great resistances to flow. When the small nozzle is installed the performance factor falls to about 0.66, which is due to its not very advantageous form as an interchangeable piece, and to several openings which it was necessary to cut to allow its insertion. The velocities attainable at the maximum output are 10.6 in the large nozzle and 12.3 m/sec in the small one.

The performance factor alone is not sufficient to permit a complete estimate of the efficiency of a tunnel; it must be supplemented by data on the uniformity of flow in time and space. The velocity fluctuations in time which are approximately proportional to the velocity itself at first amounted to about $\pm$ 2% of v_0, and could be reduced to about $\pm$ 1.5% by damping of the free surface. Another considerable improvement was accomplished by installation of a short honeycomb in front of the driving propeller. This prevents as far as possible the entry of irregular, rotating balls of liquid into the propeller which have not been sufficiently suppressed by the guide vanes in the bend ahead of the propeller, and assures a more nearly constant energy consumption. By this means the time fluctuation dropped to about $\pm$ 0.3%, which for the present purpose is adequate to obviate the necessity of installing an automatic regulator.

The local velocity distribution in the measuring section was determined by

means of a pitot tube. The clamping device for this was so arranged in a rotatable stuffing box that by tilting and shifting the tube it was possible to reach any desired point in the measuring section. The time fluctuations were eliminated while measuring the pressure drop between the apertures used for determining the performance factor by taking readings on the pitot tube manometer only when the pressure drop indicated the selected mean velocity of 4.05 m/sec in the measuring plane. Figure 6 shows the result for the large nozzle used in the subsequent propeller tests, where contours of equal velocity are plotted. By measuring about 300 points in the section and by the elimination of the time fluctuations just described, the accuracy of these curves is to some extent assured from 0.1 to 0.1%. It appears the local fluctuation over a circle of 25 cm indicated by a broken line in the figure and corresponding to about the greatest dimensions used in the models, amounts to about 1%. This distribution is to be regarded as good, above all because the effect of the bearing support close behind the measuring section has not yet faded out here, and therefore it was not regarded as necessary to increase local uniformity by the installation of sieves with unknown qualities in the cavitation zone. In the small nozzle this local fluctuation due to its greater contraction falls, over the 25 cm circle, to about 0.5%. It was possible to dispense with measurement of the distribution at higher mean velocities, since according to tests by Nikuradse, for the exponent of an exponential expression for the velocity distribution in a smooth tube,[40] the Reynolds number corresponding to the test

$$R = 2v_o \sqrt{F_o/\pi}/\nu = 1.8 \cdot 10^6$$

is already in the zone where this exponent changes only very slowly with R ($R > 1.6 \cdot 10^6$), so that a material change of the lines of equal velocity ratios can no longer occur.

Simultaneously with these measurements of local velocity, static pressure measurements were undertaken over the measuring section to investigate the freedom from rotation of the stream. When the test instrument was shifted no change in static pressure was noticeable, and therefore the jet in the measuring plane is to be regarded as free from rotation.

The cavitation tank just described differs from that built at the same time by the American Navy [41] in essential details. For one thing, all cross sections of the American tank are circular without guide vanes or honeycombs. The stream flows through the surrounding water as an open jet, the surrounding water being shut off from the outer atmosphere by the container. The reasons for this arrangement, unfavorable with respect to the performance factor and the uniformity of flow in time and space, are not evident. The unavoidable rotation of the

40) Handb. d. exp. Physik, IV, Part 4, p 70.

41) Soc. of Nav. Arch. and Marine Eng., New York, 1930.

stream consequent upon this method of construction probably causes the considerable one-sided difference between the power measurements of a propeller in the tunnel and in the towing basin reported in the cited paper.*

*N.B. The author is evidently not in touch with the American tunnel, and is unacquainted with the improvements that have been made, or he would not make such statement. U.S.E.M.B.

The plant having been described and the data required to judge of its usefulness reported, the test methods and the apparatus developed for performing cavitation tests of propeller models will be taken up.

b) Test Methods and Test Instruments.

For the complete determination of propeller characteristics it is essential to measure the following values: The speed of advance v_e, i.e. the velocity in the region of the propeller when this is imagined to be removed, its revolutions n, the static pressure p to which it is subjected, the temperature of the water in the tank t, the torque absorbed M, and the thrust delivered S. From these measured values non-dimensional coefficients can then be formed, - the thrust coefficient $c_1 = S/\rho n^2D^4$ and the torque coefficient $c_2 = M/\rho n^2D^5$, which depend only upon certain non-dimensional parameters later introduced.

α) Determination of the Speed of Advance v_e(m/sec).

This is obtained, allowing for several corrections, from the velocity of flow through the measuring section v_o, which, according to comparative model basin data, will be obtained with the greatest certainty from the local velocity readings of a pitot tube at some point alongside the propeller. From the standpoint of test procedure this is simpler than the method of determining v_o from the pressure drop in the nozzle used in obtaining the performance factor. The installation of the pitot tube in the plane of the propeller is indicated by the fact that due to the finite ratio of the propeller stream to the cross section of the tunnel corrections are necessitated, which can be found with sufficient accuracy only at points where the diameter of the propeller stream is known, i.e. in the plane of the propeller itself or very far in advance of it or very far to the rear. The latter possibility is eliminated because of the installations to the rear of the propeller, and far ahead of the propeller the velocity is so low because of the large cross sections there prevalent, that the accuracy of the measurement is vitiated. Therefore the only recourse left was to place the tube next to the propeller, which has the additional advantage that the correction mentioned has here a small value, as will be developed later on. In installing the tube care must first be taken that its distance from the blade tips of the propeller model is sufficient to avoid the effects of the tip vortices, which are hard to estimate.

A basis for this minimum distance was obtained by special tests in the model basin with a propeller having a diameter of 0.240 m, where the difference of the total pressure and the static pressure corresponding to undisturbed flow at points outside the propeller disc was established, (Fig. 7). Here it was shown that this influence becomes most noticeable for S = 0 by a change in the total pressure. In order still to obtain correct values even for this case, a distance of about 0.1 d between the blade tips and the pitot tube must be maintained, according to these data. Furthermore, it is advisable to arrange the holder for the tube and thus also the connection with the manometer vertically downward, to avoid as far as possible the influence on the manometer of air which easily separates out of the water in a high vacuum.

From the pressure (h_{st} in mm Hg) indicated by the pitot tube is obtained first the velocity of flow v_o through the measuring section without propeller and with the following corrections:

1. The tube constant, which is governed by the pressure drop at the static slit originating from the pressure distribution on the half-body, and the damming effect of the holder, overcompensating in this case. It was found to be 1.026 from comparison of the velocity reading of the tube with the velocity of the carriage of the model basin determined from time and distance, and in the range of actual velocity limits it was independent of the velocity with sufficient accuracy. Accordingly the actual velocity is $v = 1.026 \sqrt{\frac{2}{\rho}\, 12.59 \cdot h_{st}} = 0.509 \sqrt{h_{st}}$ (m/sec). It might seem questionable that calibration is carried out in still water, i.e. in extreme potential flow, while the pitot tube is subsequently used as a meter in turbulent flow. According to investigations made by Cole [42], who, as in the present case, used a tube calibrated in a liquid at rest by means of a carriage, in order to determine the mean velocity of turbulent flow in a pipe, which also could be determined by weighing, this difference can be neglected within the limits of test accuracy.

2. Correction because of the local non-uniformity of flow in the measuring section. In the large nozzle, which alone comes into consideration for propeller tests, there exists according to Fig. 6, an excess velocity of 0.2% in the locality of the pitot tube. With this and with the correction given in 1. the mean velocity is equal to $0.508 \sqrt{h_{st}}$.

3. Correction for the finite cross section of the tube F_{st} as compared to the Measuring section F_0. The displacement of the flow about the head of the tube brings about a decrease in pressure at the static slot so that the pressure difference and with it the velocity measured by it are too high. The correction factor found directly from the continuity equation $(1-F_{st}/F_0)$, with $F_{st} = 0.786$ cm² (tube diameter $\delta = 1.00$ cm), and $F_0 = 2,146$ cm², is found with sufficient

42) Trans. Amer. Soc. Mechan. Eng. 1935, pp 281-294.

accuracy to be equal to unity.

4. Correction for wall effect. In order to estimate this effect it is assumed that the curvature of the neighboring wall is negligible. Thus we obtain the correction by mirroring flow from the source, which by superposing on the parallel flow, yields a half-body of the principal dimensions of the obstruction. This consists of a circular cylinder ($\varnothing\ \delta$ = 1.00 cm) with a hemi-spherical head attached, while the half-body produced by a point source assumes the form of a circular cylinder only in infinity. Therefore, diameters being equal at infinity, there exists a difference in contour at the location of the static slot where the pressure is of interest for this correction. This difference is first to be determined in order to decide whether the half-body of the point source with the diameter δ at infinity reproduces with sufficient accuracy the tube dimensions in the vicinity of the static slot. In polar coordinates r and φ (Fig. 8) the flow function of parallel flow is $\psi_1 = v_0 \cdot r^2/2$ and that of the source, located at coordinates zero, is $\psi_2 = -\frac{e}{4\pi}(1 + \cos\psi)$, where e represents its flow. Accordingly the equation of the half-body is

$$\psi = \psi_1 + \psi_2 = v_0 \cdot r^2 - \frac{e}{2\pi}(1+\cos\varphi) = 0,$$

from which we get $e/v_0 = \pi\delta_2^2/2(1 + \cos\varphi_2)$ when the index 2 relates to the corresponding values at the static slot. In addition the continuity equation yields the relation in a cross section at an infinite distance: $e/v_0 = \pi\delta^2/4$, from which by comparison with the former equation it follows that $(\delta_2/\delta)^2 = 0.5\ (1 + \cos\varphi_2)$. Herein $\cos\varphi_2 = \frac{s - x_1}{\sqrt{(s-x_1)^2 + \delta_2^2/4}}$ and further $x_1 = \sqrt{\frac{1}{4\pi}\frac{e}{v_0}} = \frac{\delta}{4}$. With the known dimensions δ = 1.00 cm and s = 3.50 cm we obtain from the last three equations δ_2 = 0.997 cm, which within the scope of this estimate agrees sufficiently well with the tube diameter. – Since the distance to the wall is large in comparison to the tube diameter, two further assumptions are justified: First that the mirrored source has no influence on the form of the half-body, thus permitting us to retain the flow $e/v_0 = \pi\delta^2/4$ for the source and its mirror image; and second, that the average value of the velocity over the static slot (vertical section 2, Fig. 8) approximates the velocity in the axial point 2 sufficiently well. With these assumptions the pressure difference measured by the tube, with the wall regarded as distant from the tube, which is to be introduced as a relative value, will be

$$\frac{p_1 - p_2}{\frac{\varrho}{2} v_0^2} = \left(\frac{v_2}{v_0}\right)^2 = \left(1 + \frac{e}{v_0}\frac{1}{4\pi x_2^2}\right)^2 = \left(1 + \frac{1}{16\beta^2}\right)^2$$

with the symbol $\beta = x_2/\delta$. In considering the effect of the wall, the velocity in point 1 is no longer zero, but as a result of the influence of the mirrored source it has the finite components

$$v_{1x} = v_o - \frac{e}{4\pi x_1^2} - \frac{e \sin \vartheta_1}{4\pi r_1^2} \text{ und } v_{1y} = \frac{e \cos \vartheta_1}{4\pi r_1^2}.$$

From which, after introducing the corresponding values, we get $(v_1/v_0)^2 = 1/(1 + 64\alpha^2)^2$, when $\alpha = \frac{a}{\delta}$ represents the ratio of the distance of the wall to the diameter of the tube. In the same way we get for the components of the velocity in point 2:

$$v_{2x} = v_o + \frac{e}{4\pi x_2^2} + \frac{e \sin \vartheta_2}{4\pi r_2^2} \text{ und } v_{2y} = \frac{e \cos \vartheta_2}{4\pi r_2^2}$$

and from this, as resultant velocity in 2:

$$\left(\frac{v_2}{v_o}\right)^2 = \left[1 + \frac{1}{16\beta^2} + \frac{\beta}{16(\beta^2 + 4\alpha^2)^{1.5}}\right]^2 + \frac{\alpha^2}{64(\beta^2 + 4\alpha^2)^3}$$

The relation between the measured pressure difference and the dynamic pressure of the velocity of flow will then be

$$\frac{p_1 - p_2}{\frac{\varrho}{2} v_o^2} = \left(\frac{v_2}{v_o}\right)^2 - \left(\frac{v_1}{v_o}\right)^2$$

With the numerical values α = 6.90/1.00 = 6.90 and β = 3.25/1.00 = 3.25, the pressure ratio according to these equations will be: without wall = 1.0119 and with wall 1.0121, so that the effect of the proximity of the wall upon the static pressure amounts to 0.02%, which affects the velocity by .01%, and can be neglected.

5. Correction for the pressure gradient in the tunnel. This pressure drop which is included in the measurement by the tube and has the effect of rendering the velocity readings too high, can be expressed approximately on the basis of Nikuradse's tests on the pressure drop in straight cylindrical tubes; in view of the slight relative roughness of the tunnel it is sufficient here to limit ourselves to the tests in smooth tubes, which can be expressed by the interpolation formula [43]

$$\psi = [2 \log (R \sqrt{\psi}) - 0{,}8]^{-2}$$

where ψ and R are defined by the relations

$$\psi = \frac{\Delta p}{l} \frac{2D}{\varrho v_o^2} ; R = \frac{v_o \cdot D}{\nu}$$

In the present instance, we are interested in the pressure drop for a distance

43) Data of the AVA, Göttingen, IV, p 29.

equal to the distance of the static slot from the vertex of the tube, which is indicated in Fig. 8 as s, and at a pipe diameter, which, because of the slight difference of the measuring cross section from a circle with F_0 as the diameter, has equivalent area when D = 0.523 m. With these values the ratio of the pressure drop of the tunnel for s = 3.50 cm to the dynamic pressure of the mean velocity of flow through the tunnel v_0 will be

$$\frac{\Delta p}{\varrho/_2 v_0^2} = \frac{s\psi}{D} = 6.69 \cdot 10^{-2} \cdot \psi.$$

For v_0 = 5 m/s, ψ is found to be $1.07 \cdot 10^{-2}$ and with this $\frac{\Delta p}{\varrho/_2 v_0^2} = 7.14 \cdot 10^{-4}$, so that the correction factor for the static pressure obtained with this is sufficiently near unity.

These corrections are adequate, with the propeller lacking, to determine from the local velocity reading of the pitot tube the mean velocity of flow through the plane of the propeller which is equal to $v_0 = 0.508 \sqrt{h_{st}}$ in m/sec for h_{st} in mm Hg. With the propeller present, however, the velocity v_0 thus determined is not yet to be regarded as the velocity v_e at which in water of unlimited cross section and with the same RPM the same thrust is generated as in the tunnel. Equality of thrust here represents, in the sense of the simple stream theory, upon which the following calculations are built up, equality of velocity of flow through the propeller disc, since by this means, due to the constancy of RPM, equal values of incidence and relative velocity on the blade element are assured, providing that the wall effect on the tangential component of the induced velocity can be neglected. This limitation can have no great significance, since considerations based on the stream theory are limited from the start to propellers under small loads. Now if we start, say, with a propeller in a tunnel having a very large cross section which can be regarded as unlimited, where the speed of advance v_e will also be considered as having been measured by means of a pitot tube, then this tube with decreasing cross section but unaltered velocity of flow through the propeller plane will give lower readings than in unlimited water, i.e. the speed of advance v_e in open water corresponding to the tunnel velocity v_0 is greater than v_0. In order to find the relation between v_e and v_0 we first set up the equations of the propeller in a cylindrical tube. In doing this the postulates of Glauert [44] who determined the relation between the velocity far in advance of a propeller operating in a tube and the corresponding undisturbed velocity are used extensively (symbols in Fig. 9). According to the continuity equation we have the relations:

$$(1a) \quad F_2 v_2 = F_3 v_3$$

$$(1b) \quad F_0 v_1 = (F_0 - F_2) v_0 + F_2 v_2$$

44) Elements of Aerofoil and Airscrew Theory, Cambridge, 1926, pp 222–226. See also Wood and Harris, Rep. and Memor., 662.

(1c) $F_0 v_1 = (F_0 - F_3) v_3 + F_2 v_2$

Applying Bernoulli's equation in the forward and rear portions of the propeller stream we get:

$$S = F_2 \cdot \Delta p_{Schr} = F_2 \left[\left(p_3 + \frac{\varrho}{2} v_3^2\right) - \left(p_1 + \frac{\varrho}{2} v_1^2\right) \right]$$

Outside the propeller stream we have:

$$p_1 + \frac{\varrho}{2} v_1^2 = p_3 + \frac{\varrho}{2} v_3'^2$$

and with this

$$(2)\ S = F_2 \left[\left(p_3 + \frac{\varrho}{2} v_3^2\right) - \left(p_3 + \frac{\varrho}{2} v_3'^2\right) \right] = F_2 \frac{\varrho}{2} (v_3^2 - v_3'^2)$$

The law of momentum for a control surface with vertical boundaries far in advance and far to the rear of the propeller and with the wall of the tube yields as the thrust:

$S = F_3 \rho v_3 (v_3 - v_1) + (F_0 - F_3) \rho v_3' (v_3' - v_1) + F_0 (p_3 - p_1)$ or

$$(3)\ S = F_3 \rho v_3 (v_3 - v_1) + (F_0 - F_3) \rho v_3' (v_3' - v_1) + F_0 \rho/2\ (v^2_1 - v_3'^2).$$

The load factor of the propeller which is determinable by test, is

$$c_s = \frac{S}{\frac{\rho}{2} F_2 v_0^2}$$

with which the two last equations become

$$(2)\ c_s v_0^2 = v_3^2 - v_3'^2$$

$$(3)\ c_s v_0^2 = 2 v_3 (v_3 - v_1) F_3/F_2 + 2 v_3' (v_3' - v_1)(F_0 - F_3)/F_2 + (v^2 - v_3'^2) F_0/F_2$$

v_3, v'_3 and v_1 are eliminated from (2) and (3) by means of equations (1), so that now only the measured value v_0 and the velocity of flow v_2 required for comparison with the open-water propeller occur as velocities. Making $f_1 = F_2/F_0$ and $f_2 = F_3/F_2$, equations (1) become:

$$(1a)\ v_3 = v_2/f_2$$
$$(1b)\ v_1 = (1 - f_1) v_0 + f_1 v_2$$
$$(1c)\ v'_3 = (1 - f_1) v_0/(1 - f_1 f_2)$$

Herewith the equations for the thrust, expressed in terms of v_0 and v_2, when in addition $k = v_0/v_e$ become

$$(2a)\quad c_s\, k^2 f_2^2 (1 - f_1 f_2)^2 = (v_2/v_e)^2 (1 - f_1 f_2)^2 - k^2 (1 - f_1)^2 f_2^2$$

and likewise, after a lengthy calculation:

$$(3a)\quad c_s\, k^2 f_2 (1 - f_1 f_2)^2 = (v_2/v_e)^2 (1 - f_1 f_2)^2 (2 - f_1 f_2)$$

$$- k^2 (1 - f_1)^2 f_1 f_2^3 - 2(v_2/v_e) k f_2 (1 - f_1 f_2)^2 (1 - f_1)$$

For the propeller operating in an unlimited cross section the thrust, according to the law of momentum, using the symbols in Fig. 9b, is

$S = F_2 \rho\, v_2\, 2\Delta$; since $\Delta = v_2 - v_e$, we have $S = 2F_2 \rho\, v_2 (v_2 - v_e)$ from which, after introducing the load factor c_s defined above, we get the relation $v_2^2 - v_2 v_e - c_s v_o^2/4 = 0$, or $v_2/v_e = 0.5(1 + \sqrt{1 + c_s k^2})$, with a positive sign before the root, since v_2 is greater than v_e. The velocity v_e of the propeller in open water, then, is to be so determined that v_2 will have the same value in both cases. The last equation, therefore, is the relation still missing in (2a) and (3a), with which it is possible with f_1 given to determine the load factor c_s and the appropriate correction k according to the choice of parameters f_2. The numerical calculation can be simplified considerably in this case also by Glauert's process, if we write the last equation in the form: $v_2/v_e = 0.5(1 + c)$, i.e., if we define c as

(4) $c^2 = 1 + c_s k^2$. With the expression for c_s following from this, (2a) and (3a) yield equations for the two new unknowns c and k, from which by (4) follows the corresponding c_s value; by a short calculation we get

$$(5)\quad k(1 - f_1) = (1 + c)(1 - f_1 f_2)/2f_2 + (1 - c)(1 - f_1 f_2)$$

$$(6)\quad (c + 1)/(c - 1) = f_2 (1 - f_1 f_2^2)^2/(1 - f_2)(1 - f_1 f_2)^2$$

Equation (6) determines the value c when f_1 is given and with a selected parameter f_2, equation (5) yields the corresponding correction k, and from (4) follows the corresponding c_s, so that it is possible to determine k as a function of c_s and f_1 from these three last equations. The following table and Fig. 10 give the results:

f_1	f_2	c_s	k	f_1	f_2	c_s	k
0,10	0,95	0,2598	0,9997	0,25	0,95	0,3078	0,9989
	0,90	0,6200	0,9984		0,90	0,7320	0,9949
	0,85	1,1466	0,9961		0,85	1,3494	0,9876
	0,80	1,9610	0,9922		0,80	2,3242	0,9747
0,15	0,95	0,2740	0,9994	0,30	0,95	0,3298	0,9981
	0,90	0,6530	0,9976		0,90	0,7788	0,9931
	0,85	1,2069	0,9938		0,86	1,2828	0,9856
	0,80	2,0682	0,9873		0,81	2,2243	0,9706
0,20	0,95	0,2901	0,9991	0,35	0,95	0,3530	0,9977
	0,90	0,6918	0,9961		0,90	0,8321	0,9911
	0,85	1,2743	0,9909		0,86	1,3705	0,9812
	0,82	1,7691	0,9858		0,82	2,1344	0,9668
	0,80	2,1888	0,9815				

As is to be expected, the velocity proper to equality of thrust is greater in the unlimited cross-section than the measured velocity of flow through the plane of the propeller in the tunnel, and increases with increasing ratio of the propeller area to the measuring cross-section and with increasing load factor. For values generally occurring the correction is of the order of magnitude of 1%, the smallness of which renders the simplifying basis of the stream theory acceptable, although it tends to yield an inadequate correction.

A check of this result was made by carrying out complete tests of the same propeller first under atmospheric pressure in the cavitation tank and then in the model basin, it being required here to maintain the same velocity in both cases in order to eliminate scale effects which might outweigh the wall effect. The difference still existent due to the state of turbulence of the fluid has a material effect only in the neighborhood of the maximum lift of a blade section [45], i.e. at very small slips which in this case have no great interest. The propeller used, the model of a screw for a high speed vessel, is characterized by the following data: d = 0.250 m (F_a = 491 cm²); F_a/F = 0.89; pitch H at 0.7 r_o = 0.260 m; the cross-section of the tunnel amounts to F_0 = 2,146 cm², the cross-section of the basin is about 35 m² and to be regarded as unlimited as compared to the propeller area. There were obtained the test points non-dimensionally plotted in Fig. 11 as thrust coefficient c_1 and torque coefficient c_2 over the speed ratio $\lambda_o = v_o/nD$, or as the case may be, $\lambda_e = v_e/nD$. For conversion of the data obtained in the tunnel from λ_o to λ_e the values there measured have been assembled in the following table, and tne correction k applied to v_o after calculating c_s, as in Fig. 10:

Measurements in Cav. Tank; v_o = 4.50 m/s; f_1 = 491/2146 = .229

λ_o	c_1	$c_s = 8c_1/\pi\lambda_o^2$	k Fig. 10	$\lambda_e = \lambda_o/k$
0,957	0,0775	0,215	0,999	0,958
0,902	0,108	0,336	0,999	0,903
0,846	0,136	0,485	0,998	0,848
0,804	0,160	0,630	0,996	0,807
0,788	0,168	0,690	0,996	0,791
0,753	0,184	0,827	0,994	0,757
0,717	0,205	1,003	0,993	0,722
0,698	0,217	1,136	0,991	0,705

The horizontal displacement of the measured points obtained in the cavitation tank occasioned by the correction brings the corrected values closer to those measured in the towing basin, which are all somewhat higher. For the usual c_s and f_1 values encountered the correction is, however, so slight, that, particularly after the

45) Millikan, Trans. Amer. Soc. Mechan. Eng. 56, 1934.

beginning of cavitation, it lies within the limits of test accuracy and therefore is practically insignificant (see p 49).

The usefulness of the pitot tube for measuring speed is limited by the cavitation possible around it, and it was therefore necessary to determine the lowest cavitation index below which the device records false readings in consequence of deformation by the layer of vapor. For this purpose the pressure drop already used in finding the performance factor between apertures 1 and 2 in the nozzle (Fig. 4) was used as a gauge for a comparison velocity unaffected by cavitation, and the static pressure at a constant velocity was lowered until differences between the two velocity readings occurred, which then are to be attributed to cavitation on the tube. The lowest cavitation index thus obtained at several tunnel velocities referred to the center of the shaft of the propeller model is on the average $\sigma = 0.37$, which is wholly adequate for the purposes of propeller tests.

β) Determining the Revolutions n (1/sec).

It is measured by means of a revolution counter installed at the end of the drive shaft of the propeller model (Fig. 12) which is started and stopped simultaneously with a stopwatch by touching a pushbutton. It has become the custom to count revolutions over the period of a minute, which assures revolutions per second within $\pm$ 0.2%. An electrical tachometer is used to obtain required revolutions. Its transmitter is connected with the propeller shaft by a V-belt, and the recording device is located on the switchboard near the rheostat for the Leonard drive of the propeller model.

γ) Determining Static Pressure p (kg/m^2).

The static pressure, according to a definition to be given later, is to be taken at the height of the shaft center of the propeller model, and is measured by a mercury manometer as the difference in pressures between an aperture in the tunnel at the height of the shaft center and the outer atmosphere. A water tank of sufficiently large surface and the same water level as the manometer at the point of connection is connected with the second arm of the manometer and obviates geodetic correction. The connecting aperture is placed at a point of sufficiently large cross-section at some distance in front of the propeller (plane F_1, Fig. 4), where the pressure is to be regarded as independent of the propeller stream [46]. If the connection were made in the measuring plane the pressure measured there would be dependent upon the propeller stream in the sense that the pressure reading with respect to a propeller at equal velocity and in unlimited cross-section will be too high by twice the amount of the per cent velocity correction. In order

46) Because of the low velocity prevailing in this plane no certain velocity measurement is possible here.

to avoid this correction, which under certain conditions may be considerable, and the effect of which together with the velocity correction would amount to at least four times [47] the effect of the latter on the quantity σ_o defined on p 32, the cross-section F_1 was chosen as the connecting plane and the assumed independence of thrust was proven by test, by the fact that the pressure reading on this manometer did not change when the thrust was changed, v_o being equal and the pressure in the connecting tube between the pump and the tunnel being constant. The pressure difference between this plane F_1 and the measuring plane F_0 then depends only on the velocity and is known from a single check measurement (Fig. 13, where the pressure difference $\Delta h_{1.0}$ between test stations 1 and 0, both at the center of the shaft, is given in mm Hg). With a pressure p_0 (kg/m²) at the center of the shaft in the measuring plane there then corresponds a Hg column in mm in the static manometer installed over aperture 1 of $h_1 = \frac{b_0 - p_0}{12.59} - \Delta h_{1.0}$, where b_0 represents the atmospheric pressure in kg/m².

An air pump connected with the dome of the tunnel generates the pressure in the test plane (Fig. 4). Pressure can better be regulated with this than with water columns, such as had been planned originally. A rotary pump with a slide valve of the Pfeiffer type with a maximum capacity of 15 m³/h was chosen, which is sufficiently robust to enable it to draw small quantities of condensed water on occasion without detriment to its efficiency. To regulate the vacuum the pump is kept running slowly with constant revolutions during the test, and the pressure is first roughly regulated by throttling cocks in the connecting pipe line and then accurately by a pinch-cock which admits atmospheric air into the water line through a rubber tube. In this method the pump always sucks some air, among which, in addition to the fresh air, there is air from the water of the tunnel highly saturated with water vapor, so that it is impossible to prevent the entrance of condensed water at times, in spite of the installation of drying and overflow tanks. By reversing the direction of rotation the pump acts as a compressor and therefore can also be used to generate the excess pressure required at higher velocities in order to obtain atmospheric pressure in the plane of measurement.

The connecting leads to the pressure as well as the velocity manometer are of glass in order to permit a constant check of the air content and thus avoidance of errors in readings. The connecting tubes of heavy rubber are very short. Furthermore the manometers are set so low that lifting the connecting lines and the consequent small pressures are prevented. The manometers proper are ordinary U-tube manometers with three-way cocks at the ends of the arms for filling or discretionary venting of the connecting tubes or manometer arms. Slides with

47) The error per cent in σ_o obtained when e is small with respect to p_o is $\frac{d\sigma_o}{\sigma_o} = -2\frac{dv_o}{v_o}\left(1 + \frac{p_o}{p_o - e}\right) = -4\frac{dv_o}{v_o}$, while with the chosen method it amounts to only $-2\, dv_o/v_o$.

crosshair index and mirror are used to read the Hg-column. These slide over a millimeter scale which permits readings of ± 0.1 mm.

δ) Determining the Temperature of the Water in the Tunnel t (°C) and the Vapor Pressure e (kg/m²).

It is necessary to know the temperature of the water to determine the vapor pressure. This is measured by means of a thermometer installed vacuum tight a short distance behind the grid. Calibration by comparison with a standard thermometer held completely immersed in the liquid in the plane of measurement gave as correction −0.6°C, independent of velocity and temperature.

The vapor pressure e (kg/m²) is plotted as a function of t in Fig. 14 with values taken from the book "Practical Physics" by Kohlrausch, 1923, p 770.

ε) Determining Torque M (mkg).

For this purpose a Bamag torsiondynamometer was found satisfactory (Fig. 12). An elastic rod 50 cm in length interchangeable according to the maximum moment was used as the test element. Its torsion is read by means of an oscilloscope, and gives upon calibration the transmitted moment in mkg. The test rods are carefully aged and even after prolonged use show no changes in their original calibration constants. It is necessary to make a correction governed by the no-load friction, in the torque reading, which at first, with a standard grease-filled stuffing box, was found to be very high and not constant. Based on experience with the self-propelled instruments used in ship model tests, the stuffing box was thereupon made to rotate (Fig. 12) by means of an auxiliary shaft, which was likewise driven by the drive motor of the model propeller, with a reduction of 1 to 1.05 as compared to the main shaft. At the same time a tube was pushed over the part of the propeller shaft which projected into the tunnel, up to the last shaft bearing. This tube was rigidly connected with the rotating inner part of the stuffing box, which greatly decreased the relative velocity and thus also the no-load friction of the drive shaft in the stuffing box as well as in the bearing. Watertightness is obtained by means of two grease stuffing boxes, one of which shuts off the propeller shaft from the hollow shaft and the other the hollow shaft and with it the rotating part of the stuffing box from the outer fixed part. By this arrangement, a sufficiently small no-load moment was attained, amounting to about 2% of the maximum moment and in addition constant in time, since the drive of the auxiliary shaft is taken up ahead of the torsion dynamometer and the moment required for it is not included in the measurement.

ζ) Determining the Thrust S (kg).

The propeller thrust is transmitted from the drive shaft by means of knife edges and thrust bearings to a beam-arm balance outside the tank having a beam

ratio of 1:4 (Fig. 12). A coupling permits the shaft to have an axial play of ± 4 mm. To determine the mean value of the force which alone has hitherto been of interest, the scale is balanced by hand by adding weights.

The sensitivity of the balance decreases with decreasing relative velocity between the shaft and the stuffing box, while on the other hand the no-load moment decreases herewith. The selected reducing ratio of 1 to 1.05 is adequate first to assure a sufficiently small and constant no-load moment, and second to permit, in addition, a thrust balance sensitivity to a weight change of 20 g, which at a mean load of about of about 8 kg, represents a sensitivity quite adequate for the present purpose. The loading of the scale must be corrected, in order to obtain the propeller thrust, by the force originating from the pressure difference between the outer atmosphere and the tunnel, and by which the thrust reading in the usual case of negative pressure in the test plane is too large. In addition to the pressure difference, this correction is dependent only upon the shaft diameter, and results automatically in the tests as a displacement of the thrust curve not yet affected at the prevailing negative pressure with respect to that measured at atmospheric pressure.

The foregoing sufficiently explains the methods and devices used in the tests. The question now is what values of pressure, velocity, revolutions and temperature should be chosen in a given case so that a test with a similar model will simulate the flow condition about a full-scale structure, i.e. so that forces will be measured which are in definite ratio to the full-scale object. The answer to this is given by the laws of similarity, which are next to be summarized.

IV. THE LAWS OF SIMILARITY AND THE CONCLUSIONS DRAWN FROM THEM.

It is a prerequisite of model tests that the model be geometrically similar. The number of laws of similarity then to be observed is governed by the number of physically different forces involved in the flow. In the case of flow with cavitation through a propeller there must be considered: Inertia forces, friction forces, gravity when the plane of the propeller is vertical, and capillary forces in the free surfaces after the inception of cavitation. Finally there is to be considered the relation derived on p 12, which indicates that the occurrence of similar cavitation conditions with geometrically similar sections is contingent upon the constancy of the cavitation index $\sigma = (p - e)/q_r$.

Comparing the forces of inertia leads to Newton's general law of similarity which in the case of phenomena about the propeller can be expressed in the form:

$$(1a)\quad S = c_1\ \rho\ n^2\ D^4 \qquad \text{or} \qquad (1b)\quad M = c_2\ \rho\ n^2\ D^5$$

where the non-dimensional coefficients c_1 and c_2, in consequence of the requisite similarity of the velocity triangles composed of speed of progression and tip

velocity are primarily functions only of the speed ratio $\lambda_e = v_e/Dn$. The occurrence of other kinds of force as well as the requirement that σ be constant causes the coefficients to be dependent upon additional parameters.

First the requirement that σ be constant, derived previously for the individual blade, will be applied to the sections at corresponding radii in the propeller aggregate, which will yield two specifications of basic importance to the tests. These can be most easily traced if we consider a propeller blade in vertical position upward. The static pressure for a blade section at the radius r is then $p = p_o - r\,\gamma - \Delta p$, and the dynamic pressure prevailing here is $q_r = \frac{\rho}{2} v_r^2$. Here p_o represents the static pressure at the center of the shaft (air + water column) at a great distance in front of the propeller, γ the specific gravity of the liquid, Δp the pressure decrease due to centrifugal force in the propeller stream, and v_r the relative velocity at the blade section. If the unapostrophied values refer to the model and the apostrophied ones to the full-scale structure the condition of equal cavitation indices for similar cross-sections at corresponding radii will read:

$$\frac{p_o - e}{q_r} - \frac{r\gamma + \Delta p}{q_r} = \frac{p_o' - e'}{q_r'} - \frac{r'\gamma' + \Delta p'}{q_r'}$$

This expression can be identically satisfied if we carry out the model test in such a manner that the two following equations exist:

(2) $(p_o - e)/q_r = (p_o' - e')/q_r'$

(3) $(r\gamma + \Delta p)/q_r = (r'\gamma' + \Delta p')/q_r'$

Now, observing the requirement of the general law of similarity that the two similar propellers be compared at the same speed ratio and under the assumption that any viscosity effect is negligible, the ratio of the relative velocity v_r to the speed of advance v_e and likewise $\Delta p/q_r$ is independent of the scale. Thus the conditions (2) and (3) become

(2a) $(p_o - e)/\frac{\rho}{2} v_e^2 = (p_o' - e')/\frac{\rho'}{2} v_e'^2$ or $\sigma_o = \sigma_o'$

(3a) $v_e/v_e' = \sqrt{r/r'} = 1/\sqrt{L}$,

if L represents the linear scale. These two equations indicate that if the static pressure p_o in the model test has been so determined that the cavitation indices referred to unaffected values of pressure and velocity are equal for a given point in the propeller and its model - the center of the shaft being selected as the point of reference for reasons of symmetry - as in equation (2a), then determination

of the speed of advance of the model according to (3a), i.e. according to Froude's law, will assure equal cavitation indices for all the remaining corresponding radii.

The foregoing considerations already take into account the effect of gravity on the model test, and it remains to express the requirements resulting from viscosity and surface tension. The dependence of the prevailing forces upon viscosity is expressed by Reynold's law which states that the coefficients defined by (1a) and (1b) are functions of the Reynold's number

(4) $R = v_e\, d/\nu$ ($\nu = \mu/\rho$ = kinematic viscosity; m^2/sec).

or in other words, that equal coefficients can be obtained for prototype and model only with equal Reynold's numbers. Analogously, the surface tension arising after inception of cavitation in the free surface between the liquid and the vapor zone which tends to decrease the curvature of the surface, requires Weber's number [48] to be constant for similar formation of the cavities.

(5) $W = v_e^2 d/\kappa$ ($\kappa = k/\rho$ = kinematic capillarity; m^2/sec).

Summarizing, these laws result in the following dependencies of the pressure p_o and the velocity v_e in the model tests upon the scale L:

1. The law of equal cavitation indices at corresponding radii requires:

a) According to (2a): $p_o = (\rho/\rho')(v_e/v_e')^2 (p_o' - e') + e$, where in addition

b) according to (3a): $v_e = v_e'/\sqrt{L}$

2. Reynold's law requires according to (4): $v_e = v_e'\, L\, \nu/\nu'$

3. Weber's law requires according to (5): $v_e = v_e'\, \sqrt{L}\, \sqrt{\kappa/\kappa'}$

It is impossible to satisfy the three requirements for the velocity in the model test simultaneously by controlling the material characteristics and in temperature variations, even if we assume a test liquid other than water. According to Weber [49] then, we have a case of approximate mechanical similarity where the question is which law of similarity is of predominant importance. First an attempt will be made to draw conclusions from the influence of the Reynold's number on the section characteristics regarding which sufficient data are available in the literature on the subject, reciprocating with Froude's law. If we first assume Froude's corresponding velocity Eq. (3a) as being the criterion, then, in the great majority of cases, Reynold's law, which must certainly be satisfied to the extent that all cross-sections will operate beyond the appropriate critical R-number, will no longer be sufficiently considered for the sections near the boss. Let us, for example, consider a three-bladed propeller model still further used in this connection, having the dimensions d = 0.2 m; $F_a/F = 0.56$; $H/D = 1.2$,

48) Weber, JSTG 1919

49) J.S.T.G. 1919, p 386

with elliptical blade surfaces and ogival section, whose corresponding Froude velocity is v_e = 3 m/sec, and let us seek the condition of flow of the various blade sections, whether it be below or above the critical point. In his paper "Scale Effect on Marine Propellers", Gutsche [50] on the basis of scale tests of single blades established charts for the various orders of flow velocity about ogival sections, which are already adapted for propellers of elliptical surface, and which give limit curves for the sub-critical, transitional, and super-critical zones, as functions of a Reynold's number R', the radius ratio r/r_o and a thickness ratio s_i/l_m. Here $R' = (nd^2/\nu)(l_m/d) = (v_e d/\lambda\nu)(l_m/d)$, where, however, the resultant velocity is perhaps taken in sufficiently close approximation as equal to nd in consideration of the fact that the limit curves are dependent upon the condition of turbulence of the outer stream. l_m/d represents the mean blade width ratio which, according to simple geometric relations is equal to $(F_a/F)\ (1.963/z)$. Further, s_i designates the section thickness extrapolated for the center of the shaft, which amounts to 0.05 d. In the case of the present propeller we get the numerical values l_m/d = 0.366, $s_i/l_m = \frac{s_i/d}{l_m/d}$ = 0.137 and $R' = 1.88 \cdot 10^5/\lambda$, where ν, in agreement with similarly conducted tests for t = 14.1°C was written as $1.17 \cdot 10^{-6}$ m²/sec, and with this the following radius ratios are found from the paper just mentioned, beyond which the propellers operate supercritically, depending upon λ:

λ	:	0.8	0.9	1.0	1.1
$r/10^5$	:	2.35	2.09	1.88	1.71
r/r_o	:	0.25	0.28	0.30	0.32

According to this the inner portions of the propeller still lie in the transition zone, and therefore in this case, when Froude's law is satisfied, we must accept a scale effect due to viscosity, which under certain conditions may become very considerable, as is evident from Gutsche's measurements of pressure distribution dependent upon the Reynold's number [51]. These show that the pressures in the subcritical zone, particularly in thick sections such as occur in the vicinity of the boss, amount to only about half of those in the supercritical zone over a large extent of the width of the blade but that the differences decrease directly with the thickness of the section. Accordingly the effect, even when the transitional zone extends farther than in the example as will usually be the case because of the small corresponding velocity, will be noticeable not so much in the thrust and torque, which are only small in the inner parts which are most affected, as in the external appearance of cavitation, and with it in the prognostication of the extent of erosion. In this connection it must also be considered that it

50) J.S.T.G. 1935

51) Reports of Preuss. Versuchsanstalt f. Wasserbau u. Schiffbau, No. 10.

is a peculiarity of the constant pitch propellers chiefly used in actual practice that cavitation sets in in the inner parts. In these propellers, the beginning of cavitation, if the corresponding velocity is low, will occur only at a greater angle of attack, i.e. a smaller λ, than is the case in a full-scale propeller, and will shift in the direction of higher λ when v_e increases but σ_o remains constant, until a v_e is attained at which the inner parts too operate supercritically. This is confirmed by subsequent tests (Fig. 16).

According to this, care must be exercised – less in consideration of the forces than similarity in form of the cavitation zone – that all sections will lie in the supercritical zone. This requirement can be satisfied, at the same time observing Froude's law (3a), by heating the water in the tunnel. An increase in temperature to 50°C will approximately double the Reynold's number at normal temperature in consequence of the decrease in ν, and in the case of our example all the sections will lie beyond the critical point. This solution, however, because of the difficulty of working with a heated tank as evidenced chiefly by high grease consumption in the packing and the consequent turbidity of the water, is not satisfactory, and therefore the question arises to what extent the propeller forces depend upon Froude's number, in order, if this dependence is slight, deviating from the requirement of equal local cavitation indices at corresponding sections and observing only Eq. (2a) $\sigma_o \quad \sigma_o'$, to arrive at a greater speed of advance v_e which will assure supercritical flow for all propellers at a normal water temperature.

In order to obtain the order of magnitude of this dependence, we consider the cavitation index and the force curve governed by it for a blade element on the radius r as a function of the turning angle, and strike the desired average of the force for the prototype and the model [52]. Here it can be assumed first that the model sections will operate beyond the critical point since now there is involved only the influence of unequal local σ, and second that with λ equal the derived induced velocities dependent upon the forces will not be materially altered by the effect under investigation. This again requires v_e/v_r and the centrifugal negative pressure $\Delta p/q_r$ to be approximately independent of the scale for equal λ. The last assumption, however, is justified only if the dependence of the propeller forces upon Froude's number is found to be small.

The cavitation index of the element under consideration at a turning angle of φ calculated clockwise from the upward vertical, using the designation on p 32 and with $r/r_o = x$, will be

$$\sigma = \frac{(p_o - r\gamma\cos\varphi - \Delta p) - e}{\frac{\varrho}{2} \cdot v_r^2} \left(\frac{v_e}{v_r}\right)^2 \left[\sigma_o - r_o \frac{2 g x \cos\varphi}{v_e^2}\right] - \frac{\Delta p}{q_r}$$

52) See Lerbs, WRH, 1934, No. 6.

Here σ_o again represents the cavitation index taken with respect to the shaft center and formed with the speed of advance of the propeller, which is brought into agreement in both cases by the pressure in the model test. If, as before, the apostrophied values refer to the full-scale model and taking into consideration the assumptions just mentioned and the speed ratio being equal, we will have

$$\sigma' = \left(\frac{v_e}{v_r}\right)^2 \left[\sigma_o - r_o \frac{2\,g\,x\cos\varphi}{v_e'^2}\right] - \frac{\Delta p}{q_r} \qquad \text{and}$$

$$\sigma = \left(\frac{v_e}{v_r}\right)^2 \left[\sigma_o - r_o \frac{2\,g\,x\cos\varphi}{v_e^2}\right] - \frac{\Delta p}{q_r}$$

For the sake of clearness in the following, the mean cavitation index and the fluctuation about this mean value are introduced. The mean value is found to be

$$\sigma'_m = \sigma_m = \left(\frac{v_e}{v_r}\right)^2 \sigma_o - \frac{\Delta p}{q_r} = \bar{\sigma}$$

and the amplitudes of the fluctuations are

$$(1)\quad \sigma'_1 = \left(\frac{v_e}{v_r}\right)^2 r'_o \frac{2\,g\,x}{v'^2_e} \quad \text{and} \quad \sigma_1 = \left(\frac{v_e}{v_r}\right)^2 r_o \frac{2\,g\,x}{v_e^2} \qquad \text{respectively.}$$

With these symbols we can write briefly

$$(2)\quad \begin{cases} \sigma' = \bar{\sigma} - \sigma'_1 \cos\varphi \\ \sigma = \bar{\sigma} - \sigma_1 \cos\varphi \end{cases}$$

In agreement with all the preceding, σ'_1 will be equal to σ_1, i.e. $\sigma' = \sigma$ for every r and φ when $r_o'/r_o = v_e'^2/v_e^2$ or when $v_e = v_e' \sqrt{r_o/r_o'}$ i.e. when Froude's law is fulfilled. Here we have to investigate the case that $v_e = n\, v_e' \sqrt{r_o/r_o'}$, where n generally is greater than unity. The relative course of the cavitation indices is easily noted with this number n if we form their differences $\sigma - \sigma' = \sigma_1 \cos\varphi\,(n^2-1)$. Since σ_1 is always positive, the model cavitation index for the usual case where $n > 1$ will be greater in the upper half of the propeller disc, and smaller in the lower half, than in the case of the full-scale propeller.

The estimation of the error in the load factor of a blade element caused by this difference in cavitation indices at any arbitrary speed of advance of the model will be made using a frictionless propeller as a basis. For this we get

$$(3)\quad c_{sr} = \frac{1}{\varrho/2\, v_e^2} \frac{dS}{dF} = (v_r / v_e)^2 \cdot c_a \cdot \cos\beta.$$

where β represents the angle of the resultant velocity with the propeller plane and the lift coefficient c_a is to be regarded as a function of σ. For this we

use the relation

$$(4)\quad c_a = \frac{\pi}{2}\,\alpha+\sigma$$

given by Betz and noted on p 13. This is used beyond its range of applicability for fully developed cavitation up to the uncertain conjunction with the range of lift coefficients independent of σ, which permits sufficiently accurate presentation of section test results for this purpose. In the independent zone the blade element is replaced by an ogival section, and accordingly we write: [53]

$$(5)\quad c_a = 2\pi(\alpha+2f/t).$$

The error with a mean load factor then depends essentially upon whether σ and σ' both remain either in the linearly rising or in the independent zone of c_a during a revolution, or whether a transition from one zone to the other occurs. Only in the latter case is the error in the mean value finite. In the former case it is always zero, independently of n. Two cases must be distinguished which lead to the maximum errors and which are characterized by Fig. 15a and 15b.

In the first case c_a just barely remains within the linear zone, while at the cavitation index σ^x (corresponding turning angle φ^x), c_a' passes into the independent zone. Accordingly, by using Eq. (2), (3) and (4) we have for the model:

$$c_{sr} = (v_r/v_e)^2 \cos\beta\,\left(\frac{\pi}{2}\,.\,\alpha+\bar{\sigma}-\sigma_1\,.\cos\varphi\right)$$

and the mean value for one revolution

$$\overline{c_{sr}} = (v_r/v_e)^2 \cos\beta\,\left(\frac{\pi}{2}\,.\,\alpha+\bar{\sigma}\right).$$

For the full scale structure the linear law is applicable from $\varphi = 0$ to φ^x and from $(2\pi - \varphi^x)$ to 2π, while the lift coefficient is constant between φ^x and $(2\pi - \varphi^x)$. Using the same equations and considering this c_a curve we get for the mean load factor of the full scale structure:

$$\overline{c_{sr}} = \left(\frac{v_r}{v_e}\right)^2 \cos\beta\left[\frac{\varphi^x}{\pi}\left(\bar{\sigma}+\frac{\pi}{2}\,\alpha\right)-\frac{\sin\varphi^x\,.\,\sigma_1'}{\pi}+\left(1-\frac{\varphi^x}{\pi}\right)c_a\right]$$

From these two last equations we now get the error in per cent of the mean value:

$$(6)\quad \frac{\overline{c'_{sr}}-\overline{c_{sr}}}{\overline{c_{sr}}} = \Delta c_a = \frac{\left(1-\frac{\varphi^x}{\pi}\right)\left(c_a-\bar{\sigma}-\frac{\pi}{2}\,\alpha\right)-n^2\,\sigma_1\,\frac{\sin\varphi^x}{\pi}}{\bar{\sigma}+\frac{\pi}{2}\,\alpha}$$

where $\sigma_1' = \sigma_1' n^2$ was written as in Eq. (1). In the equation c_a represents the expression according to (5) independent of σ, and further φ^x is determined as the turning angle at which the full scale structure attains the maximum cavitation index of the model, which according to (2) is found from the relation

53) See Hütte, 26th edition, p 401.

$\bar{\sigma} - \sigma_1' \cdot \cos\varphi^x = \bar{\sigma} + \sigma_1$, to be

$$(7)\quad \cos\varphi^x = -\sigma_1/\sigma_1' = -1/n^2;\ \sin\varphi^x = \sqrt{1-1/n^4}.$$

With a given section and the cavitation indices in the order here assumed $\bar{\sigma}$ and σ_1 are no longer independent of each other. Rather, according to Fig. 15a

$$(8)\quad \bar{\sigma} = \sigma^x - \sigma_1;$$

and in addition, σ^x can be expressed as abscissa of the point of intersection of the two postulates (4) and (5) in terms of section values:

$$(9)\quad \sigma^x = \frac{3\pi}{2}\alpha + 4\pi \cdot f/t$$

With Eq. (5), (8) and (9) we get from (6) as the ultimate value of the error per cent the expression

$$(10)\quad \Delta c_s = \frac{\sigma_1\left[\left(\frac{\varphi^x}{\pi} - 1\right) + n^2\frac{\sin\varphi^x}{\pi}\right]}{\sigma_1 - c_a}\ .$$

which for n = 1, i.e. when Froude's law is valid, becomes zero with $\sin\varphi^x = 0$, $\varphi^x = \pi$, according to Eq. (7).

In the second postulated case where the cavitation index follows the curve in Fig. 15b, which likewise leads to a maximum error, c_a is still barely in the constant zone, while on the other hand c'_a shifts to the linearly decreasing zone with σ^x. With the same postulates as above: $\overline{c_{sr}} = (v_r/v_e)^2 \cos\beta\ c_a$ and for $\overline{c'_{sr}}$ we obtain the same expression as in the first case considered, with the exception that now φ^x represents the angle at which the element of the full scale propeller attains the cavitation index σ_{min} : $\sigma - \sigma_1' \cdot \cos\varphi^x = \sigma - \sigma_1$, from which follows $\cos\varphi^x = \sigma_1/\sigma_1' = 1/n^2$. . The error per cent of the mean load factor now is:

$$\Delta c_s = \frac{\varphi^x\left(\frac{\pi}{2}\alpha + \bar{\sigma} - \sigma_1'\frac{\sin\varphi^x}{\varphi^x} - c_a\right)}{\pi \cdot c_a}\ .$$

which, by using (5), (8) and (9) becomes

$$(11)\quad \Delta c_s = \frac{\varphi^x\,\sigma_1\left(1 - n^2\frac{\sin\varphi^x}{\varphi^x}\right)}{\pi \cdot c_a}$$

The validity of the two equations (10) and (11) must be limited with decreasing c_a where the error becomes excessively large due to the neglected section drag.

With the value prevailing in the zone of greatest thrust $v_r/v_e = 3.0$ [54] in normal operating conditions for x = 0.7, and the customary model radius

54) By using the simple stream theory we get $(v_r/v_e)^2 = (\pi \cdot x/\lambda)^2 + (1 + c_s)$. from which we get the above value for $c_s = 0.5$; $\lambda/\pi = 0.25$. , the operating condition of a high speed propeller.

r_o = 0.1 m the amplitude σ_1 will be equal to 0.006 according to equation (1) when in addition v_e = 5 m/s is taken as the speed of advance in the tunnel. Let this velocity differ by double the value from the Froude velocity, i.e. let n = 2. With this the error per cent in the elementary load factor measured on the model assuming c_a = 0.4 will in the first instance be found to be -1.2% and in the second instance also -1.2%. The load factor of the blade element measured in the model test accordingly will be too high, when a higher speed of advance is chosen, to correspond to the Froude speed. The error for the entire propeller, however, is surely smaller than the amounts give, since the unfavorable cases considered may be valid for one of the blade elements, but will not occur for the aggregate. So long as we consider a frictionless propeller, the error in torque amounts to the same as the error in thrust, and from this we can conclude that deviations from the Froude speed for the propeller as a whole will be unnoticeable within the fluctuations connected with these tests, (see p 50) which is due essentially to the small value of the amplitude

According to these investigations it is safe, with respect to the propeller forces, to proceed to those higher speeds of advance at which all sections will lie in the supercritical zone. However, it is questionable whether with the differences now existing in the cavitation indices on corresponding radii there are connected discrepancies in the condition for the occurrence of cavitation on a single blade $\sigma = p'/q_r$ given on p 8 , which render prognostication of the zone of erosion just as impossible as the non-uniformity in pressures on the section caused by subcritical flow, which would then mean only shifting the difficulty from the section to the propeller stream. Although the mean values of the cavitation indices are the same on each radius for model and prototype since the condition $\sigma_o = \sigma_o'$ is satisfied by the pressure, the super-posed cosine function entails a difference in the sense that the model has greater σ-values in the upper half of the propeller and smaller ones in the lower half. The difference for r = 0 is likewise zero and increases with increasing radius (Eq. (1)) and (2). For example, with the numerical values of the example cited above, σ is equal to $\sigma_o/9.3$ when $\Delta p/q_r$ is neglected, and the amplitudes of the superposed cosine are 0.006 and 0.024 respectively in the full-scale propeller. While according to this the differences in σ around the parts near the boss which are important in the inception of cavitation in constant pitch propellers are only slight, important differences can occur in the outer parts (difference at blade tip: 0.024 - 0.006 = 0.018) since $\sigma_o/9.3$ is of the order of magnitude 0.1. On the other hand these difference are of the same order of magnitude as those that occur at the upper or lower tips of the model blade in vertical position (equal to 2 · 0.006 = 0.012), where, however, it was impossible to perceive by means of careful observation with the stroboscope any difference in the external aspects of the cavitation zone. This finding is important and justifies tne surmise that in the case of these

briefly superposed fluctuations, relatively small in comparison with the mean value, the mean value which is the same in both cases is the decisive factor, that is, that the liquid possesses a property which might be called "dynamic delay in boiling". However, no analogous findings or theories could be found in the literature on the subject, and our own investigations had to be limited to the scale measurements cited in the following.

It remains to elucidate the effect of Weber's Law, given on p 33 under 3, which leads to a velocity $v_e = v_e' \sqrt{L}\sqrt{\varkappa/\varkappa'}$ which can hardly be attained experimentally. As yet very few data regarding this are available, only, according to Ackeret's reports [55] it seems to be definitely proven that the capillary forces become significant only at an advanced stage of cavitation which is outside the present scope of interest. For that reason this law has been given no further consideration in the tests reported below.

To test these conclusions drawn from the laws of similarity some of which are based on highly simplifying assumptions, similarity tests were undertaken with the three-bladed propeller given as an example on p 33: d = 0.20; F_a/F = 0.56; H/D = 1.2 (elliptical contours, ogival sections), by varying the speed of advance and the water temperature. The results of these tests will be given here in this connection, before taking up analysis of the immediate test data. The tests were first carried out at normal water temperatures for v_e values of 3, 5, and 7 m/sec, in each case over an extensive range of the speed ratio, and in each speed series at cavitation indices σ_o = 1.9; 1.6; 1.3. In conjunction with this, the water in the tunnel was heated to 48.5°C average and the test repeated with the same cavitation indices as those just used for v_e = 5 m/sec. The following table gives the static pressure at the center of the shaft requisite for the velocity and temperature values at a given moment which corresponds to the intended σ_o value.

v_e (m/s)	3.0			5.0			7.0			5.0		
σ_o	1.9	1.6	1.3	1.9	1.6	1.3	1.9	1.6	1.3	1.9	1.6	1.3
t° C	13.4	14.4	14.5	13.2	13.5	14.0	11.0	12.6	14.6	49.0	48.4	48.2
e (kg/m³) Fig. 14	156	167	168	154	157	162	133	148	169	1196	1160	1150
p_o (kg/m²)	1028	902	765	2576	2197	1820	4882	4147	3418	3618	3200	2808

Let us now regard the speed of advance v_e = 3 m/sec in accordance with the statements on p 33 as the corresponding Froude velocity at which, particularly for higher speed ratios, considerable portions of the propeller are still in the transition zone, while for v_e = 7 m/s all sections are supercritical. According to scale measurements of single sections the speed ratio at which cavitation sets in must then shift, with increasing v_e and σ_o constant, to higher λ, as must also

55) Hydrom. Probleme d. Schiffsantriebes, 1932, p 230.

the zone in which cavitation first appears move inward, while the non-dimensional coefficients for thrust and torque obtained at the various speeds will evidence no material differences. In Fig. 16 the speed ratios for the beginning of suction-side cavitation are plotted as functions of a coefficient $E = v_e/\nu$, and in Fig. 17 c_1 and c_2 as functions of λ. First we see in Fig. 16 the expected shifting of the beginning of cavitation, and we find that with average area ratios and a diameter d = 0.2, a speed of advance of 5 m/s is adequate at a normal temperature to assure satisfactory observation of the zone of erosion. In the subsequently executed tests with smaller area ratios, v_e was increased to 5.5 m/s in order to offset the higher critical R number of the relatively thicker sections. In addition the measured points in Fig. 17 give no indication of a one-sided course with increasing v_e, and we must therefore assume that at normal temperature there is no influence of the Froude and Reynold's numbers within the limits of test accuracy. These numbers, it is true, cannot be separated now, but according to calculations and scale measurements with single sections both have the effect of slightly increasing the coefficients as v_e increases. The tests carried out at increased temperatures in contrast to those at normal temperature permit an increase in the R number with constant Froude number, and the result now is a slight increase in c_1 with a simultaneous increase in c_2, especially large for smaller values, which it was impossible to clear up, since at the low temperature only small inner portions of the propeller still lie in the zone of transition.

Aside from this discrepancy it is sufficient according to the tests as well as the reasoning, to carry out the model tests at a speed of advance which will result in supercritical flow about the propeller elements, and to arrange the pressure at the shaft center in such a manner that the condition $\sigma_o = \sigma_o'$ will be satisfied. Then the mean value of the cavitation index at each radius of the model will also be the same as in the prototype. Therefore Eq. (2a) on p 32 is to be regarded as the essential law of similarity. The independence of Froude's law expressed hereby also signifies an increase in test accuracy so far as the very low pressures connected with the relatively low Froude velocity may easily lead to the separation of air in the zones of low pressure, for the air dissolved in the water cannot always be wholly removed in spite of long de-aeration under very low pressure and low velocity of flow. The possible effect of this on the tests becomes the slighter the higher the pressure and the shorter the time during which the water flows through the zones of low pressure, i.e. the higher v_e becomes. [56]

V. RESULTS OF TESTS WITH SYSTEMATICALLY ALTERED MODEL PROPELLERS.

In order to obtain an idea of the dependence of cavitation characteristics

56) See Reinhardt, Zum Aehnlichkeitsgesetz für Hohlraumbildung, VDI.- Report 370, 1935.

upon the form parameters of a propeller, area, pitch and number of blades exclusive of the section, investigation of which is not relevant here, a series of three-bladed propellers with d = 0.20 m and symmetrical elliptical surfaces, constant pitch on the pressure side and ogival sections (Series B_3) within the limits: F_a/F = 0.42; 0.56; 0.70 and H/D = 0.8; 1.0; 1.2; and 1.4 was tested by the developed methods, and likewise the four-bladed series (B_4) within the limits F_a/F = 0.56; 0.70 and H/D = 0.8; 1.0; 1.2.

An easily worked white metal alloy was first used as material for the propellers. However, it was impossible to obtain reproducible results with this, and thrust and torque increased from test to test, all other conditions being equal. This gave rise to the surmise that the propellers became bent inelastically through the load in the sense of greater pitch, as was confirmed by subsequent measurements. Therefore it was impossible to avoid adopting bronze models. These were built by the method usually followed by the model basin. Radial lines were milled into the rough casting to the depth corresponding to the section and it was then cut down by hand, tested with a machine gauge, recut to the gauge marks and finally measured. By this method it is possible to attain an accuracy of section coordinates of $\pm$ 0.05 mm.

Tests were made with each propeller at a constant speed of advance of 5 m/sec and with constant pressure, thrust, and torque over a range of speed ratios sufficient for the purpose. Then the tests were repeated with an altered cavitation index graduated in intervals of .3 to .3. With the propellers with F_a/F = .42, v_o was raised to 5.5 m/sec for the reasons given above. In addition, by observation, the range of speed ratios was determined over which the propeller is in danger of erosion, viz., beginning and end of cavitation, and the exact condition at which the condensation impact passes into the liquid (fully developed cavitation). Before taking up the results of the tests, we shall first describe the external aspects of cavitation and the effects on the propeller forces connected therewith.

a) The Cavitation Picture and the Forces.

The various phases of the external aspects of the phenomenon of cavitation can best be followed by changing the speed ratio from large to small values at a constant cavitation index. With a large λ there is cavitation starting at the leading edge on the pressure side, an indication that the forward impact point is located on the leading edge of the suction side the extent of which increases with decreasing σ_o and increasing λ, and when sufficiently advanced leads to a deviation in thrust and torque from atmospheric values. With decreasing λ this pressure side cavitation, and with it the difference in thrust and torque, recede until the propeller in general operates entirely without cavitation (exceptions with small σ_o, see p 45), when the forces too will no longer differ from those measured under

atmospheric pressure. When the revolutions are further increased, the point arrives at which the thrust decrease at the blade tip and with it, the circulation about the tip vortex has become sufficiently large to introduce cavitation here, by which the contour of the propeller stream is rendered visible in sharp distinction against the outer flow and having the typical appearance of a vortex surface (Fig. 18). By the distribution of light and shadow in the photograph it is possible to recognize the wave-formed structure of the free surface in the direction of a vortex line, such as was investigated in detail in conjunction with a theory [57] published by Ackeret, in the boundary vortex of a single airfoil – Fig. 19 shows one of the possible wave formations. As a result of this investigation, the relation between the circulation about the vortex line, the section depth and wave height and length developed by Ackeret was satisfactorily confirmed. When this cavitation sets in in the tip vortices, the suction side still lies in homogeneous flow, which begins to cavitate only at smaller λ and, starting at about half-chord (shock-free entry) begins at the sections near the boss. With this a range of speed ratios is attained where the condensation impact lies upon the blade but the forces are not yet affected due to the slight importance of the immediately affected inner portions, and therefore erosion of the suction side can be expected without effect on the efficiency. Thrust and torque assume smaller values only when suction side cavitation has reached the stage shown in Fig. 20, when, since the condensation impact still lies upon the propeller blade, erosion and influencing of the forces occur simultaneously. In this connection it is a peculiarity of these B-series propellers that first the thrust and then at a somewhat smaller λ the torque also begins to deviate, i.e. that the efficiency likewise decreases with the decrease in forces and the transitory slight improvement in the L/D ratio of ogival sections does not become evident in an improvement in performance at positive angles of attack. This probably is due to the fact that when the conditions for an improvement in the L/D ratio in the outer portions which are essential to the generation of forces exist, the inner portions where cavitation begins but where a slight improvement in the L/D ratio on the whole does not become effective, operate with considerably poorer characteristics. – When the revolutions are further increased the condensation impact shifts towards the trailing edge and gradually entirely into the liquid, thus reaching the stage of fully developed cavitation and eliminating the possibility of erosion of the suction side. The only remaining effect of cavitation is a strong reduction of the propeller forces with rapidly growing decrease in the efficiency. Fig. 21 shows in extreme form the flow condition corresponding to this, where the blade is nearly covered by a vapor zone attached to it, bell-shaped in the photograph, and where now the condensation impact shifts widely from place to place. With this are connected corresponding fluctuations of thrust and torque.

57) Ing.-Archiv I, 1930, p 399.

b) Limits of Validity of the Earlier Series Tests and Limits of Corrosion.

The limits of validity of tests reported by Schaffran [58] for series B_2 and B_4 which were carried out in the open towing basin, i.e. under atmospheric pressure, are primarily determined for small λ-values by the speed ratio beginning with which the thrust assumes smaller values than measured under atmospheric pressure due to the influence of cavitation, since the slight difference in the speed ratio already mentioned between the effect on thrust and torque is always such that the beginning of the thrust deviation is connected with the greater speed ratio, and this is therefore to be taken as the limit of the previous systematic tests. These limit speed ratios appear within a series as functions of the three parameters H/D, F_a/F and σ_o, which, with respect to clear plotting, gives rise to the question whether there are concepts according to which the number of these parameters can be reduced. In order to obtain a law under simplified assumptions we revert to the lift of a single blade which we shall study first with cavitation developed and then in homogeneous flow. In the former case, according to Betz (p 13) $c_a = \frac{\pi}{2} \alpha + \sigma$; in the second we substitute for the section its midline, an arc with the curvature ratio f/t, and by means of known equations get $c_a = 2\pi(\alpha + f/t)$. Since we are dealing with a blade in the propeller aggregate at small loads, where the angles of attack in the field of operation are small, and since furthermore no quantitative data are required of the equations, it will be sufficient to consider only the case of $\alpha = 0$. Thus we find that beginning with the cavitation index $\sigma = 2\pi f/t$ the lift coefficient of the single blade and therewith also the propeller thrust are influenced. In the propeller aggregate the local cavitation index of the section has the relation $\sigma = \sigma_o \ (v_e/v_r)^2$ to σ_o when the negative pressure in the stream is neglected, where v_e/v_r depends also upon the thrust in addition to λ because of the accelerations, while the thrust within a series, as is known from the results of systematic tests, depends predominantly only upon H/D, and the much smaller dependence from F_a/F can be neglected. Accordingly it is proper to write $(v_e/v_r)^2 = \phi \ (\lambda, H/D)$. Since, furthermore, f/t is inversely proportional to the area ratio within a series, $f/t = \frac{\text{constant}}{F_a/F}$, we finally obtain from the relation for the single blade the following relation for the speed ratio at which deviation occurs: $\sigma_o \ \phi \ (\lambda, H/D) = \frac{\text{constant}}{F_a/F}$ or $\sigma_o F_a/F = \phi_1 \ (\lambda, H/D)$. With this information derived from known laws, according to which the product of σ_o and F_a/F determines the speed ratio at which there is a cavitation effect under small loads, the plotting of data and also the extent of the necessary measurements are greatly simplified. Figures 22a and b show the results when they are plotted, where it is evident that the test points satisfy the developed relation sufficiently closely. These charts can be used directly, for example with given

58) Schiffbau 1916.

values of λ, σ_o and H/D, to determine the area required to prevent cavitation within the F_a/F values investigated, where λ and H/D correspond approximately to the optimum propeller of the problem concerned which was interpolated according to earlier tests [59], both of which depend only to a negligible extent upon the area and can therefore be picked out with an approximate F_a/F value. Comparison of the two figures also shows that the required product $\sigma_o F_a/F$, other conditions being equal, is greater if we select a four-bladed propeller than for a three-bladed one. This can be explained by the fact that the sections of the four-bladed propeller with an equal total area have a greater thickness ratio than those of the three-bladed one, and that therefore a greater area ratio is needed to balance this.

For the sake of completeness the speed ratios at which torque begins to be affected are given in Fig 23a and 23b. These, as already mentioned, are somewhat smaller than the corresponding values for thrust. The chart in Fig. 23b can be checked with the trial run data of the BREMEN given on p 7 . With the values there given we get $\lambda_2' = \frac{v_s (1-w)}{nD} = 0.751$ when in addition the mean wake factor w measured on the model and corrected for the full-scale is taken as 0.15. On the other hand, with the shaft center at a depth of 6.5 m in accordance with the trial run conditions $\sigma_o = \frac{(10,330 + 6,500) - 200}{51 \times 1.025(14 \times .825)^2} = 2.38$, where the factor 1.025 takes into account the difference in density between fresh and salt water, and $\sigma_o F_a/F = 1.335$. With H/D = 1.04, Fig. 23b gives us for this: $\lambda_2' = 0.754$, which practically agrees with the trial run value.

From these curves we see that the thrusts and torques delivered as yet uninfluenced, other conditions being the same, increase directly with increasing surface, but the less so, the greater the area, so that we may assume a maximum limit of area beyond which cavitation is no longer materially postponed by increasing the area. This limit, which can be explained by increasing grid effect is found by extrapolation about at $F_a/F = 0.85$.

The atmospheric tests, the limits of whose validity are set in the direction of small speed ratios by the relations just cited, are likewise limited on the side of large λ-values due to cavitation on the pressure side by the fact that at small σ_o-values and large λ, face cavitation causes a difference in thrust and torque. These differences, however, are small in the zone of positive thrust unless back cavitation has already so far developed at the point of vanishing face cavitation that the atmospheric values do not occur, under certain conditions, in the entire range of λ. In Fig. 24a and 24b are given the σ_o-values for which the thrusts and torques measured under atmospheric pressure are just barely reached, while with smaller σ_o this no longer occurs. The interval $\Delta\sigma_o = 0.3$, adequate elsewhere, was not adequate to express these values. Instead, a series of tests at intervals of $\Delta\sigma_o = 0.1$, and some at 0.05 were instituted in

59) See Schmidt, Zusammenfassende Darstellung von Schraubenversuchen, VDI-Pub.Co., 1926.

the vicinity of the surmised point of contact, and from these the actual point of contact was interpolated.

A propeller whose area satisfies the boundary curves of Fig. 22, just barely misses being affected in its power turnover but it will no longer operate free of erosion. The erosionless stretch of the suction side is governed by the speed ratios prevailing when suction side cavitation begins and the condensation impact has just shifted wholly into the liquid, and the erosionless condition of the pressure side by speed ratios which are smaller than those corresponding to the point of vanishing pressure side cavitation. These observations also have been plotted in Fig. 25–27 as functions of the variable $\sigma_o F_a/F$, which is useful also for this even though the scattering of the points is greater, due to the uncertainty of visual observation, than in Fig. 22 and 23, which resulted from tests. Furthermore slight irregularities in the surface can have a sharp influence on the observed results, and it was possible to obtain satisfactory results only after the most careful workmanship.

In Fig. 25 another curve is plotted as a dotted line, which combines th points of intersection of corresponding curves of beginning back and vanishing face cavitation with each other. To the left of this cross–curve, therefore, back cavitation begins while there is still cavitation on the face, while back cavitation occurs only for condition points to the right of the curve.

In comparing the curves of Fig. 22 with Fig. 25 it is obvious that the beginning of the effect on thrust is generally connected with smaller speed ratios than the beginning of suction side cavitation, but that for large pitch ratios the curves intersect, and that thrust then decreases before cavitation is fully developed on the suction side. These zones in which performance is affected without erosion, are shown by cross–hatching in Fig. 22. At first it seems unreasonable that the properties of the propeller should change without a change in flow about the section, but it is evident from the figures that this condition does occur with large H/D and small λ, i.e. at large thrusts and accompanying violent tip vortices. As a result of their great circulation, these rapidly assume the form of cavitation and in the condition of diminishing thrust are so far advanced that the tips of the propeller blades are completely enveloped and the extreme portions contribute only slightly to the thrust. In Fig. 20 and 28 the tip vortex for propeller B_2: $F_a/F = 0.70$, $H/D = 1.4$, is shown in the condition in which thrust begins to be affected, viz., in Fig. 20 for $\sigma_o F_a/F = .70$, $\lambda = 1.070$ where back cavitation is already developed and in Fig. 28 for $\sigma_o F_a/F = 1.333$; $\lambda = 0.906$, where as yet no cavitation has occurred on the back. The difference in the extent of the cavitating zone in the boundary vortex is plainly recognizable.

c) Results of Thrust and Torque Measurements in the Cavitating Zone.

As an example of the analysis of these tests, Propeller B_2 – $H/D = 1.4$,

$F_a/F = 0.56$ has been selected, which was tested at $v_o = 5$ m/sec, and in addition to tests at atmospheric pressure, was tested at cavitation indices $\sigma_o = 2.2$ to .7 at intervals of .3. The following table shows first the pressure column required in the static manometer for each σ_o taking into account the water temperature t and air pressure b_o, which, according to p 29 is

$$h_1 = \frac{b_o - p_o}{12.59} - \Delta h_{1,o} \text{ with } p_o = \sigma_o \frac{\varrho}{2} v_o^2 + e$$

when for the time being the difference between v_o and v_e is disregarded.

σ_o	t °Cels	e kg/m²	$\sigma_o \frac{\varrho}{2} v_o^2$ kg/m²	p_o kg/m²	b_o mm Hg	b_o kg/m²	$\frac{b_o - p_o}{12.59}$ mm Hg	(Fig. 13) $\Delta h_{1,e}$ mm Hg	h_1 mm Hg
2,2	24,0	304	2805	3109	766,6	10423	580,7	97,2	483,5
1,9	24,2	308	2423	2731	"	"	610,7	"	513,5
1,6	24,5	314	2040	2354	"	"	640,6	"	543,4
1,3	24,9	320	1658	1978	766,5	10421	670,3	"	573,1
1,0	24,2	308	1275	1583	767,2	10431	702,4	"	605,2
0.7	24,8	319	893	1212	"	"	731,9	"	634,7

In testing under atmospheric pressure at the shaft center of the propeller plane the pressure difference $\Delta h_{1:0}$ is to be set as positive on the manometer.

With these pressures, first always under the assumption that v_o and v_e do not differ from each other, the following thrust and torque values are obtained as functions of the speed ratio $\lambda_o = v_o/nD$ which are plotted in Fig. 29 nondimensionally and as c_1 and c_2.

$v_o = 5{,}0$ m/sec; $h_{st} = (v_o/0{,}508)^2 = 96{,}9$ mm Hg; $d = 0{,}20$ m.

Atmospheric pressure

N U/M	λ_o	S/4 kg	S kg	M Sk.-T.	Leerr. Sk.-T.	M Sk.-T.	M mkg	c_1	$10 \cdot c_2$
1053	1,424	0,16	0,64	12,0	1,4	10,6	0,156	0,0127	0,1551
1104	1,358	0,76	3,04	17,2	"	15,8	0,232	0,0550	0,2100
1193	1,256	1,64	6,56	26,6	"	25,2	0,370	0,1016	0,2868
1258	1,192	2,30	9.20	34,2	"	32,8	0,482	0,1280	0,3358
1337	1,122	3,22	12,88	44,5	"	43,1	0,634	0,1588	0,3910
1404	1,068	4,04	16,16	54,4	"	53,0	0,779	0,1806	0,4358
1463	1,025	4,86	19,44	63,3	"	61,9	0,910	0,2002	0,4688
1541	0,974	6,04	24,16	75,4	"	74,0	1,088	0,2239	0,5052
1603	0,936	7,04	28,16	86,2	"	84,8	1,247	0,2412	0,5350
1677	0,895	8.28	33,12	101,4	"	100.0	1,470	0,2597	0,5764

σ_0 = 2,2. ΔS = 0,66 kg.

N U/M	λ_0	(S/4) kg	S/4 kg	S kg	M Sk.-T.	Leerr. Sk.-T.	M Sk.-T.	M mkg	c_1	$10 . c_2$
1147	1,308	1,79	1,13	4,52	21,5	1,4	20,1	0,296	0,0758	0,2482
1227	1,222	2,64	1,98	7,92	30,5	"	29,1	0,428	0,1160	0,3134
1303	1,151	3,45	2,79	11,16	40,2	"	38,8	0,571	0,1450	0,3710
1377	1,089	4,49	3,83	15,32	50,4	"	49,0	0,721	0,1782	0,4192
1455	1,031	5,44	4,78	19,12	61,6	"	60,2	0,886	0,1992	0,4615
1542	0,973	6,71	6,05	24,20	75,9	"	74,5	1,096	0,2242	0,5084
1625	0,923	8,02	7,36	29,44	90,9	"	89,5	1,317	0,2458	0,5500
1488	1,008	5,93	5,27	21,08	66,9	"	65,5	0,964	0,2098	0,4800
1603	0,936	7,67	7,01	28,04	86,6	"	85,2	1,253	0,2408	0,5382
1661	0,903	8,58	7,92	31,68	96,8	"	95,4	1,403	0,2530	0,5680
1685	0,890	8,84	8,18	32,72	101,4	"	100,0	1,471	0,2542	0,5718

σ_0 = 1,9. ΔS = 0,71 kg.

N U/M	λ_0	(S/4) kg	S/4 kg	S kg	M Sk.-T.	Leerr. Sk.-T.	M Sk.-T.	M mkg	c_1	$10 . c_2$
1091	1,374	1,34	0,63	2,52	15,9	1,4	14,5	0,214	0,0466	0,1978
1164	1,289	2,02	1,31	5,24	23,4	"	22,0	0,324	0,0853	0,2638
1250	1,200	2,89	2,18	8,72	33,4	"	32,0	0,471	0,1230	0,3320
1324	1,133	3,73	3,02	12,08	42,6	"	41,2	0,606	0,1520	0,3812
1420	1,056	4,96	4,25	17,00	56,6	"	55,2	0,812	0,1859	0,4445
1487	1,009	6,07	5,36	21,44	67,8	"	66,4	0,976	0,2138	0,4872
1551	0,967	6,87	6,16	24,64	77,6	"	76,2	1,121	0,2258	0,5142
1634	0,918	8,04	7,33	29,32	92,4	"	91,0	1,337	0,2423	0,5520
1701	0,882	8,39	7,68	30,72	100,2	"	98,8	1,452	0,2342	0,5538
1455	1,031	5,48	4,77	19,08	62,0	"	60,6	0,891	0,1987	0,4640
1537	0,976	6,64	5,93	23,72	75,2	"	73,8	1,086	0,2214	0,5068
1576	0,952	7,30	6,59	26,36	81,9	"	80,5	1,184	0,2338	0,5255
1603	0,936	7,70	6,99	27,96	86,6	"	85,2	1,253	0,2400	0,5378
1670	0,898	8,24	7,53	30,12	96,9	"	95,5	1,404	0,2382	0,5551

σ_0 = 1,6. ΔS = 0,75 kg.

N U/M	λ_0	(S/4) kg	S/4 kg	S kg	M Sk.-T.	Leerr. Sk.-T.	M Sk.-T.	M mkg	c_1	$10 . c_2$
1047	1,432	1,00	0,25	1,00	11,7	1,4	10,3	0,152	0,0201	0,1528
1139	1,317	1,79	1,04	4,16	20,8	"	19,4	0,286	0,0708	0,2430
1234	1,216	2,80	2,05	8,20	31,5	"	30,1	0,443	0,1187	0,3210
1307	1,148	3,59	2,84	11,36	40,4	"	39,0	0,573	0,1466	0,3692
1386	1,082	4,58	3,83	15,32	51,4	"	50,0	0,736	0,1758	0,4218
1471	1,020	5,73	4,98	19,92	64,4	"	63,0	0,926	0,2028	0,4722
1546	0,970	6,82	6,07	24,28	76,3	"	74,9	1,102	0,2239	0,5080
1629	0,921	7,45	6,70	26,80	86,5	"	85,1	1,251	0,2228	0,5204
1693	0,886	7,71	6,96	27,84	91,2	"	89,8	1,330	0,2142	0,5082
1581	0,949	7,29	6,54	26,16	81,1	"	79,7	1,171	0,2308	0,5170
1517	0,989	6,41	5,66	22,64	71,9	"	70,5	1,037	0,2170	0,4970
1663	0,902	7,64	6,89	27,56	89,0	"	87,6	1,289	0,2198	0,5138

σ_0 = 1,3. ΔS = 0,79 kg.

N U/M	λ_0	(S/4) kg	S/4 kg	S kg	M Sk.-T.	Leerr. Sk.-T.	M Sk.-T.	M mkg	c_1	$10 . c_2$
1073	1,398	1,28	0,49	1,96	14,2	1,6	12,6	0,185	0,0376	0,1772
1171	1,281	2,16	1,37	5,48	24,4	"	22,8	0,335	0,0881	0,2692
1239	1,211	2,89	2,10	8,40	32,1	"	30,5	0,448	0,1206	0,3220
1310	1,145	3,65	2,86	11,44	41,2	"	39,6	0,582	0,1470	0,3740
1379	1,088	4,53	3,74	14,96	50,5	"	48,9	0,719	0,1736	0,4172
1455	1,031	5,44	4,65	18,60	62,0	"	60,4	0,888	0,1937	0,4628
1520	0,987	6,02	5,23	20,92	69,7	"	68,1	1,001	0,1997	0,4778
1601	0,937	6,22	5,43	21,72	74,8	"	73,2	1,076	0,1868	0,4630
1689	0,888	6,45	5,66	22,64	80,6	"	79,0	1,161	0,1752	0,4489
1434	1,046	5,27	4,48	17,92	58,9	"	57,3	0,843	0,1924	0,4520
1484	1,011	5,73	4,94	19,76	65,8	"	64,2	0,944	0,1978	0,4728
1559	0,962	6,19	5,40	21,60	72,8	"	71,2	1,047	0,1960	0,4760

σ_o = 1,0. ΔS = 0,83 kg.

N U/M	λ_o	(S/4) kg	S/4 kg	S kg	M Sk.-T.	Leerr. Sk.-T.	M Sk.-T.	M mkg	c_1	10 . c_2
1144	1,311	1,94	1,11	4,44	21,2	1,6	19,6	0,288	0,0748	0,2428
1216	1,234	2,67	1,84	7,36	29,5	"	27,9	0,410	0,1098	0,3060
1295	1,158	3,49	2,66	10,64	39,9	"	38,3	0,563	0,1399	0,3704
1384	1,084	4,15	3,32	13,28	48,9	"	47,3	0,696	0,1528	0,4008
1545	0,971	4,56	3,73	14,92	57,5	"	55,9	0,822	0,1377	0,3800
1594	0,941	4,67	3,84	15,36	58,5	"	56,9	0,837	0,1334	0,3632
1691	0,887	4,98	4,15	16,60	63,4	"	61,8	0,909	0,1280	0,3506
1271	1,180	3,27	2,44	9,76	36,3	"	34,7	0,510	0,1332	0,3480
1336	1,123	3,80	2,97	11,88	44,2	"	42,6	0,626	0,1467	0,3868
1452	1,033	4,37	3,54	14,16	53,1	"	51,5	0,758	0,1482	0,3962

σ_o = 0,7. ΔS = 0,87 kg.

N U/M	λ_o	(S/4) kg	S/4 kg	S kg	M Sk.-T.	Leerr. Sk.-T.	M Sk.-T.	M mkg	c_1	10 . c_2
1085	1,382	1,07	0,20	0,80	10,8	1,6	9,2	0,135	0,0150	0,1265
1171	1,281	1,65	0,78	3,12	19,8	"	18,2	0,268	0,0502	0,2156
1235	1,215	2,22	1,35	5,40	26,4	"	24,8	0,365	0,0781	0,2638
1304	1,150	2,68	1,81	7,24	31,8	"	30,2	0,444	0,0939	0,2882
1385	1,083	2,82	1,95	7,80	35,5	"	33,9	0,499	0,0897	0,2868
1471	1,020	3,03	2,16	8,64	38,2	"	36,6	0,538	0,0881	0,2742
1561	0,961	3,08	2,21	8,84	42,0	"	40,4	0,594	0,0800	0,2688
1659	0,904	3,31	2,44	9,76	45,1	"	43,5	0,640	0,0782	0,2564

It is further to be noted that the calibration constant of the torsion dynamometer amounted to 68 (mkg = Sk.T/68), and that the number ΔS represents the thrust increase caused by the difference in pressure between atmosphere and tunnel, which, deducted from the figures in column (S/4) gives the true thrust. Furthermore, the no-load friction is the mean value of a calibration before and after each test series, which was accepted only when the two no load torques coincided within the fluctuations that amount to a few tenths on the scale. Within this limit of fluctuation no dependence of the no load friction on the revolutions could be established.

The circumstance that the "free" velocity v_e, dependent upon the load factor and the section ratio differs from v_o brings about a double effect upon the curves σ_o = constant; first, since $v_e > v_o$, a test point shifts horizontally towards a greater λ, and further σ_o is no longer constant on one curve, but decreases the more from the given number the higher the load factor. Strictly speaking it is therefore requisite to repeat the tests first carried out on the assumption that $v_o = v_e$, by so adjusting the pressure and velocity from RPM to RPM with the load factors of the first test series that the tunnel velocity suitable for v_e = 5 m/sec and the static pressure required for the momentarily prevailing σ_o at this velocity will exist. This has been carried out for σ_o = 1.3 with the correction factor k determined in Fig. 30 from Fig. 10 for F/F_o = 314/2146 = 0.146. The test points thus obtained and plotted in Fig 30 show no systematic difference as compared to the first test, which is understandable in view of the smallness of the correction which at the highest load factor encountered amounts to 0.998.

Within the limits of the lightly loaded series B_2 and B_4 in which the propeller taken as an example belongs, among those having the greatest pitch ratio and therefore the greatest load factors, it is accordingly permissible to take v_o and v_e as equal to each other.

To judge of the accuracy of the force measurements which represent mean values of fluctuating quantities, thrust readings were made self-recording temporarily, a residual force remaining after the placing of the weight being taken up by a spring, the extension of which was recorded on a revolving drum. The per cent value of the mean fluctuation in thrust with respect to the mean force is approximately constant at atmospheric pressure, and otherwise increases according to the following table with decreasing values of σ_o and λ. It attains higher values after the condensation impact has gone into the liquid, where corresponding fluctuations in the forces are connected with its local fluctuations.

	λ: 1.057	0.882	0.750
Atm.-Druck	$\pm$ 0.4	+ 0.3	+ 0.4
σ_o = 1.9		$\pm$ 0.3	+ 0.5
σ_o = 1.3		$\pm$ 0.5	$\pm$ 0.8

With a view to simple application of the data which exist in a series of curves c_1 and c_2 as functions of λ and σ_o, the question arises whether this multiplicity of curves can be reduced under a definite assumption, so that the final result will be presented in a clear form. After several vain attempts, it was found possible, at least for the curves which touch upon those measured at atmospheric pressure, i.e. precisely for those cases exclusively available for practical use, to plot them in readable form, in which the ratio of $c_{1.0}$ to c_1, formed at a given speed ratio, where $c_{1.0}$ signifies the coefficient measured at σ_o and c_1 at atmospheric pressure, are considered as functions of the ratio λ/λ_1', where λ_1' is the speed ratio at which a change in thrust begins (Fig. 22). We get for the relative drop in c_1 and likewise c_2, where the abscissa is to be taken with respect to λ_2', the two curves shown in Fig. 32, with the surprising result that within a series these curves are first independent of σ_o, F_a/F and H/D, and furthermore do not change in going over to Series B_4. The numerous test series available scatter about the two mean curves with the exception of isolated points within ranges indicated by cross-hatching in the figure. This scattering, however, which increases as λ/λ' decreases, is to be attributed more to test inaccuracy than to the method of plotting, since there is no systematic course recognizable in the individual series. As proof to what extent it is possible to reconstruct the tests by means of these two curves and the values λ_1' or λ_2' respectively in Fig. 22 and 23, the thrust and torque coefficients thus obtained were plotted in Fig. 17, 29, and 31 which contain direct test data, and comparison shows that the tests are reproduced with sufficient accuracy for both series. It

is to be noted that it was not possible to find an adequate theoretical basis for this method of plotting, which probably is valid only for small loads, and that therefore it has merely the value of a working hypothesis useful only within the limits of the material available herein.

The loss in efficiency from that at atmospheric pressure and equal λ is found from $\eta_0/\eta = \frac{c_{\lambda 0}/c_1}{c_{\lambda 0}/c_2}$ and can therefore also be expressed by means of the two curves in Fig 32 and represented by the dotted curve there plotted. This curve at first drops only slightly, and beginning at about $\lambda/\lambda' = 0.8$, which coincides approximately with the condition of fully developed cavitation, rapidly decreases in correspondence with the great increase in ε which then begins.

The curves of relative decrease in thrust and torque lose their significance for σ_0 values at which the atmospheric value are no longer attained, i.e. for lower σ_0 values than those given in Fig. 24, since now the quantities λ_1' or λ_2' as the case may be, can no longer be determined. The coefficients measured under these conditions are contained in the following tables, where the choice of the smallest σ_0 value was limited by the possibility of practical usefulness.

Serie B_2.

$F_a/F=0{,}56$; $H/D=1{,}4$. $\sigma_0=0{,}7$.			$F_a/F=0{,}56$; $H/D=1{,}2$. $\sigma_0=0{,}7$.			$F_a/F=0.56$; $H/D=1{,}0$. $\sigma_0=0{,}7$.		
λ	c_1	$10 \cdot c_2$	λ	c_1	$10 \cdot c_2$	λ	c_1	$10 \cdot c_2$
1,382	0,015	0,127	1,193	—0,008	0,066	0,960	0,028	0,096
1,281	0,050	0,216	1,105	0,046	0,159	0,905	0,049	0,126
1,215	0,078	0,264	1,026	0,068	0,203	0,855	0,055	0,134
1,150	0,094	0,288	0,974	0,075	0,207	0,804	0,061	0,135
1,083	0,090	0,287	0,915	0,077	0,199	0,768	0,063	0,138
1,020	0,088	0,274	0,858	0,075	0,186	0,728	0,063	0,130
0,961	0,080	0,269	0,812	0,076	0,180	0,696	0,056	0,121
0,904	0,078	0,256	0,769	0,062	0,161	0,642	0,050	0,110

Serie B_4.

$F_a/F=0.56$; $H/D=1{,}2$. $\sigma_0=1{,}0$.			$F_a/F=0.56$; $H/D=1{,}0$. $\sigma_0=1{,}3$.			$F_a/F=0{,}56$; $H/D=0{,}8$. $\sigma_0=1{,}9$.		
λ	c_1	$10 \cdot c_2$	λ	c_1	$10 \cdot c_2$	λ	c_1	$10 \cdot c_2$
1,205	0.020	0.114	0,961	0,027	0,117	0,792	0,026	0,083
1,079	0.066	0,187	0,916	0.045	0,143	0,744	0.045	0,108
1,023	0.086	0,214	0,872	0,055	0,160	0.710	0,056	0,126
0,967	0.092	0,225	0,831	0,063	0,169	0,685	0,061	0,131
0,917	0,090	0.228	0,792	0.062	0,167	0,654	0,064	0,138
0.874	0,080	0,217	0,759	0.061	0,163	0.635	0.067	0,133
			0,737	0.059	0,159	0,610	0,064	0,130
			0,709	0,052	0,160	0,591	0,063	0,126
			0,686	0,049	0,154			

$F_a/F=0,56$; $H/D=0,8$. $\sigma_0=1,6$.			$F_a/F=0,70$; $H/D=1,2$. $\sigma_0=1,0$.			$F_a/F=0,70$; $H/D=1,2$. $\sigma_0=0,7$.		
λ	c_1	$10 \cdot c_2$	λ	c_1	$10 \cdot c_2$	λ	c_1	$10 \cdot c_2$
0,797	0,006	0,058	1,206	0,026	0,145	1,045	0,021	0,120
0,746	0,028	0,079	1,114	0,081	0,219	0,949	0,048	0,176
0,704	0,040	0,101	1,036	0,116	0,279	0,872	0,066	0,178
0,665	0,044	0,112	0,970	0,127	0,309	0,811	0,050	0,171
0,637	0,046	0,110	0,930	0,126	0,321			
0,615	0,042	0,105	0,889	0,123	0,313			
0,614	0,045	0,111	0,838	0,115	0,301			
			0,789	0,100	0,279			

$F_a/F=0,70$; $H/D=1,0$. $\sigma_0=1,0$.			$F_a/F=0,70$; $H/D=0,8$. $\sigma_0=1,3$.		
λ	c_1	$10 \cdot c_2$	λ	c_1	$10 \cdot c_2$
0,959	0,023	0,098	0,824	—0,005	0,032
0,903	0,052	0,142	0,779	0,015	0,059
0,855	0,065	0,168	0,735	0,033	0,083
0,808	0,066	0,170	0,704	0,043	0,105
0,776	0,064	0,178	0,681	0,046	0,109
0,770	0,066	0,179	0,666	0,049	0,117
0,735	0,062	0,177	0,645	0,048	0,118
0,722	0,065	0,179	0,639	0,047	0,116
0,706	0,060	0,179	0,614	0,049	0,118
0,691	0,059	0,172	0,590	0,044	0,117
			0,568	0,044	0,114

With these data and Fig. 32 together with Fig. 22 and 23 the thrust and torque measurements carried out in the cavitation zone with Series B_2 and B_4 are presented in brief but none the less complete form. Report of the values obtained at atmospheric pressure is rendered unnecessary since these can be derived from Schaffran's well known tests, which, with the exception of slight differences explainable by scale effect, were confirmed by the water tunnel tests.

The series tests carried out have the disadvantage of all tests with a group of models which are varied according to geometrical viewpoints, i.e. that only conclusions within the limits of the varied form parameters can be drawn. Farther-reaching results are obtained if the variation is made according to physical viewpoints and if we ask, in our case, what thrust distribution goes with the greatest possible security against the occurrence of cavitation. The results thus obtained are then restricted only to the limits of the special assumption for the thrust distribution, but even with the simplest assumptions are more inclusive than the conclusions from propeller tests which differ among themselves only through geometrical variations.

VI. THRUST DISTRIBUTION WITH GREATEST POSSIBLE SECURITY FROM CAVITATION.

To answer this question we shall consider a propeller with an infinite number of blades, which, in the fully developed propeller stream produces the induced velocity components w_a in axial and w_t in tangential direction. To a circular element dr on the radius r there will then belong, under the assumption that friction is of no importance in the production of forces, and according to the laws of momentum, the thrust element

(1) $dS_\infty = 2r\pi\rho\,(v_e+w_a)\,w_a\,.\,dr - (p_o-p)\,2r\pi\,.\,dr$

and the element of torque

(2) $dM_\infty = dT_\infty\,.\,r = 2r^2\pi\rho\,(v_e+w_a)\,w_t\,.\,dr,$ where the radial pressure difference, due to centrifugal force, stands in the following relation with w_t:

(3) $(p_o-p) = \varrho \int_r^{r_o} \frac{w_t^2}{r}\,dr$

For greater clearness these three equations are written non-dimensionally with $x = r/r_o$ and $q_e = \rho/2\, v_e^2$, as the elementary load and torque factor

$$(1a)\quad dc_{s\infty} = \frac{dS_\infty}{\frac{\varrho}{2} r_o^2 \pi v_e^2} = 4\left(1 + \frac{w_a}{v_e}\right)\frac{w_a}{v_e}\,x\,dx - 2\frac{p_o - p}{q_e}\,x\,dx$$

$$(2a)\quad dc_{d\infty} = \frac{dM_\infty}{\frac{\varrho}{2} r_o^3 \pi v_e^2 r_o} = 4\left(1 + \frac{w_a}{v_e}\right)\frac{w_t}{v_e}\,x^2\,dx$$

$$(3a)\quad \frac{p_o - p}{q_e} = 2\int_x^1 \frac{(w_t/v_e)^2}{x}\,dx$$

The equations can be materially simplified if the assumption, valid only for the propellers of fast ships (c_s small) which alone are of interest here, is made, that $(w_t/v_e)^2$ is negligible as compared to the accelerations of the first order, which will eliminate the force component in (1) and (1a) emanating from the pressures as compared to those caused by the (Impulsflusz). Then we get from (1) and (2):

(4) $dS_\infty/dT_\infty = w_a/w_t,$

i.e. the resultant acceleration, on the assumption of a lightly loaded frictionless propeller, is perpendicular to the relative velocity (Fig. 33). As long as the effect of negative pressure can be disregarded, as in this case, the accelerations at the blade have reached half the values in the fully developed stream, and therefore, according to the conclusion drawn from Eq. (4), stand in the relation (Fig. 33)

(5) $\dfrac{v_e + \frac{w_a}{2}}{\omega r - \frac{w_t}{2}} = \dfrac{w_t}{w_a}$ or nondimensionally

$$(5a)\quad \left(1+\frac{w_a}{2v_e}\right)\frac{w_a}{2v_e}=\pi\,\frac{x}{\lambda}\,\frac{w_t}{2v_e}\,.$$

if, once more, the quadratic term of the tangential acceleration velocity is negligible compared to the terms of the first order.

In judging the danger of cavitation of a section on radius x, the criterion is the local cavitation index $\sigma_x = (p_x - e)/q_x$, where x indicates that the values concerned relate to the nondimensional radius x. If it is now assumed for simplification that p_x can be interchanged with the pressure at the shaft center p_o, i.e. that its mean value can be substituted for it, then $\sigma_x = (p_o - e)/q_x$. Further we have

$$(6)\quad \sigma_x/\sigma_o = q_o/q_x \qquad \text{with}$$

$$(7)\quad q_x/q_e = \frac{\left(v_e+\frac{w_a}{2}\right)^2+\left(\omega r-\frac{w_t}{2}\right)^2}{v_e^{\,2}}$$

$$= \left(1+\frac{w_a}{2v_e}\right)^2+\left(\pi\,\frac{x}{\lambda}-\frac{w_t}{2v_e}\right)^2 = 1+\pi^2\left(\frac{x}{\lambda}\right)^2-\left(\frac{w_a}{2v_e}\right)^2.$$

where $(w_t/v_e)^2$ was again neglected and the relation (5a) used. The problem now is so to distribute the acceleration velocities that the cavitation index with a given total thrust will be as large as possible on each radius, i.e. that a blade element of the propeller will find conditions in the basic flow which will postpone the inception of cavitation as far as possible. Since σ is always greater than 0, this requirement, by neglecting the boss diameter, can be so formulated that $\int_0^1 \sigma_x$ with the additional condition that $c_{s\infty} = \int_0^1 \frac{dc_{s\infty}}{dx}\,dx$ = constant can be brought to a maximum.

The load factor and the cavitation index appear according to the foregoing equations as functions of the axial acceleration velocity w_a/v_e, and therefore the integrals may be regarded as dependent upon the coefficients of an expression in terms of wholly rational functions for w_a/v_e, which are to be so determined that $\int_0^1 \sigma_x\,dx = \text{Max}$ for c_s = constant. Thus the original isoperimetric problem is reduced to an ordinary maximum-minimum problem of several variables with a secondary condition, but at the same time the limitation is set that the sought for distribution of σ_x can be expressed only within the special thrust distributions which it is possible to represent by means of the expression for w_a/v_e.

In order to avoid complex integrations for σ_x, which according to Eq. (6) and (7) and with a whole rational expression for w_a/v_e becomes fractionally rational, it is advisable so to express the problem that the minimum of the integral over $1/\sigma_x$, for $c_{s\infty}$ = constant, will be:

$$(8)\quad \int_0^1 \frac{1}{\sigma_x}\,dx = \frac{1}{\sigma_0}\int_0^1 \frac{q_x}{q_e}\,dx = \text{Min};\ c_{s\infty} = \int_0^1 \frac{dc_{s\infty}}{dx}\,dx = \text{const}.$$

which is admissible, since σ_x is never capable of reaching zero.

To satisfy both these conditions an expression for w_a/v_e with at least two constants is required. In this expression the initial condition that $w_a/v_e = 0$ for $x = 0$ was set at first, which is valid only for the propeller under a light load, and the calculation was accordingly carried out with one linear and one quadratic term. In this, however, negative values of w_a/v_e resulted in determining the constants according to (8) in the outer portions of the propeller disc, which because of the concomitant negative thrust can not be regarded as a logical solution. The most obvious procedure then is to introduce for w_a/v_e the square of the first term, which, however, gives two general equations of the sixth order for determining the two constants, the solution of which requires more time than is justifiable in view of the simplifying assumptions. Now, in order to satisfy the requirement of the first expression within the limits of simple calculation, – decrease of the accelerating velocity in the outer portions of the propeller, w_a/v_e was made equal to zero for $x = 1$ as well as for $x = 0$:

$$(9)\quad w_a/v_e = (a_1 \cdot x + a_2 \cdot x^2)\ (1-x).$$

This expression for the acceleration velocity of a propeller with an infinite number of blades has only a formal significance in consequence of the uniform decrease towards the blade tips, but when applied to a propeller with a finite number of blades it will yield physically reasonable values, since this transition requires multiplication of the velocity distribution by a function, which precisely in the neighborhood of the blade tip is small, and for $x = 1$, is zero.

According to the rules for determining an extreme with secondary conditions, the problem expressed by Eq. (8) can be formulated as follows:

$$(10)\quad \begin{aligned} &\frac{\partial J_1}{\partial a_1} + m\frac{\partial J_2}{\partial a_1} = 0\\ &\frac{\partial J_1}{\partial a_2} + m\frac{\partial J_2}{\partial a_2} = 0, \quad \text{where} \end{aligned}$$

$$(11)\quad \begin{aligned} J_1(a_1, a_2) &= \int_0^1 \frac{dx}{\sigma_x} = \frac{1}{\sigma_0}\int_0^1 \frac{q_x}{q_e}\,dx\\ J_2(a_1, a_2) &= 0 = c_{s\infty} - \int_0^1 \frac{dc_{s\infty}}{dx}\,dx \end{aligned}$$

Equations (10) determine together with the given value $c_{s\infty}$ according to (1a) the three unknowns a_1, a_2 and m.

Expression (9) yields first the following expression for q_x/q_e according to (7):

$$(7a)\quad \frac{q_x}{q_e} = 1 + x^2\left(\frac{\pi^2}{\lambda^2} - \frac{a_1^2}{4}\right) - x^3\frac{a_1}{2}(a_2 - a_1) - x^4\left(\frac{a_2^2}{4} - a_1 a_2 + \frac{a_1^2}{4}\right) + x^5\frac{a_2}{2}(a_2 - a_1) - x^6\frac{a_2^2}{4}$$

Further, the elementary load factor, neglecting the negative pressure in the stream, becomes according to Eq. (1a):

$$(1b)\quad \frac{1}{4}\frac{dc_{s\infty}}{dx} = x^2 a_1 + x^3(-a_1 + a_2 + a_1^2) + x^4(-a_2 + 2a_1 a_2 - 2a_1^2) + x^5(-4a_1 a_2 + a_1^2 + a_2^2) + x^6(2a_1 a_2 - 2a_2^2) + x^7 a_2^2$$

With these expressions there result from Eq. (11):

$$(11a)\quad J_1 = \frac{1}{\sigma_o}\left(1 + \frac{\pi^2}{3\lambda^2} - \frac{a_1^2}{120} - \frac{a_2^2}{420} - \frac{a_1 a_2}{120}\right)$$
$$J_2 = c_{s\infty} - 4\left(\frac{a_1}{12} + \frac{a_2}{20} + \frac{a_1^2}{60} + \frac{a_2^2}{168} + \frac{2}{105}a_1 a_2\right)$$

The corresponding expressions according to (11a) introduced into (10) yield the following conditional equations for a_1 and a_2:

$$(10a)\quad \frac{\partial J_1}{\partial a_1} + m\frac{\partial J_2}{\partial a_1} = -\frac{2a_1 + a_2}{120\sigma_o} - 4m\left(\frac{1}{12} + \frac{a_1}{30} + \frac{2}{105}a_2\right) = 0$$
$$\frac{\partial J_1}{\partial a_2} + m\frac{\partial J_2}{\partial a_2} = -\frac{7a_1 + 4a_2}{840\sigma_o} - 4m\left(\frac{1}{20} + \frac{2}{105}a_1 + \frac{a_2}{84}\right) = 0$$

By eliminating 4m we finally get as the relations between a_1 and a_2:

$$(12)\quad 7(2a_1 + a_2)\left(\frac{1}{20} + \frac{2}{105}a_1 + \frac{a_2}{84}\right) = (7a_1 + 4a_2)\left(\frac{1}{12} + \frac{a_1}{30} + \frac{2}{105}a_2\right)$$

The second conditional equation is obtained by integration of (1b) from the specified load factor of the propeller:

$$(1c)\quad \frac{c_{s\infty}}{4} = \frac{a_1}{12} + \frac{a_2}{20} + \frac{a_1^2}{60} + \frac{a_2^2}{168} + \frac{2}{105}a_1 a_2$$

The numerical determination of the coefficients, which is best carried out by calculating the a_2 and $c_{s\infty}$ values appropriate to a_1 in terms of the two last expressions, leads to quadratic equations the solutions of which for positive c_s -values are given in Fig. 34.

In the following the thrust distribution of a propeller that satisfies the derived conditions will be calculated for $c_{s\infty} = 0.5$, and compared with the distribution of a propeller with the lowest loss in efficiency. According to Fig. 34, with $c_{s\infty} = 0.5$ independent of λ and σ_o, $a_1 = -0.57$, $a_2 = 2.95$, and accordingly the thrust distribution according to Eq. (1b) is

$$\frac{1}{4}\frac{dc_{s\infty}}{dx} = -0{,}57 \cdot x^2 + 3{,}845 \cdot x^3 - 6{,}964 \cdot x^4 + 15{,}756 \cdot x^5 - 20{,}770 \cdot x^6 + 8{,}703 \cdot x^7$$

The thrust distribution of an equivalent three-bladed propeller is obtained from this approximately by multiplying with Prandtl's reduction factor $\varkappa$, which, strictly speaking, however, is justifiable only for the propeller with the least efficiency loss. In Helmbold's paper "The Betz-Prandtl Theory of the Screw Propeller" [60], $\varkappa$ is given as a function of the variable X (1 - x), where $X = \frac{Z}{2}\frac{\sqrt{1 + b_o^2}}{b_o}$, with b_o = tangent β for x = 1. For the purposes of this calculation it is accurate enough to take b_o as equal to the speed factor λ/π, which was assumed to be $\lambda = .25\pi$. Integration of $dc_s/dx \sim \varkappa\, dc_s/dx$ then yields the value $c_s = 0.419$ as the load factor of the equivalent three-bladed propeller.

Calculation of the thrust distribution of the corresponding frictionless propeller with least energy loss can be carried out directly according to the relations developed by Helmbold in the cited paper. We get from the universally valid equation

$$\frac{dc_s}{dx} = \frac{z}{\pi} c_a \frac{t}{r_o} \frac{q_x}{q_e} \cos\beta .$$

which is obtained directly from consideration of the forces on the blade element, using the expressions for q_x/q_e and $z\, c_a\, t/r_o$ valid for the smallest energy loss and reported in Helmbold's paper, the relation

$$\frac{dc_s}{dx} = 8\varkappa \frac{(b_o - \frac{\lambda}{\pi})\frac{b_o}{x}}{(1 + \frac{b_o^2}{x^2})^2} \left(\frac{\pi x}{\lambda}\right)^2 \left(1 + \frac{\lambda b_o}{\pi x^2}\right).$$

where b_o, which is a function of c_s and λ, has the value 0.290 [61].

Comparison of the thrust distributions in Fig. 35 shows that the thrust of the propeller with the greatest possible σ_x is concentrated more towards the inside and that at the places having the smallest cavitation indices there is a reduction in load. In order to test how far this conclusion is tenable, two propellers having the same load and speed factors were made, which differed only in the thrust distribution because of differing pitch, but otherwise had the same area ratio, area distribution and sections, and which were tested at various σ_o -values in addition to atmospheric pressure.

Using the value $c_s = 0.419$ for $\lambda = 0.25\pi$ obtained in determining the thrust distribution, the propeller with greatest possible σ_x was constructed according to the following calculations:

1. Calculation of the required product $c_a \cdot t$. For this we get from the

60) WRH 1926, No. 23 and 24.

61) See Lerbs, WRH, No. 13

forces on the blade element and considering the section drag, the expression

$$c_a \cdot t = \frac{r_o \pi \frac{dc_s}{dx}}{z \frac{q_x}{q_e} \cos\beta (1 - \varepsilon \tan\beta)}$$

Here dc_s/dx was determined according to Eq. (1b), q_x/q_e according to Eq. (7), and $\tan\beta = w_t/w_a$ according to Eq. (5) and (9) with $a_1 = -0.57$; $a_2 = 2.95$, and furthermore $\varepsilon = 0.025$ was introduced as a mean value approximately to be realized. Herewith we get the following table for radii outside the boss:

x	dc_s/dx	w_a/v_e	w_t/v_e	q_x/q_r	tangβ	$c_a \cdot t$ (cm)
0,2	0,005	0,003	0,002	1,640	0,667	0,037
0,3	0,085	0,066	0,056	2,440	0,849	0,487
0,4	0,262	0,146	0,098	3,555	0,671	0,944
0,5	0,543	0,226	0,128	4,987	0,567	1,330
0,6	0,838	0,288	0,138	6,739	0,480	1,408
0,7	1,042	0,314	0,130	8,815	0,414	1,354
0,8	0,964	0,287	0,102	11,220	0,356	1,051
0,9	0,403	0,187	0,056	13,951	0,299	0,318
1,0	0,000	0,000	0,000	17,000	0,250	0,000

The propeller radius r_o was set at 0.1 m. For comparison we shall choose a three-bladed propeller of constant pitch of the Series B_2 with $F_a/F = 0.56$, whose blade width as well as section thickness d are determined by these data. Since the area of the two screws is to agree both as to magnitude and distribution we get with these values of t and d/t the required lift coefficient and the pitch of the propeller with the greatest σ_x from the product $c_a \cdot t$ of the last table:

x	t cm	c_a	d cm	d/t	α_∞	$H/2\pi = r \cdot \tan(\alpha+\beta)$ cm
0,2	4,82	0,008	0,81	0,168	—3,2	1,178
0,3	6,08	0,081	0,72	0,118	—2,8	2,301
0,4	7,24	0,130	0,63	0,087	—2,5	2,440
0,5	8,16	0,163	0,54	0,066	—2,0	2,605
0,6	8,69	0,162	0,45	0,052	—1,4	2,706
0,7	8,74	0,155	0,36	0,041	—0,3	2,856
0,8	8,17	0,129	0,27	0,033	—0,0	2,848
0,9	6,40	0,050	0,18	0,028	—1,4	2,457
1,0	0,00	0,000	0,00	0,000	—1,5	2,220

The resulting pitch curve is represented in Fig. 36 and is characterized essentially by the fact that the pitch decreases outward and inward from a maximum at about $2/3\ r_o$.

The test data of this propeller at atmospheric pressure show first that the assumed load factor of $c_s = 0.419$ is not attained at $\lambda = 0.25\ \pi$, but only the value $c_s = 0.384$. This error of 9%, which is due to the simplifying assumptions of the theory, is immaterial in the comparison with the constant pitch propeller if

the latter is so chosen that it yields the same load factor as was measured with the first propeller. Accordingly the pitch ratio of the propeller used for comparison was taken as 0.885 according to interpolation between the earlier tests with B_2; $F_a/F = 0.56$, whose thrust corresponds with sufficient accuracy with the calculated propeller according to the measurements in Fig. 38.

The comparison tests were carried out for $\sigma_o = 1.9$, 1.6 and 1.3 and the observed beginning of suction side cavitation plotted in Fig. 37, where a considerable difference is evident in that cavitation sets in the earlier in the constant pitch propeller, the smaller σ_o . In this connection it is important that the beginning of cavitation in the case of the propeller with the greatest possible occurs approximately at 2/3 r_o, i.e. at the point of greatest thrust concentration. Corresponding with this difference in the inception of cavitation, the beginning of thrust deviation according to Fig. 38 also shifts towards small λ-values for the propeller with $(\sigma_x)_{max}$, but after the cavitation has developed sufficiently the thrust produced by this propeller becomes less than that delivered by the constant pitch propeller. The reason is that although cavitation begins later in the first propeller, it sets in at the points of greatest thrust where the thrust decrease is also large in comparison with the total thrust.

At all events it has been shown by these tests that with the developed thrust distribution it is possible to specify propellers which with the same form elements begin to cavitate later than propellers of Series B_2 which is important for fast merchant ships, where the curves of thrust loss must be avoided as far as possible.

With these considerations the studies, which have been limited to open-water propellers, will be concluded. It remains to thank those who participated in the preparation of the paper; First the Notgemeinschaft der Deutschen Wissenschaft for presentation of the means for building the cavitation tank, H. Hoppe, Eng., for his aid in the construction of the plant, H. Schultze, Eng., for his extensive participation in carrying out the tests and analysing them, Mechanic Dierks for tending the plant, and not least Dr. Kempf, Director of the Hamburg Model Basin for the facilities as well as the time he placed at our disposal for this compilation.

SYMBOLS IN FREQUENT USE

D	Propeller diameter
d	" "
H	Pitch of pressure side
r_o	Propeller radius
r	Intermediate value of the radius
F	Propeller disc area
F_p/F	Ratio of propeller area projected into the plane of rotation to the disc area
F_a/F	Ratio of developed propeller area to disc area
z	Number of blades
S	Thrust
M	Torque
n	Revolutions per second
N	Revolutions per minute
ω	Angular velocity
v_s	Speed of ship
v_e	Speed of advance of the propeller
v_o	Mean velocity of flow through the measuring plane of the tunnel
v'	Maximum local velocity at blade element
v_r	Relative velocity of basic flow
F_o	Section of tunnel in the plane of the model propeller
g	Acceleration due to gravity
$\rho = \gamma/g$	Specific mass of fresh water = 102 kg sec^2 m^{-4}
$q_e = \rho/2\ v^2_e$	Dynamic pressure of the speed of advance
$q_r = \rho/2\ v^2_r$	Dynamic pressure of the relative velocity
$\lambda = v/nd$	Speed ratio
$\lambda_s = v_s/nd$	Speed ratio with respect to velocity of ship
$\lambda_e = v_e/nd$	Speed ratio with respect to speed of advance of the propeller
$\lambda_o = v_o/nd$	Speed ratio with respect to the velocity in the measuring section of the tunnel (when the index is lacking the speed ratio of the speed of advance is meant)
p	Static pressure
p_o	Static pressure at the height of the shaft center far ahead of the propeller
$-p'$	Maximum local negative pressure on the blade element
b_o	Air pressure
e	Vapor pressure
$\sigma = (p - e)/q_r$	Cavitation index
$\sigma_o = (p - e)/q_e$	Cavitation index taken with respect to shaft center
α	Angle of incidence of blade element
α_∞	Angle of incidence of blade element taken with respect to aspect ratio zero

c_w Drag coefficient of the blade element

c_a Lift " " " " "

$\varepsilon = c_w/c_a$ Reciprocal of L/D ratio

$c_1 = S/\rho\, n^2 d^4$ Thrust coefficient

$c_{1.0}$ " " for σ_o

$c_2 = M/\rho\, n^2 d^5$ Torque coefficient

$c_{2.0}$ " " for σ_o

SHP Output measured on the shaft (immediately ahead of thrust bearing) in HP

IHP Indicated output in HP

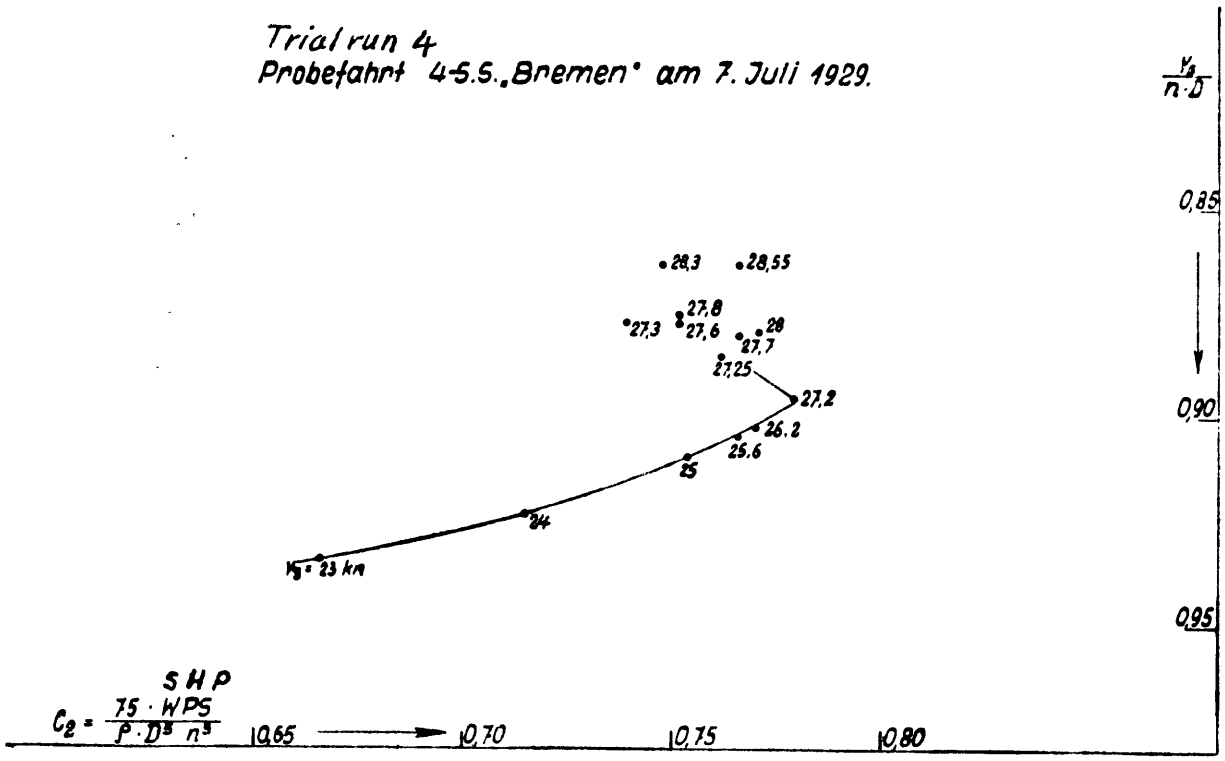
Trial run 4
Probefahrt 4-S.S. „Bremen" am 7. Juli 1929.
$\frac{V_s}{n \cdot D}$
0,85
0,90
0,95
28,3
28,55
27,8
27,6
27,3
28
27,7
27,25
27,2
26,2
25,6
25
24
V_s = 23 km
$C_2 = \frac{75 \cdot WPS}{\rho \cdot D^5 \cdot n^3}$
SHP
0,65
0,70
0,75
0,80

Fig. 1

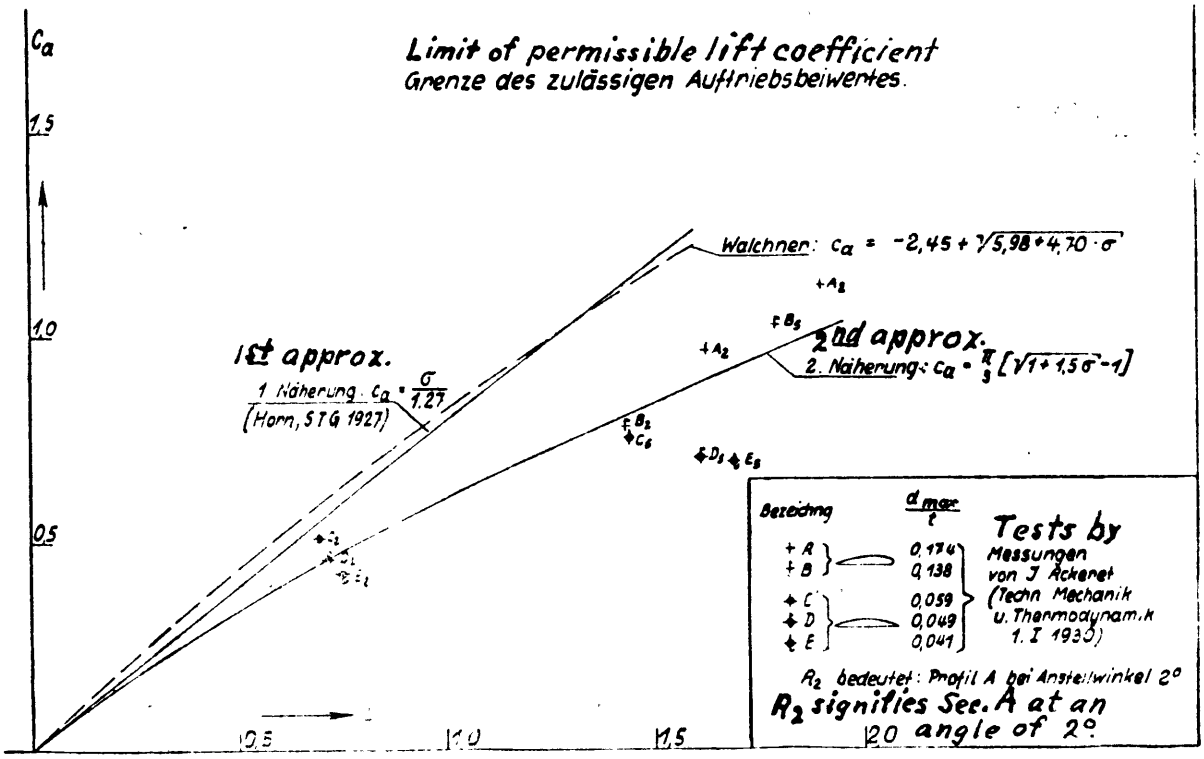
C_a
Limit of permissible lift coefficient
Grenze des zulässigen Auftriebsbeiwertes.
1,5
1,0
0,5
Walchner: $c_a = -2,45 + \sqrt{5,98 + 4,70 \cdot \sigma}$
1st approx.
1 Näherung $c_a = \frac{\sigma}{1,27}$
(Horn, STG 1927)
2nd approx.
2. Näherung: $c_a = \frac{\pi}{3}[\sqrt{1 + 1,5\sigma} - 1]$
Bezeichng
$\frac{d}{l}$ max
+ A
+ B
0,174
0,138
+ C
+ D
+ E
0,059
0,049
0,041
Tests by
Messungen
von J Ackeret
(Techn Mechanik
u. Thermodynam. I
1. I 1930)
R_2 bedeutet: Profil A bei Anstellwinkel 2°
R_2 signifies Sec. A at an
angle of 2°
0,5
1,0
1,5
2,0

Fig. 2

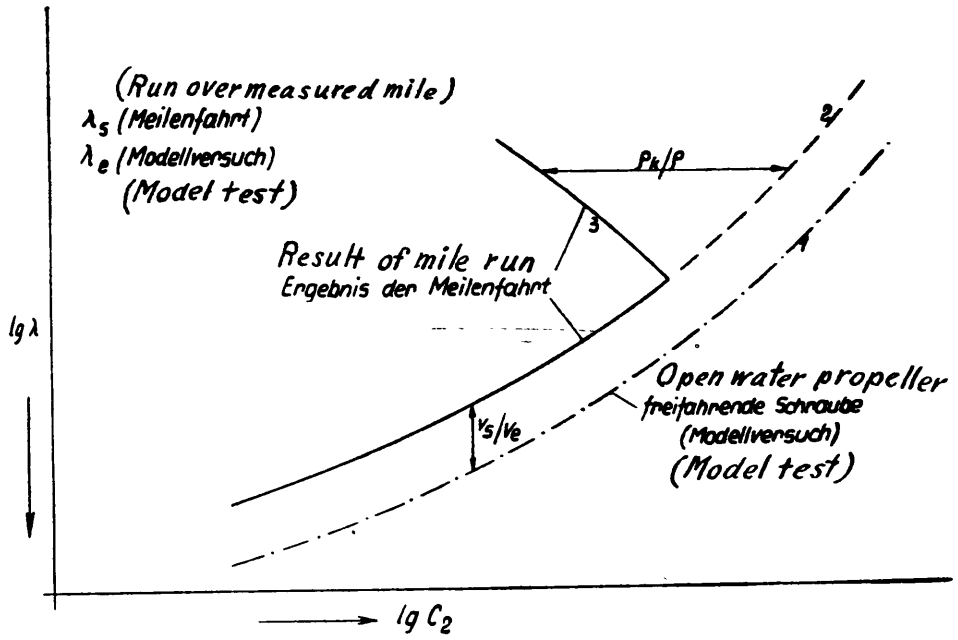
(Run over measured mile)
λ_s (Meilenfahrt)
λ_e (Modellversuch)
(Model test)
P_k/P
2
3
4
Result of mile run
Ergebnis der Meilenfahrt
lg λ
V_s/V_e
Open water propeller
freifahrende Schraube
(Modellversuch)
(Model test)
lg C_2

Fig. 3

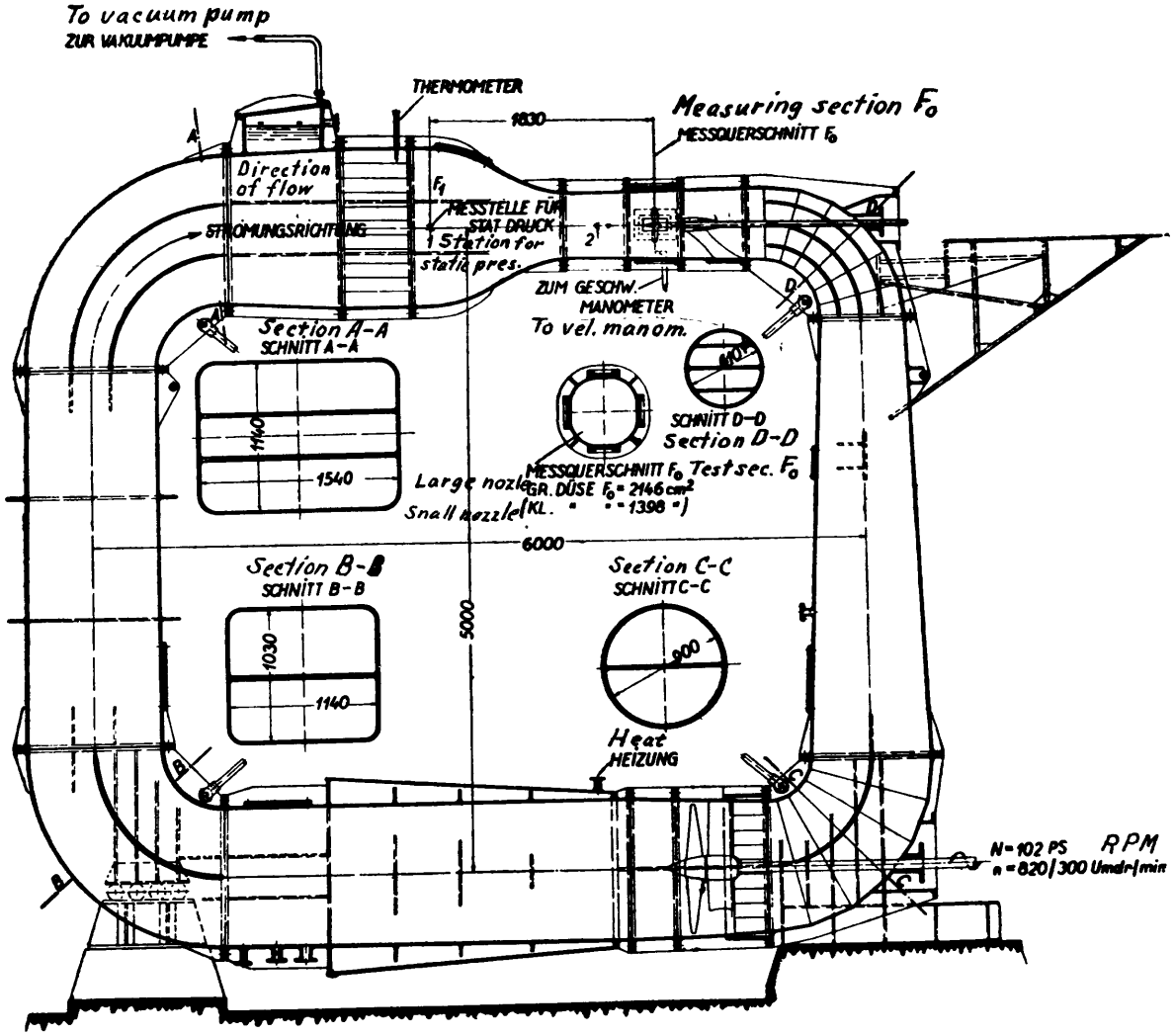
To vacuum pump
ZUR VAKUUMPUMPE
THERMOMETER
1830
Measuring section F_o
MESSQUERSCHNITT f_o
Direction of flow
STRÖMUNGSRICHTUNG
f_1
MESSTELLE FÜR STAT. DRUCK
1 Station for static pres.
ZUM GESCHW. MANOMETER
To vel. manom.
Section A-A
SCHNITT A-A
1140
1540
SCHNITT D-D
Section D-D
MESSQUERSCHNITT F_o Test sec. F_o
GR. DÜSE F_o = 2146 cm²
KL. " " = 1398 "
Large nozzle
Small nozzle
6000
Section B-B
SCHNITT B-B
1030
1140
5000
Section C-C
SCHNITT C-C
900
Heat
HEIZUNG
N = 102 PS
n = 820/300 Umdr/min
RPM

Fig. 4

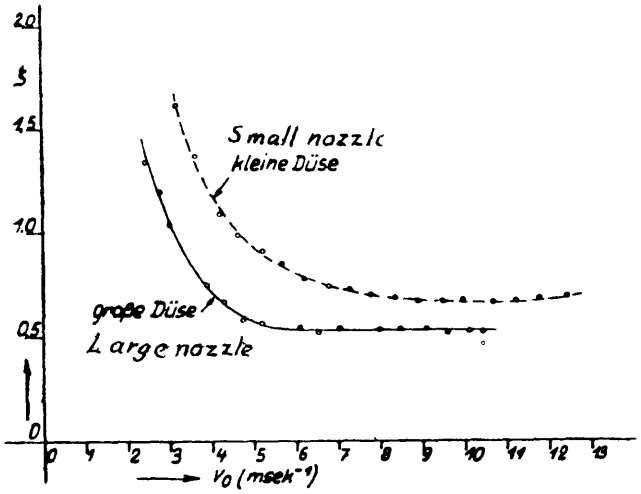

Fig. 5

Velocity distribution $\frac{v}{v_0}$ in the measuring plane
Geschwindigkeits-Verteilung $\frac{v}{v_0}$ in der Meßebene
$v_0 = 4{,}05$ msek^{-1} (große Düse). (large nozzle)
Gegen Stromrichtung gesehen.
Looking counter to direction of flow

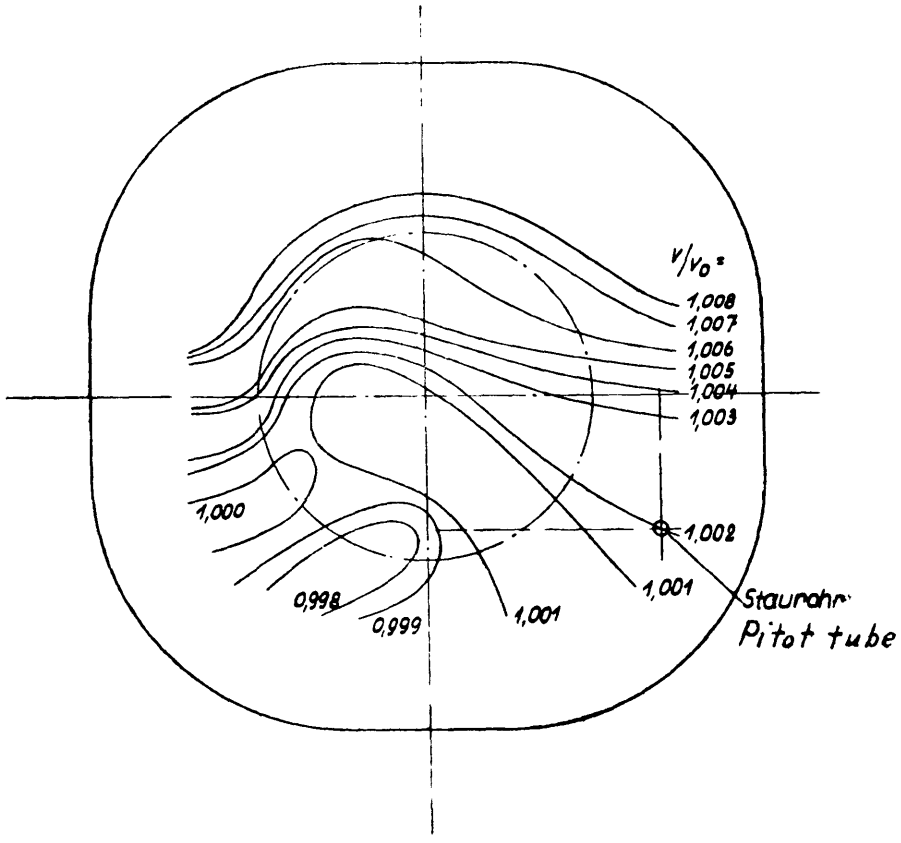

Fig. 6

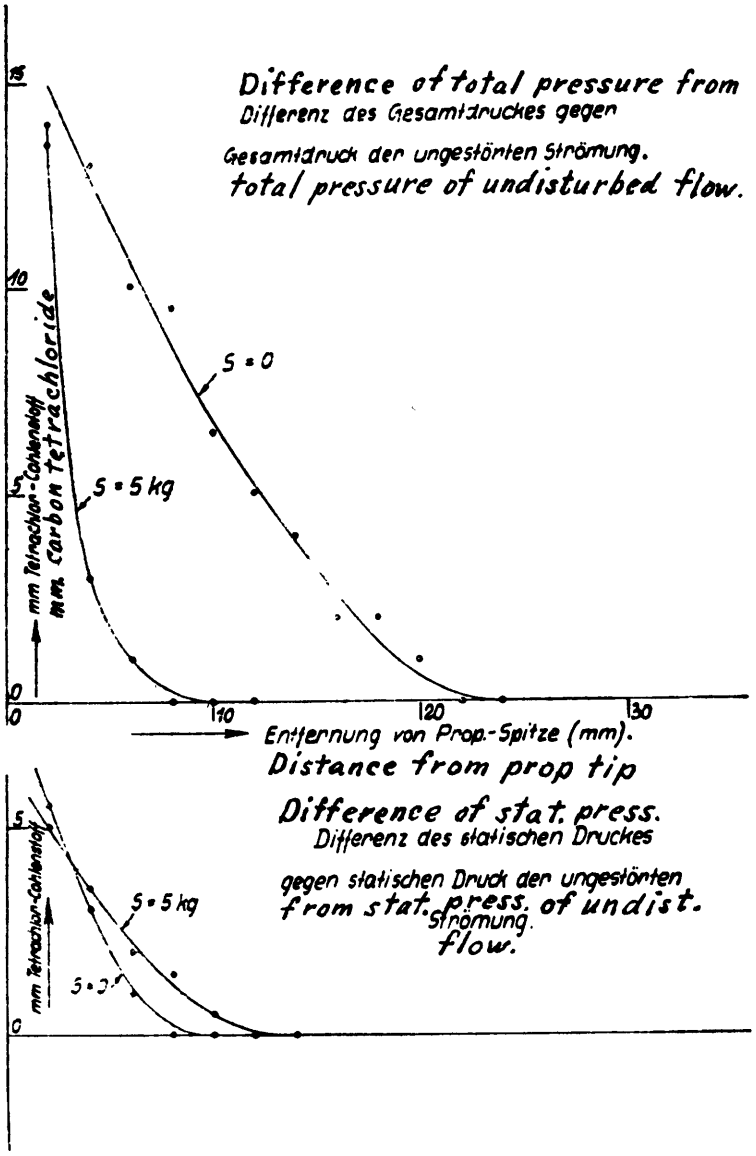
Difference of total pressure from
Differenz des Gesamtdruckes gegen
Gesamtdruck der ungestörten Strömung.
total pressure of undisturbed flow.
mm Tetrachlor-Cohlenstoff
mm carbon tetrachloride
S = 0
S = 5 kg
0
10
20
30
Entfernung von Prop.-Spitze (mm).
Distance from prop tip
Difference of stat. press.
Differenz des statischen Druckes
gegen statischen Druck der ungestörten
from stat. press. of undist.
Strömung.
flow.
S = 5 kg

Fig. 7

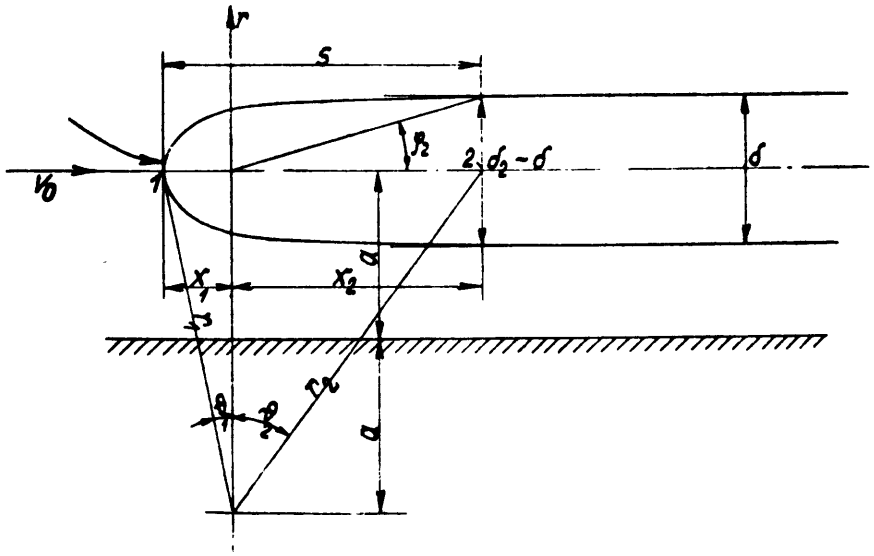
r
s
δ_2
$2\delta_2 - \delta$
δ
v_0
1
x_1
x_2
a
3
ϑ_1
ϑ_2
r_2
a

Fig. 8

a

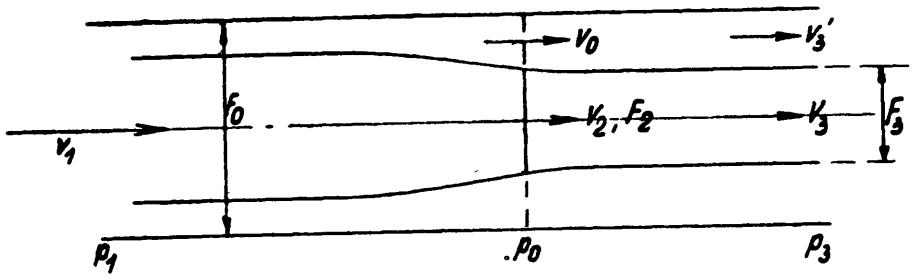

b

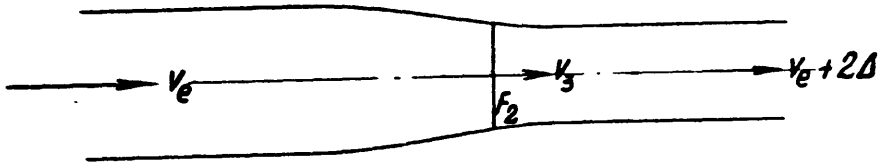

Fig. 9

Fig. 10

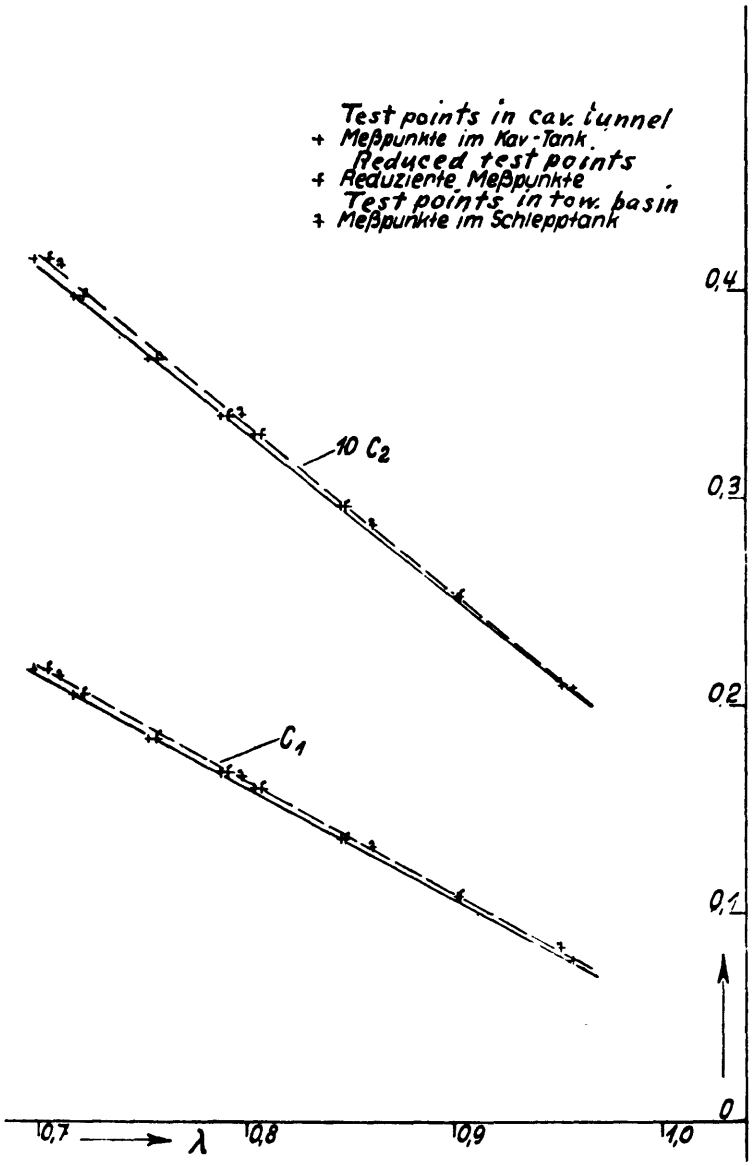

Fig. 11

Fig. 12, 12b, 12c on following pages.

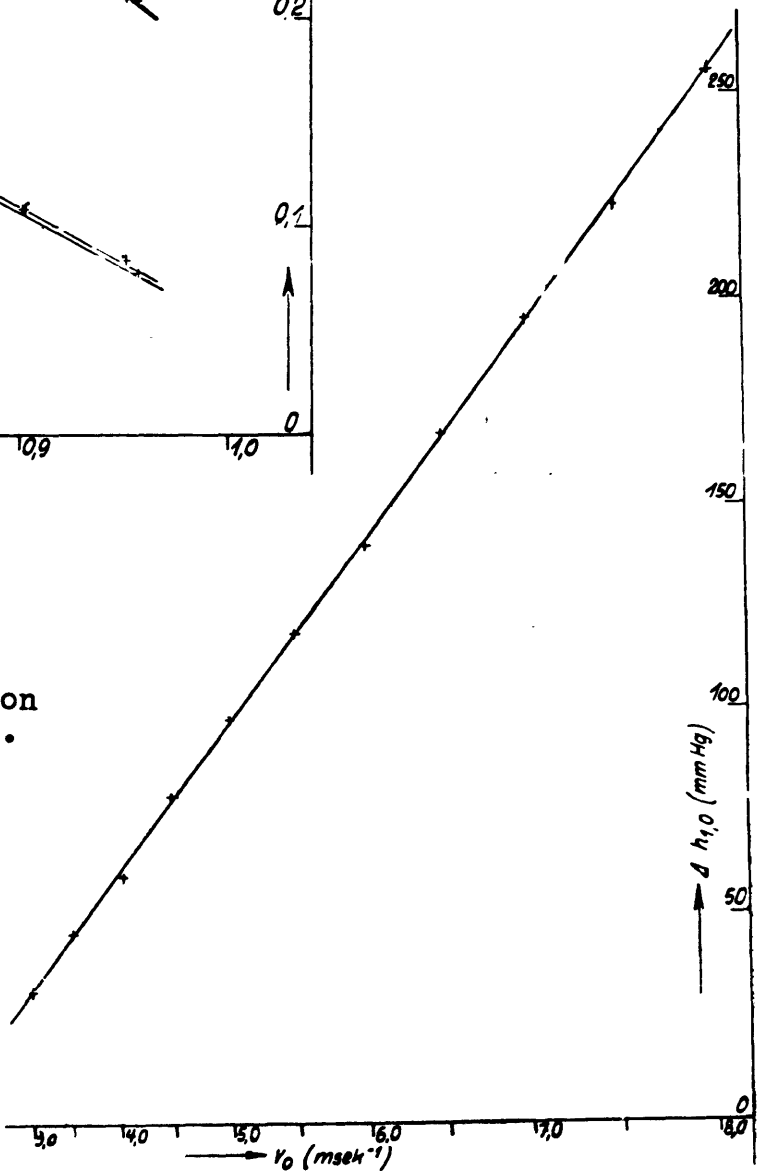

Fig. 13

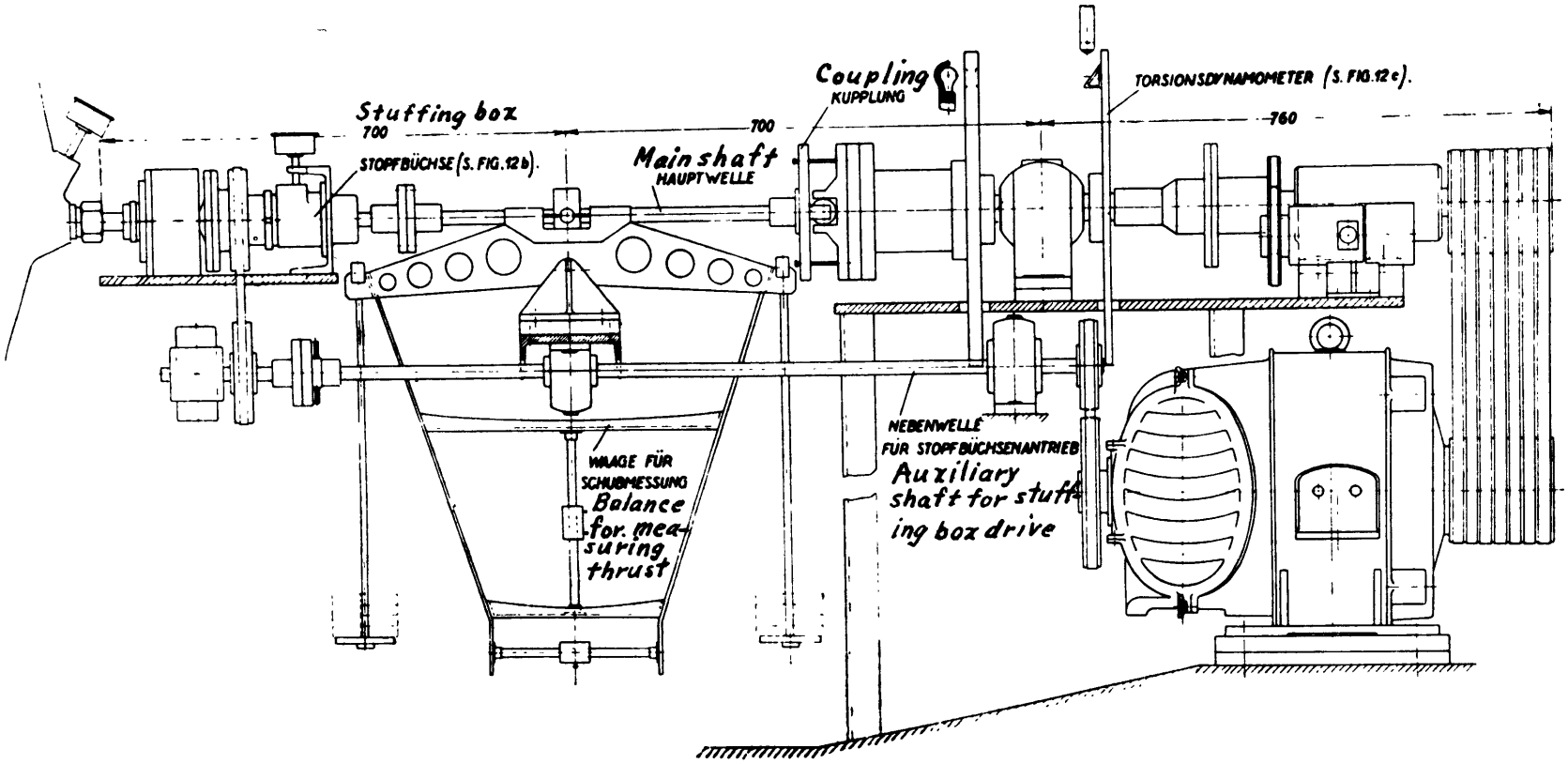
Stuffing box
700
STOPFBÜCHSE (S. FIG. 12b).
700
Mainshaft
HAUPTWELLE
Coupling
KUPPLUNG
TORSIONSDYNAMOMETER (S. FIG. 12c).
760
WAAGE FÜR SCHUBMESSUNG
Balance for measuring thrust
NEBENWELLE FÜR STOPFBÜCHSENANTRIEB
Auxiliary shaft for stuffing box drive

Fig. 12

Stopfbüchse
Stuffing box

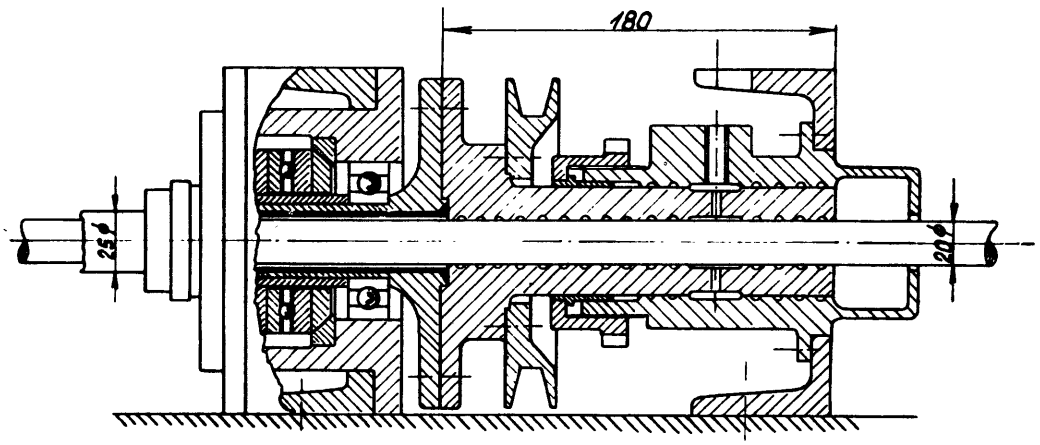

Fig. 12 b

Torsionsdynamometer

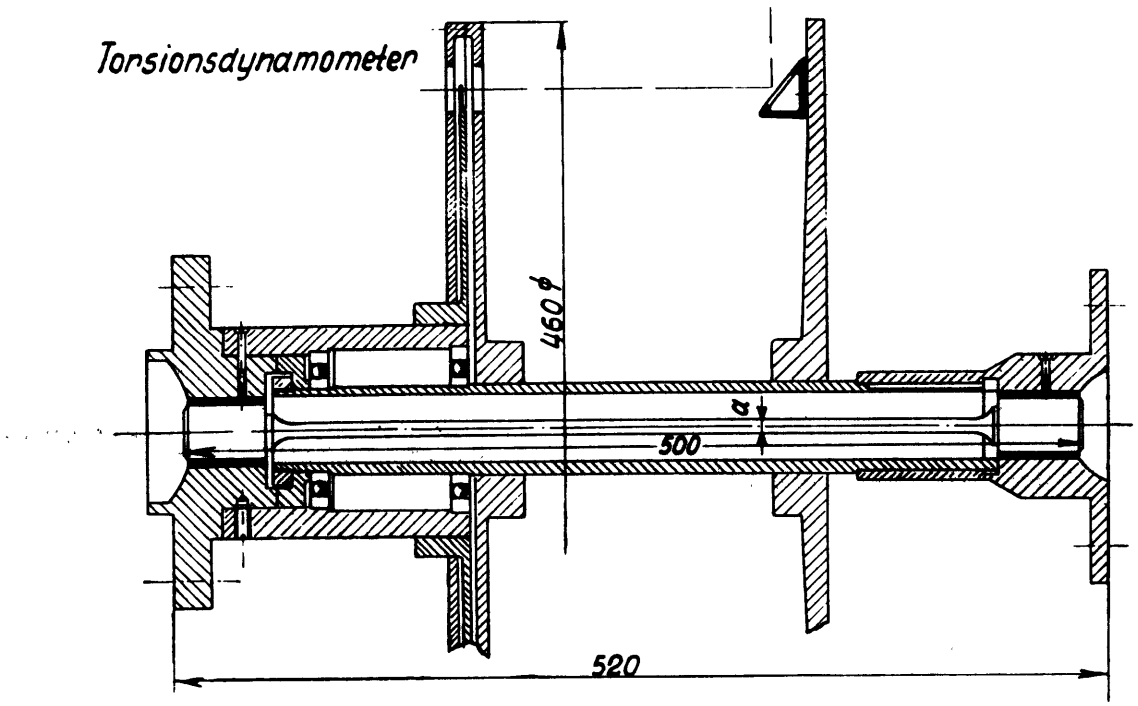

Fig. 12 c

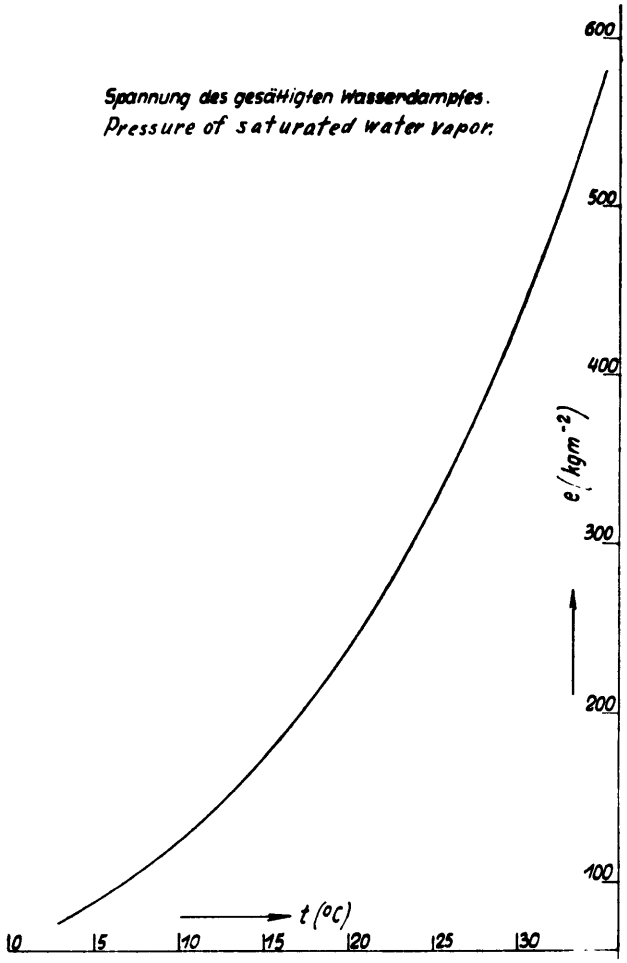
Spannung des gesättigten Wasserdampfes.
Pressure of saturated water vapor.
600
500
400
300
200
100
e (kgm⁻²)
t (°C)
10
15
110
115
120
125
130

Fig. 14

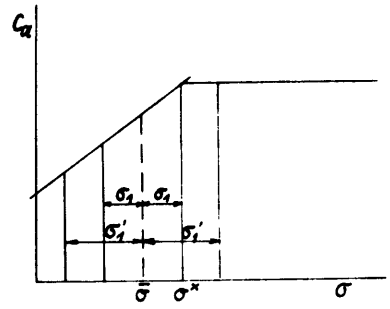
C_a
σ_1
σ_1
σ_1'
σ_1'
$\bar{\sigma}$
σ^x
σ

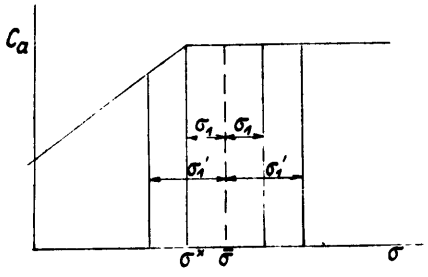
C_a
σ_1
σ_1
σ_1'
σ_1'
σ^x
$\bar{\sigma}$
σ

Fig. 15

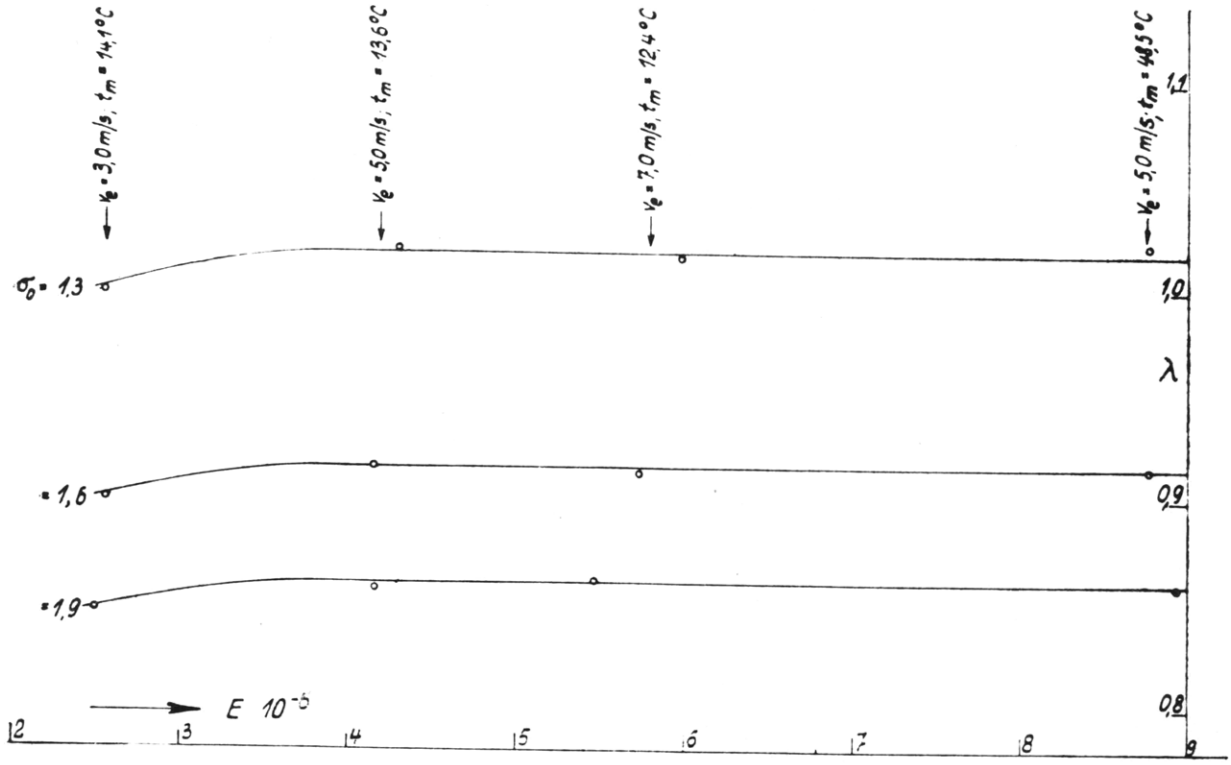

Fig. 16

Fig. 17 on next page.

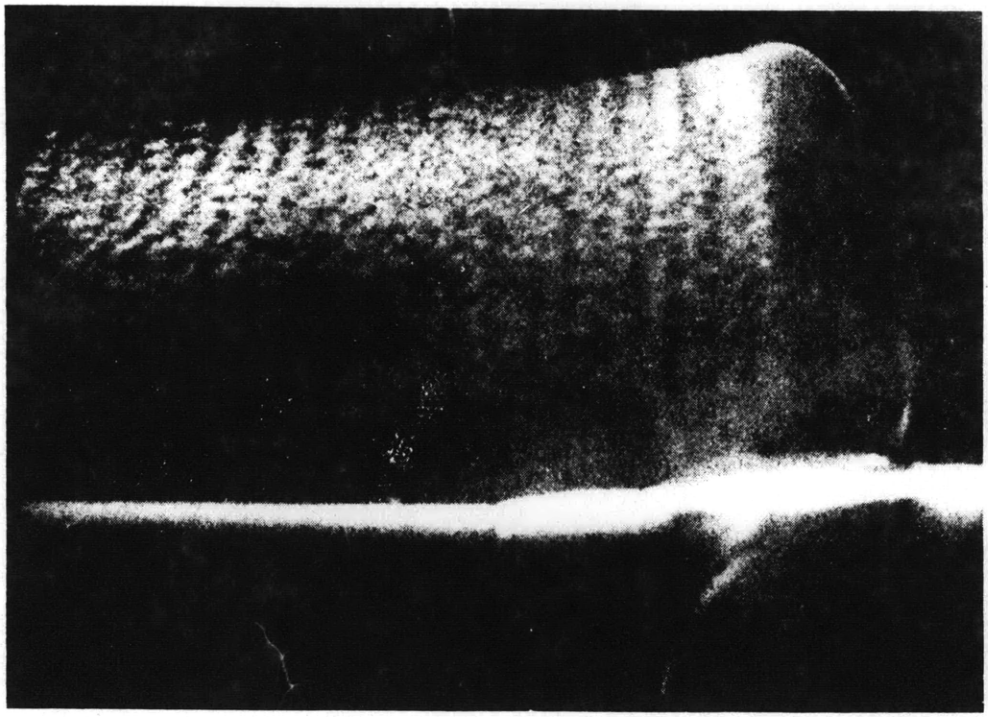

Fig. 18

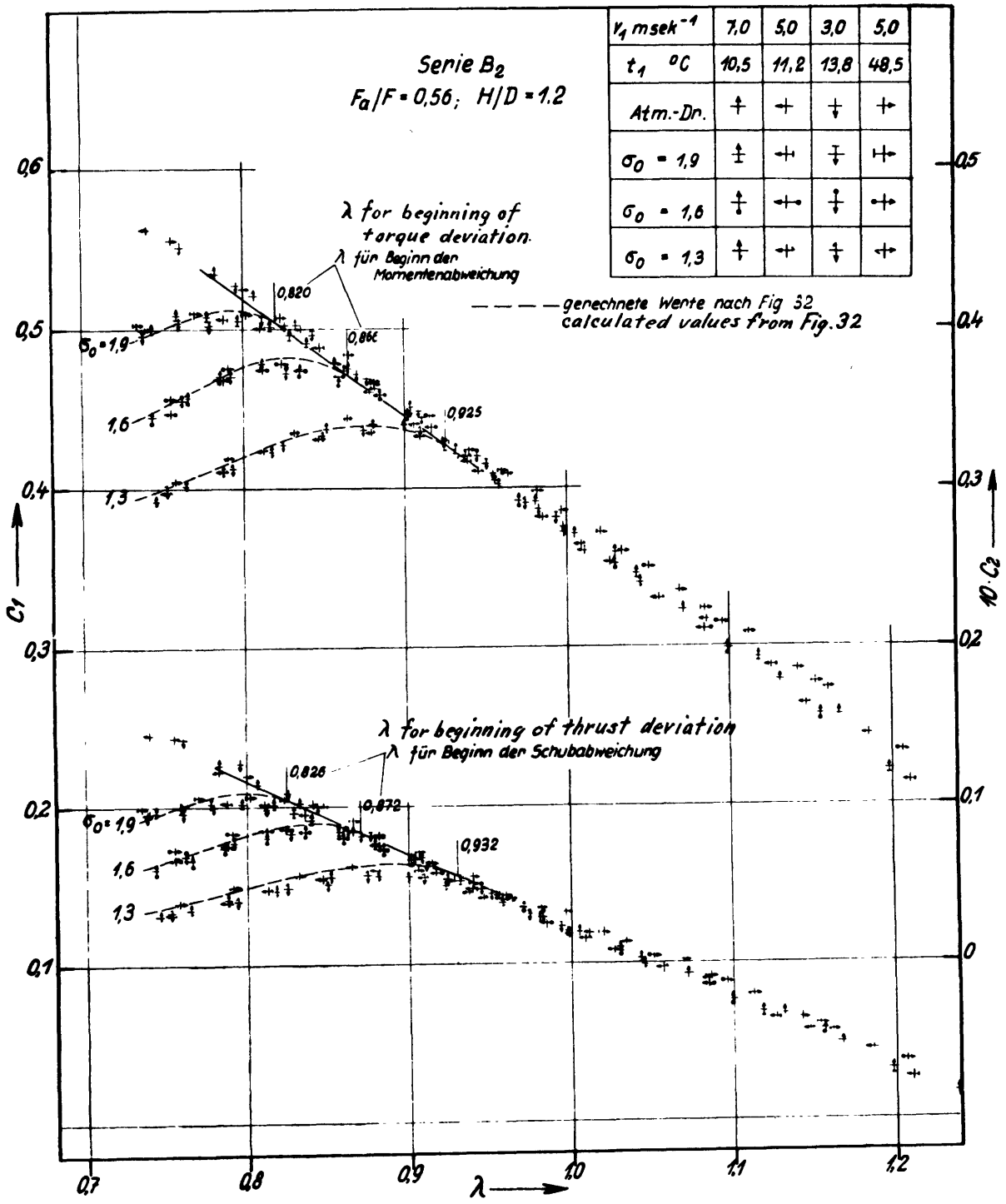
Serie B_2
$F_a/F = 0{,}56$; $H/D = 1{,}2$
v_1 msek^{-1} | 7,0 | 5,0 | 3,0 | 5,0
t_1 °C | 10,5 | 11,2 | 13,8 | 48,5
Atm.-Dr.
$\sigma_0 = 1{,}9$
$\sigma_0 = 1{,}6$
$\sigma_0 = 1{,}3$
λ for beginning of torque deviation.
λ für Beginn der Momentenabweichung
0,820
0,866
0,925
1,9
1,6
1,3
genechnete Werte nach Fig 32
calculated values from Fig. 32
λ for beginning of thrust deviation
λ für Beginn der Schubabweichung
0,826
0,872
0,932
C_1
$10 \cdot C_2$
0,6
0,5
0,4
0,3
0,2
0,1
0
0,7
0,8
0,9
1,0
1,1
1,2
λ

Fig. 17

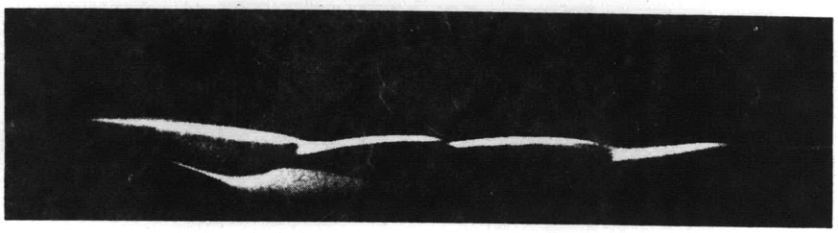

Fig. 19

α_∞ 6.5°; σ_0 1.30. In Richtung der Spannseite gesehen.
Seen in direction of suction side.

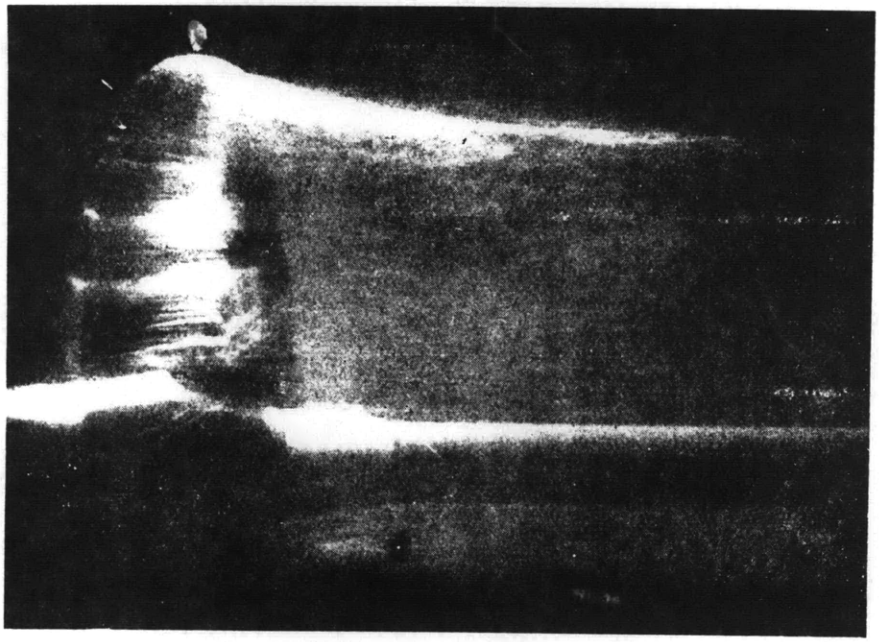

Fig 20

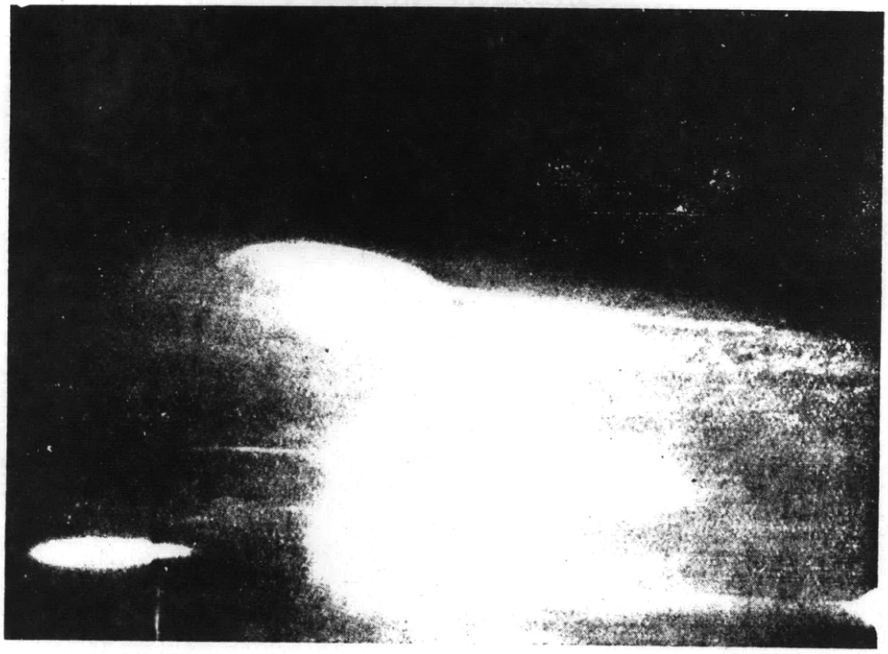

Fig. 21

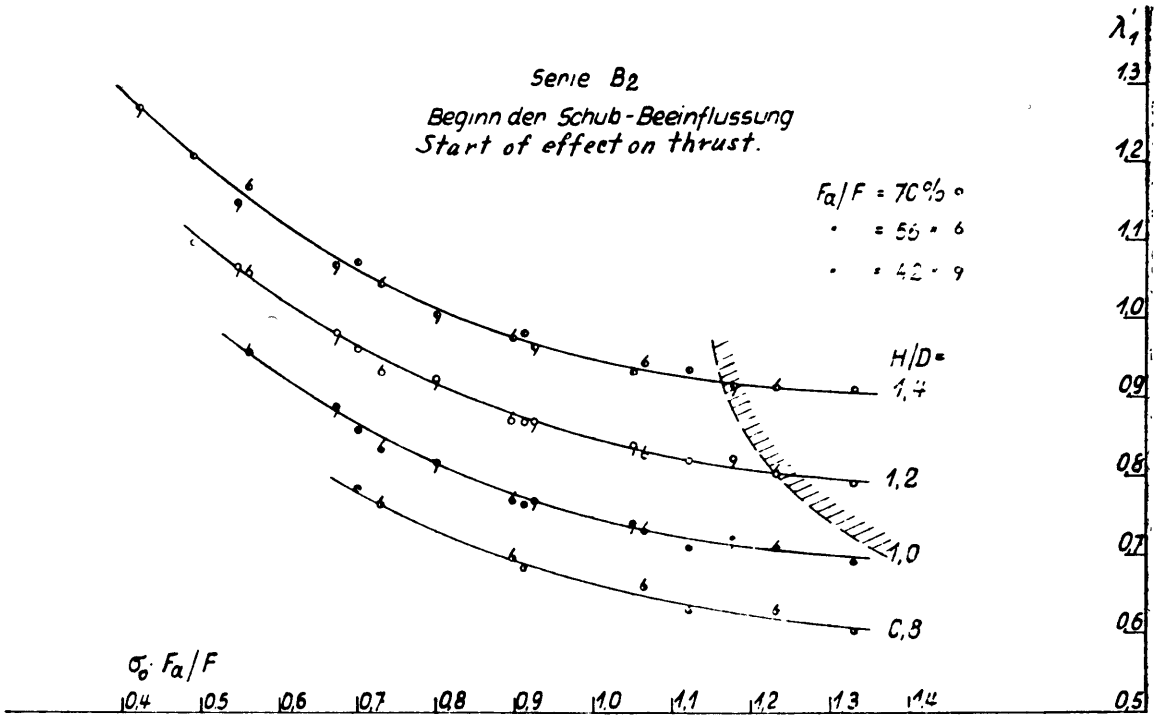

Fig. 22a

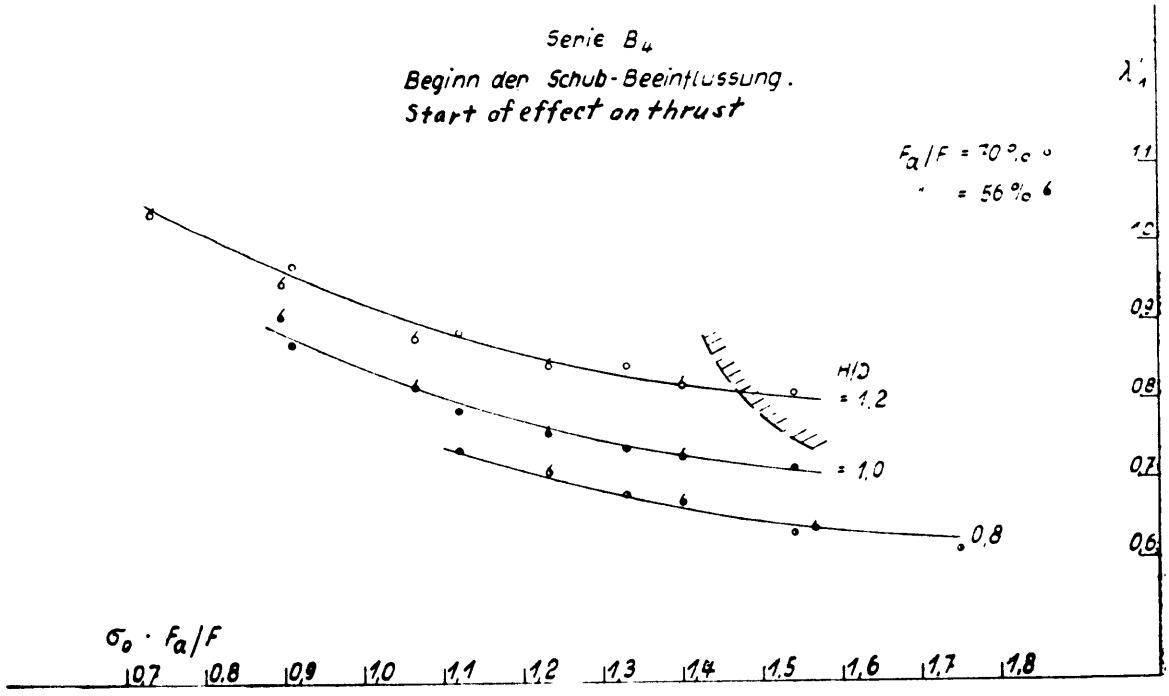

Fig. 22b

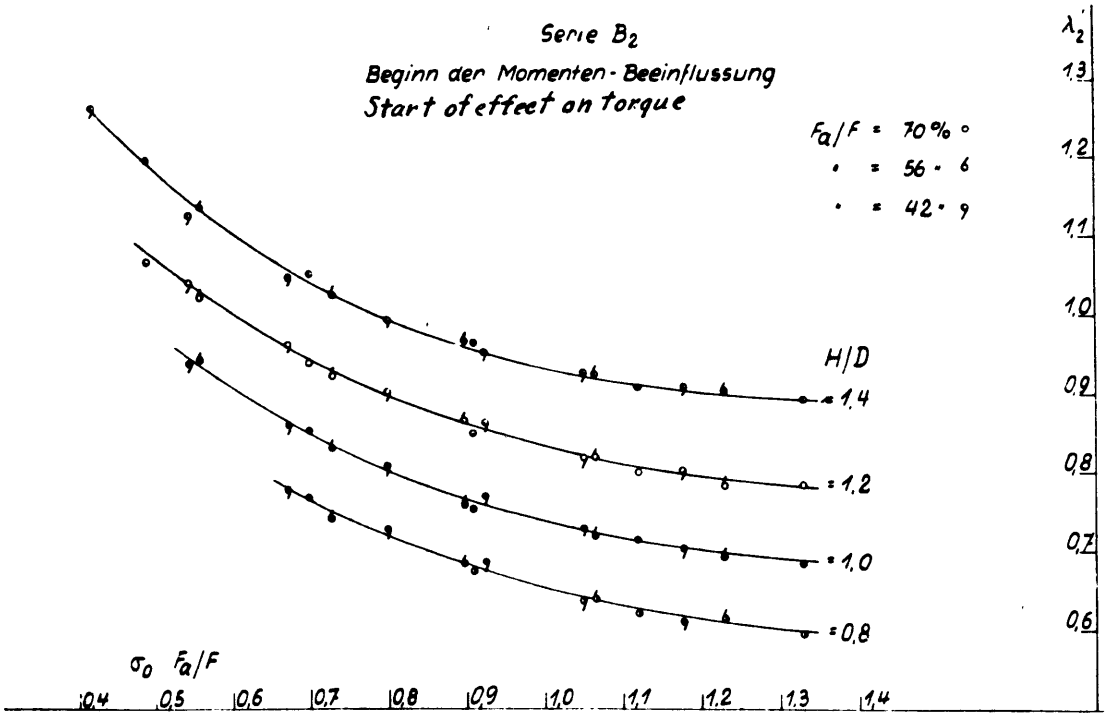

Fig. 23a

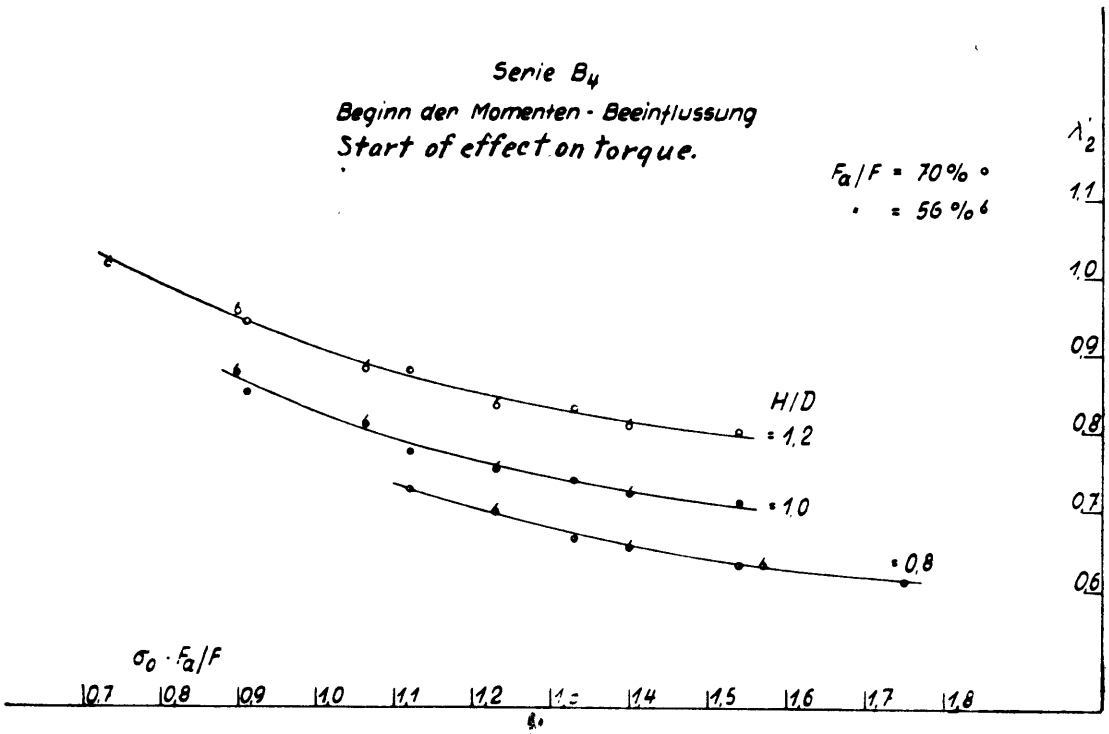

Fig. 23b

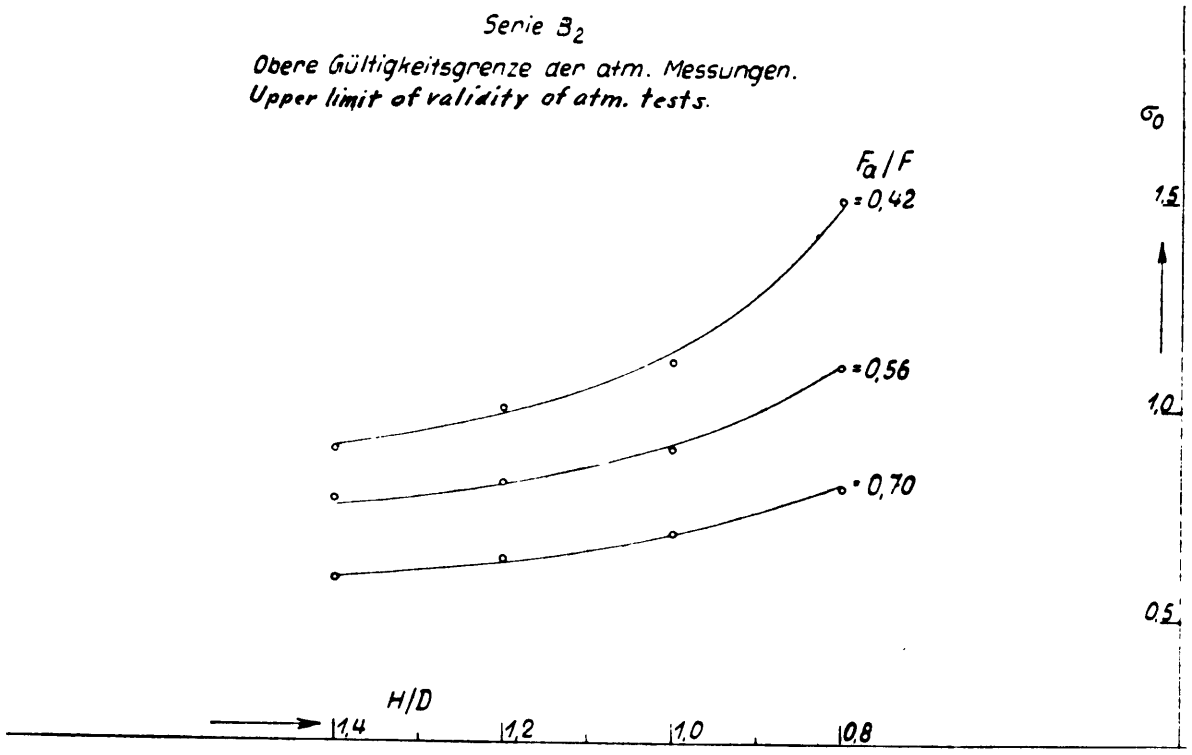

Fig. 24a

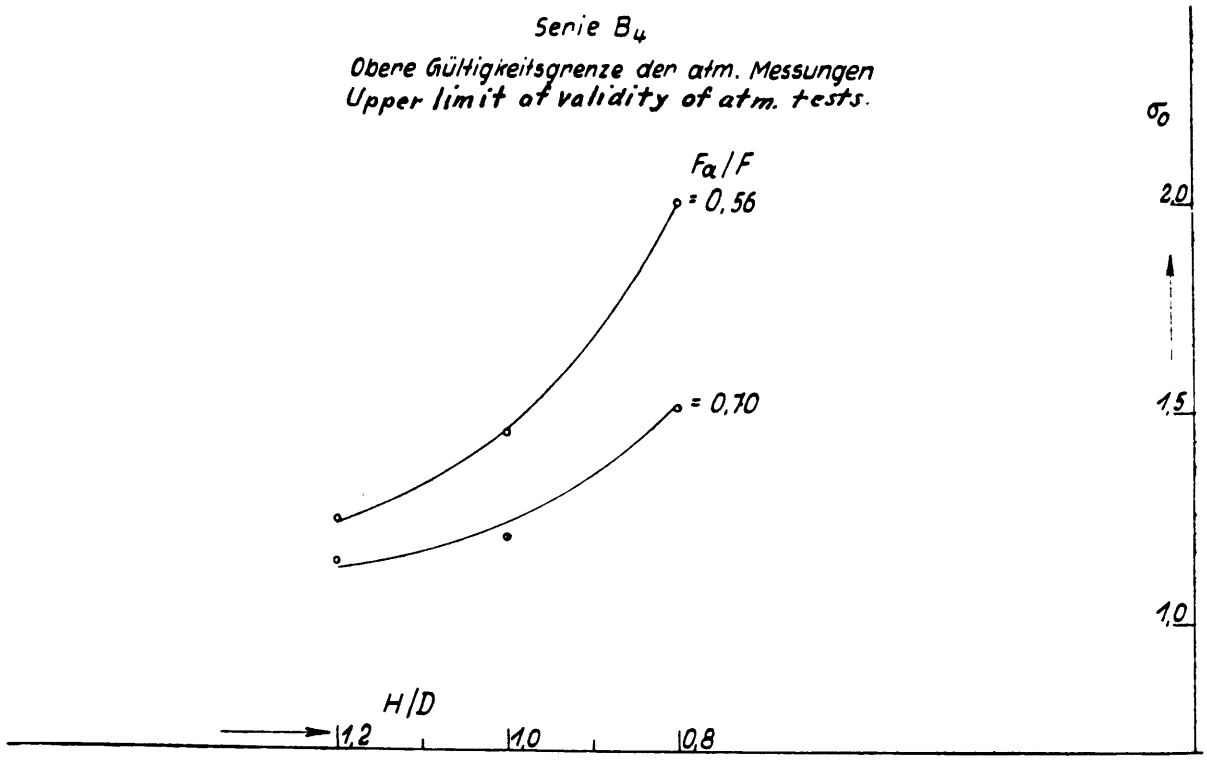

Fig. 24b

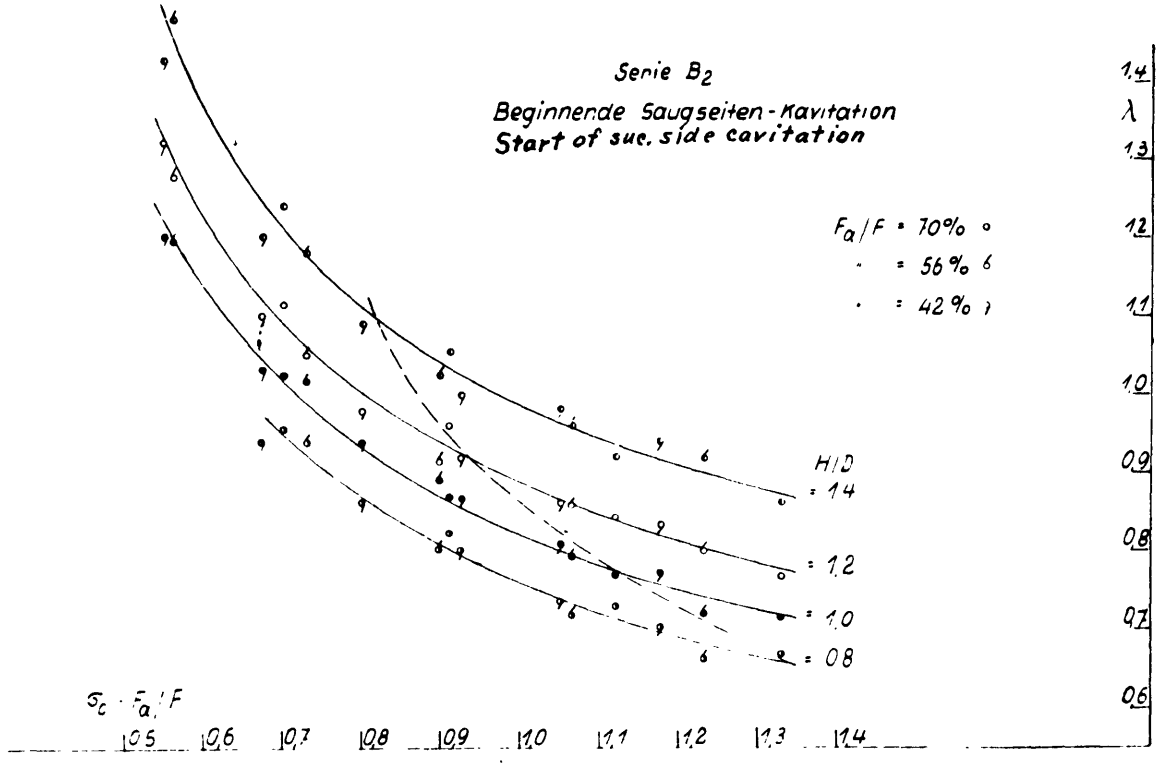

Fig. 25a

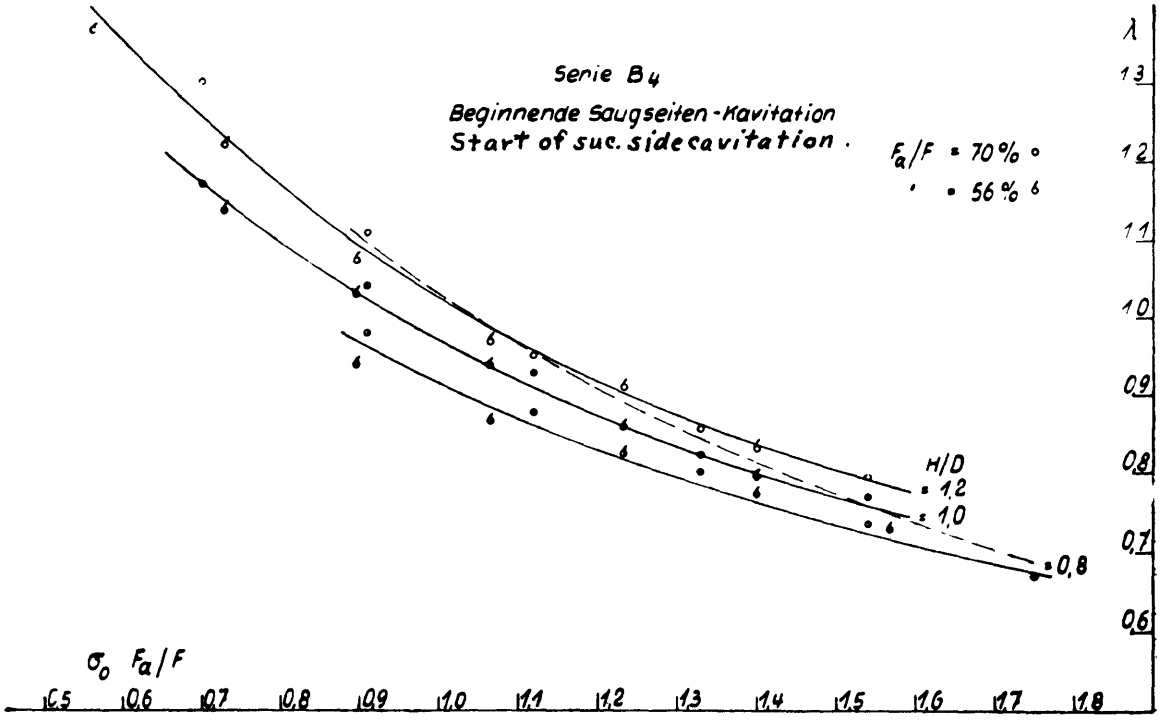

Fig. 25b

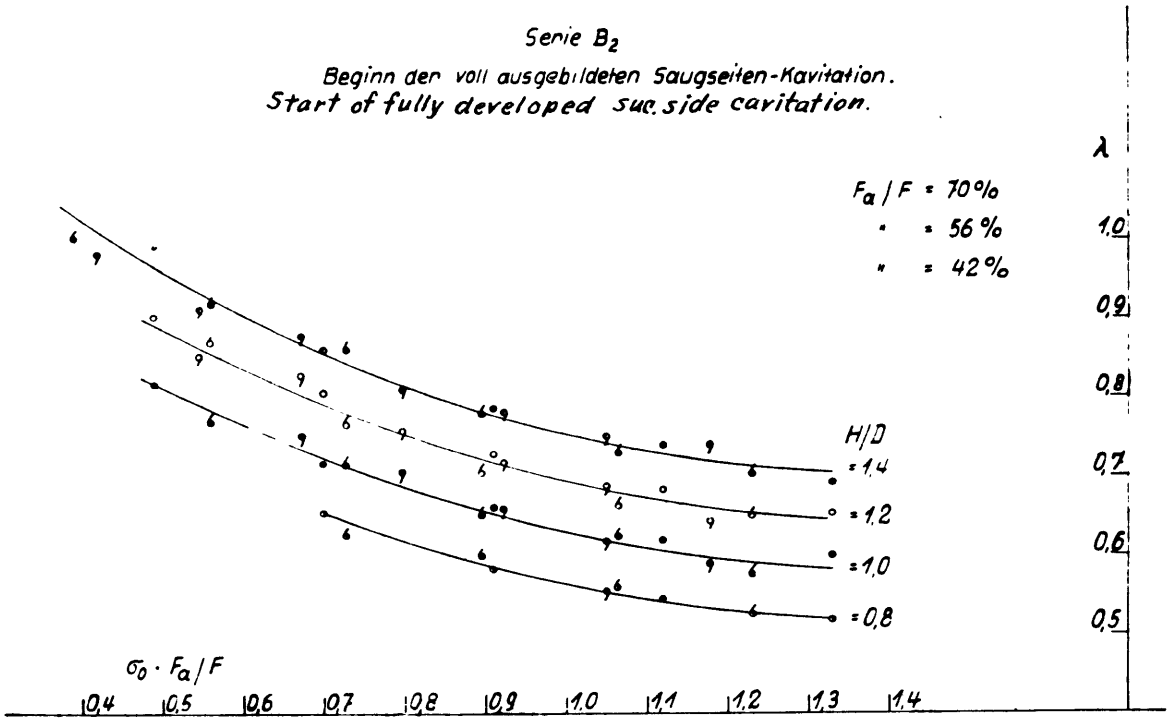

Fig. 26a

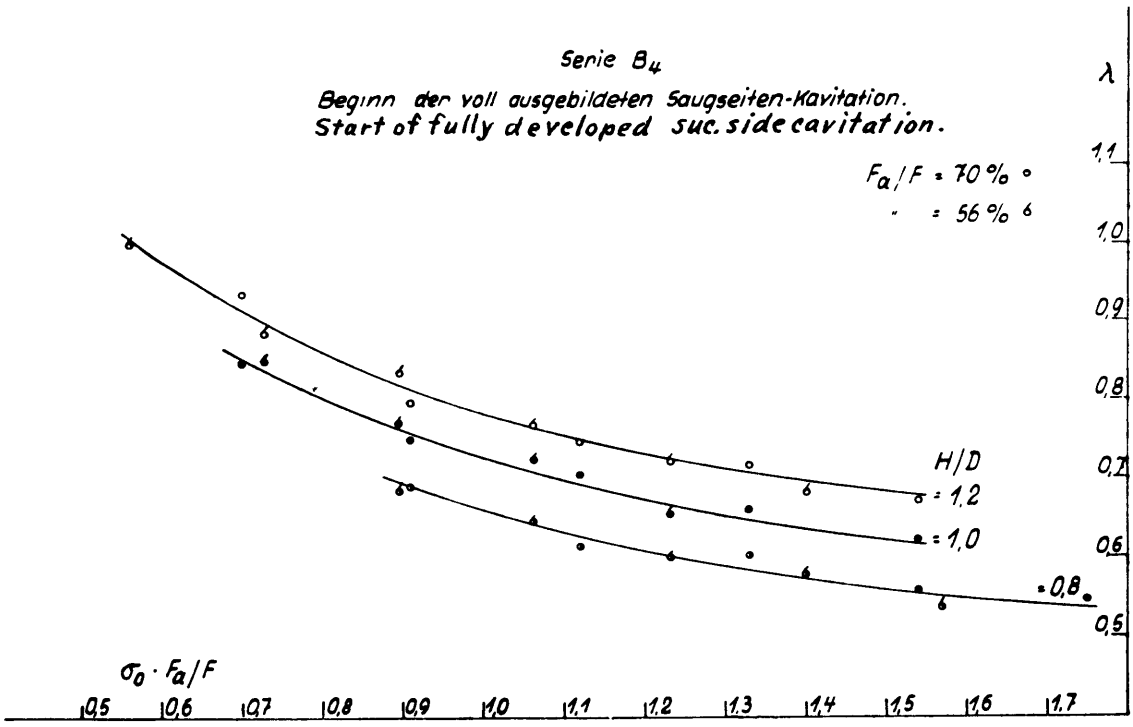

Fig. 26b

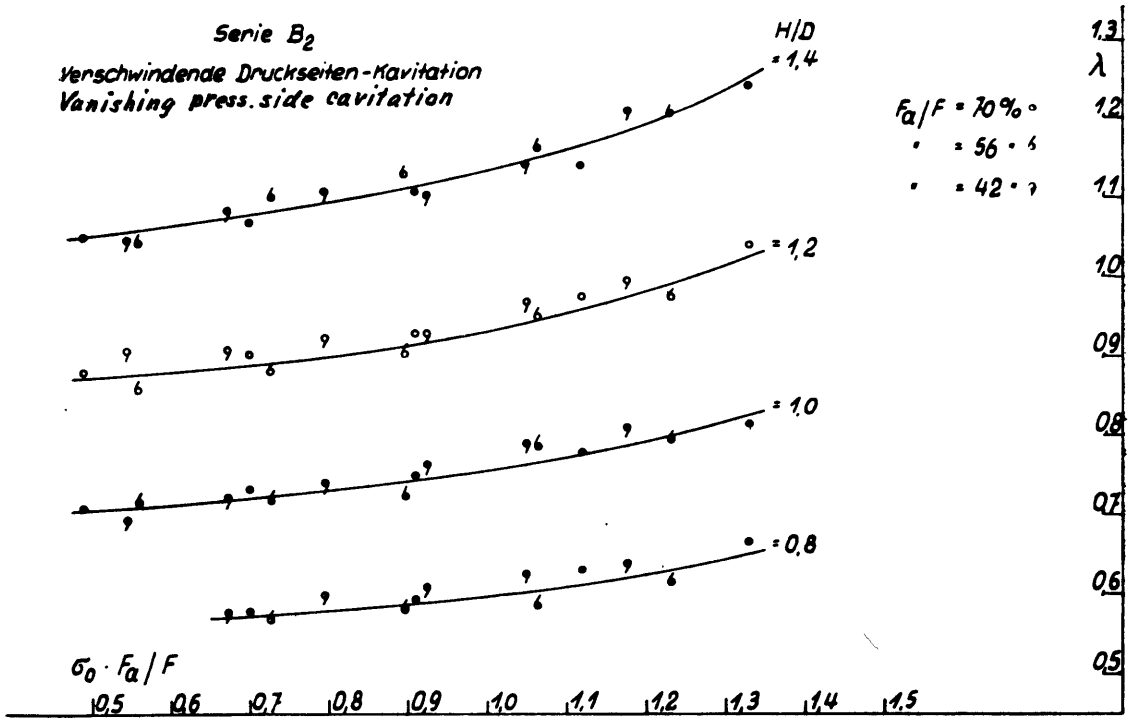

Fig. 27 a

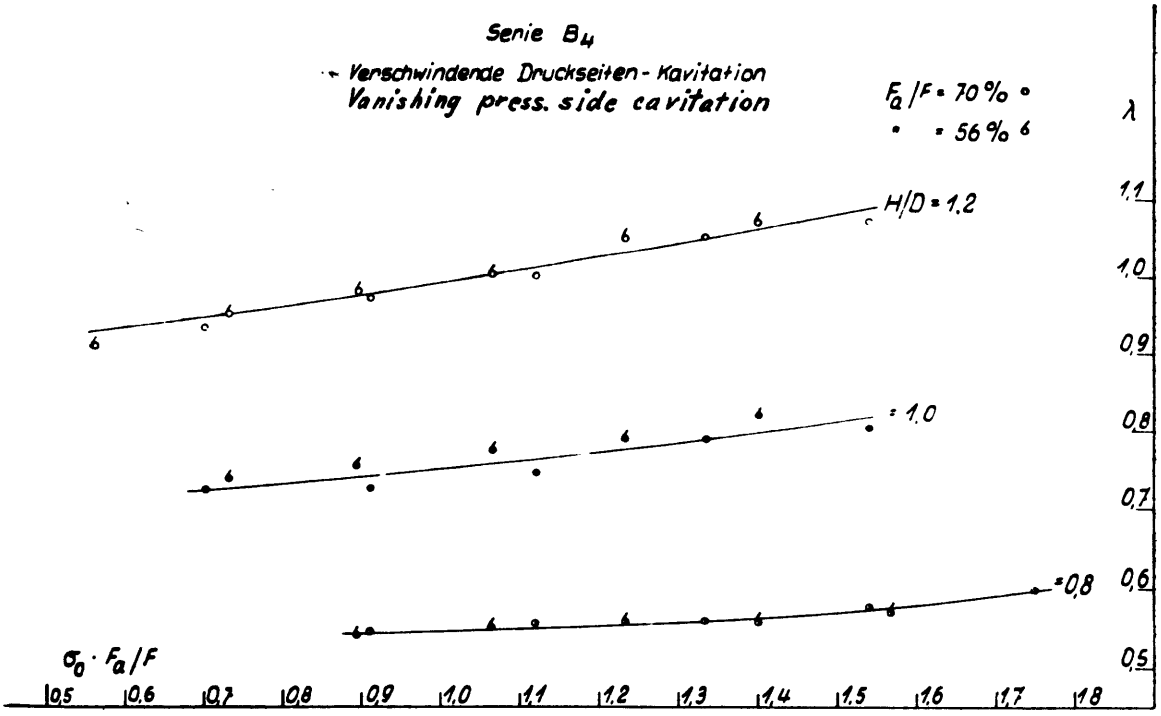

Fig. 27 b

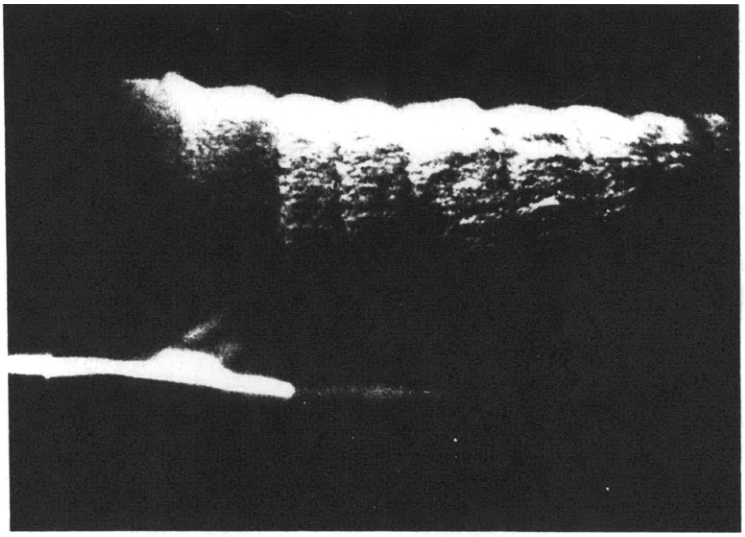

Fig. 28

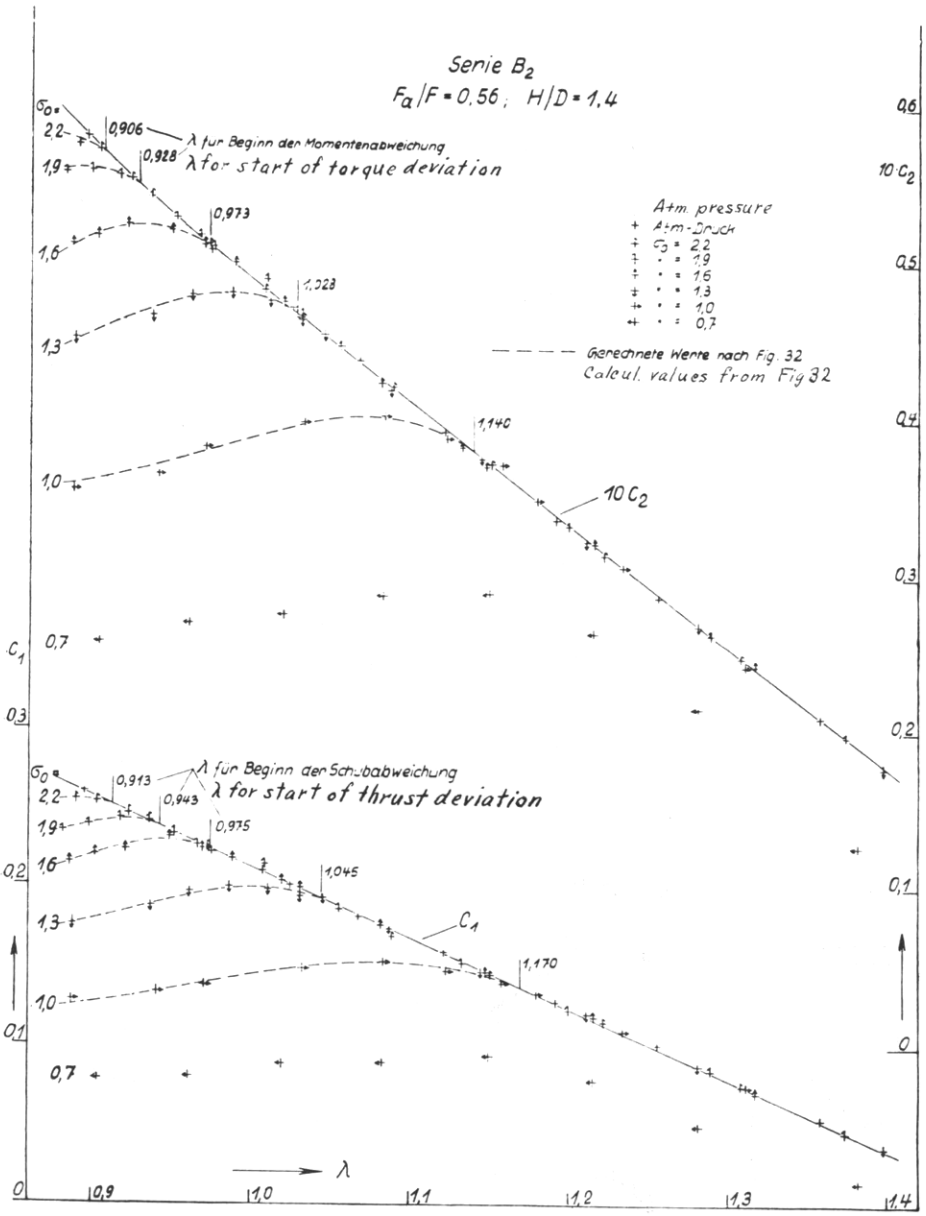
Serie B_2
$F_a/F = 0.56$; $H/D = 1.4$
σ_0 =
2,2
1,9
1,6
1,3
1,0
0,7
0,906
0,928
0,973
1,028
1,140
λ für Beginn der Momentenabweichung
λ for start of torque deviation
$10\,c_2$
Atm. pressure
Atm.-Druck
σ_0 = 2,2
" = 1,9
" = 1,6
" = 1,3
" = 1,0
" = 0,7
Gerechnete Werte nach Fig. 32
Calcul. values from Fig. 32
c_1
0,913
0,943
0,975
1,045
1,170
λ für Beginn der Schubabweichung
λ for start of thrust deviation
c_1
λ
0,9
1,0
1,1
1,2
1,3
1,4
0,6
0,5
0,4
0,3
0,2
0,1
0

Fig. 29

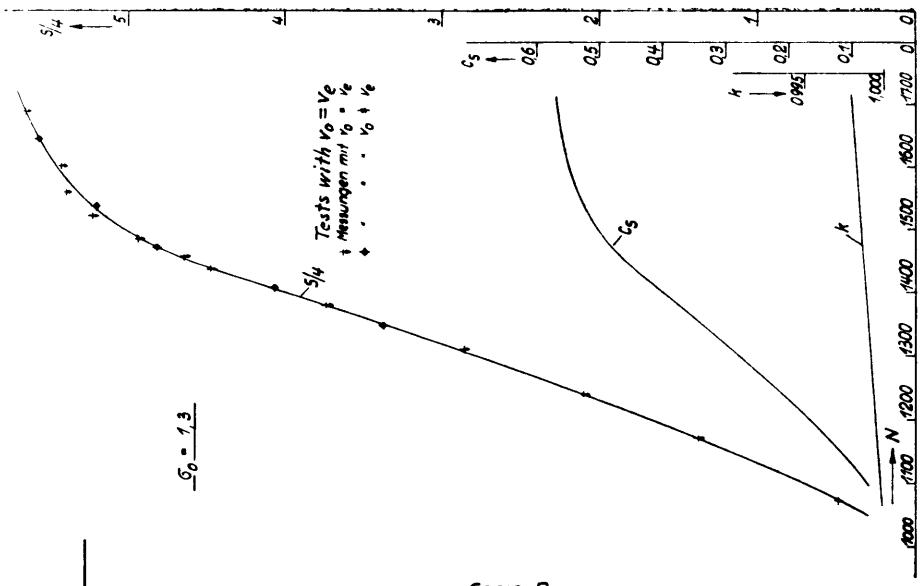
Tests with $v_o = v_e$
Messungen mit $v_o = v_e$
$\sigma_o = 1,3$
c_s
k
N

Fig. 30

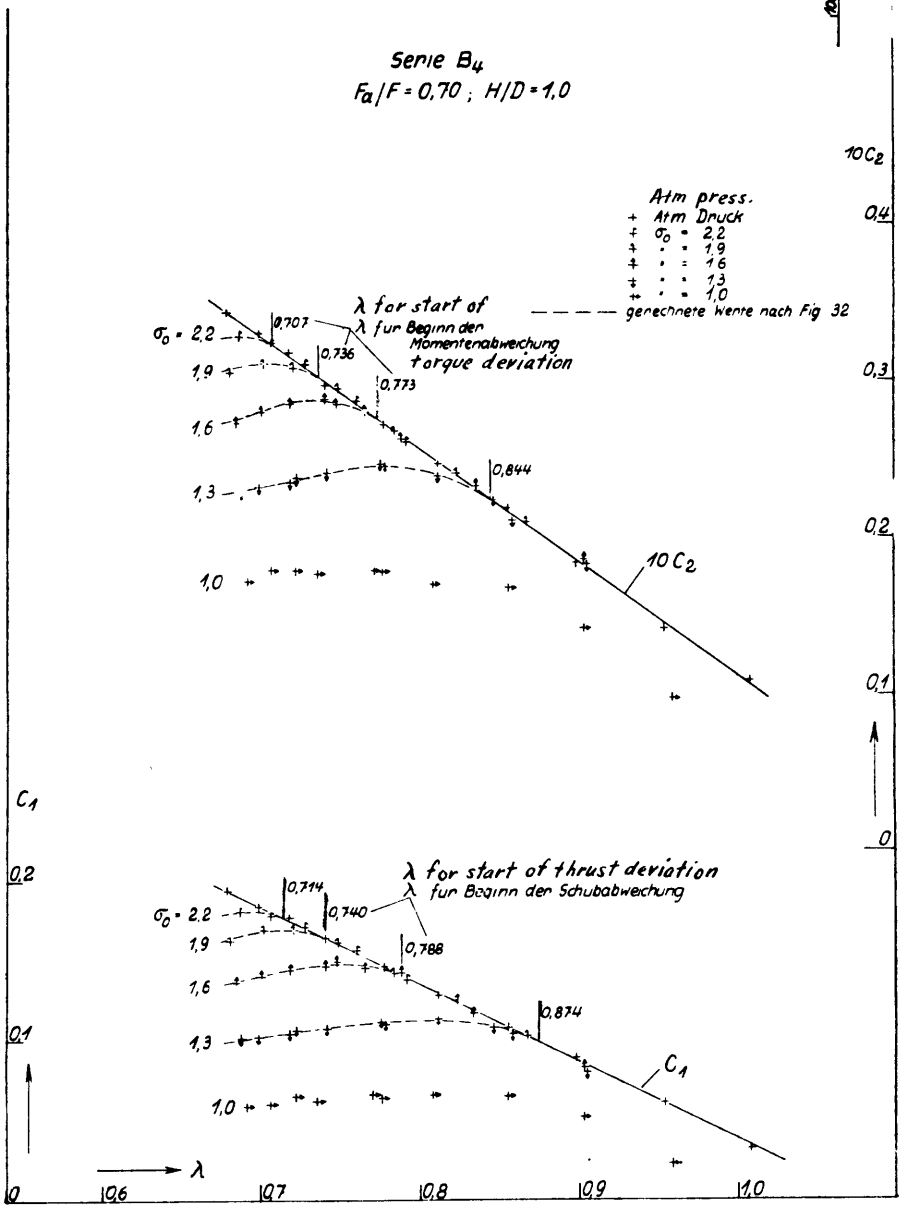
Serie B_4
$F_a/F = 0,70$; $H/D = 1,0$
Atm press.
Atm Druck
σ_o = 2,2
1,9
1,6
1,3
1,0
genechnete Werte nach Fig. 32
λ for start of
λ fur Beginn der
Momentenabweichung
torque deviation
0,707
0,736
0,773
0,844
$10 C_2$
C_1
λ for start of thrust deviation
λ fur Beginn der Schubabweichung
0,714
0,740
0,788
0,874
0,6
0,7
0,8
0,9
1,0

Fig. 31

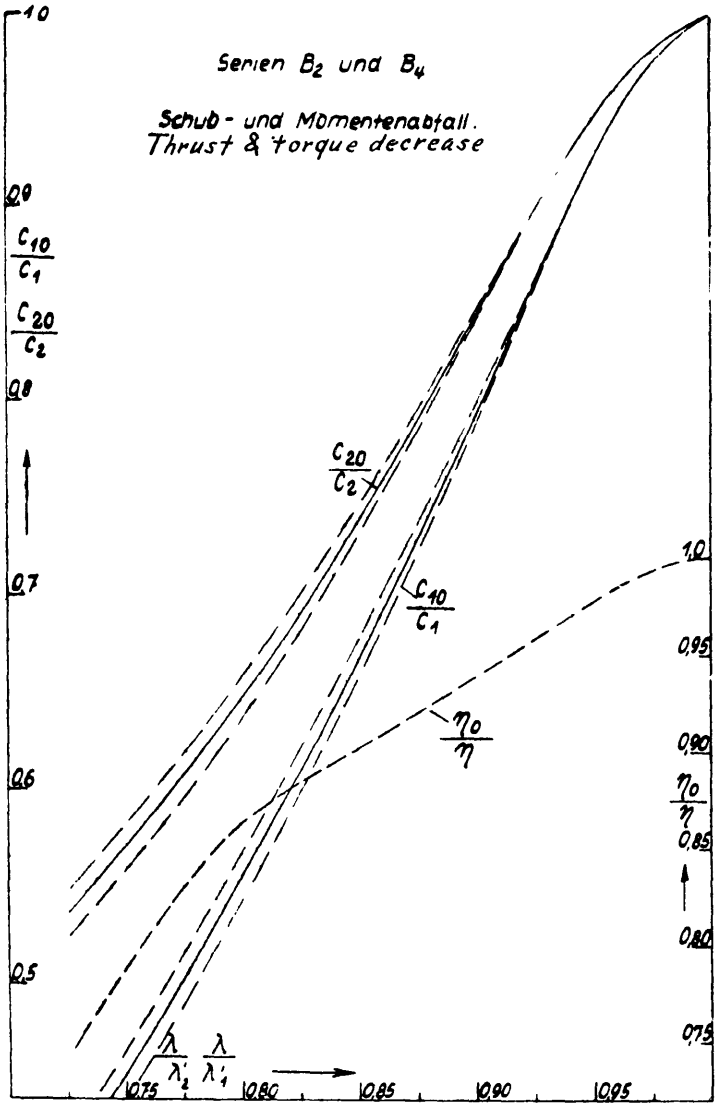
Serien B_2 und B_4
Schub- und Momentenabfall.
Thrust & torque decrease
1.0
0.9
$\frac{c_{10}}{c_1}$
$\frac{c_{20}}{c_2}$
0.8
0.7
0.6
0.5
$\frac{c_{20}}{c_2}$
$\frac{c_{10}}{c_1}$
η_0/η
1.0
0.95
0.90
0.85
0.80
0.75
$\frac{\lambda}{\lambda_2}$ $\frac{\lambda}{\lambda_1}$
0.75
0.80
0.85
0.90
0.95

Fig. 32

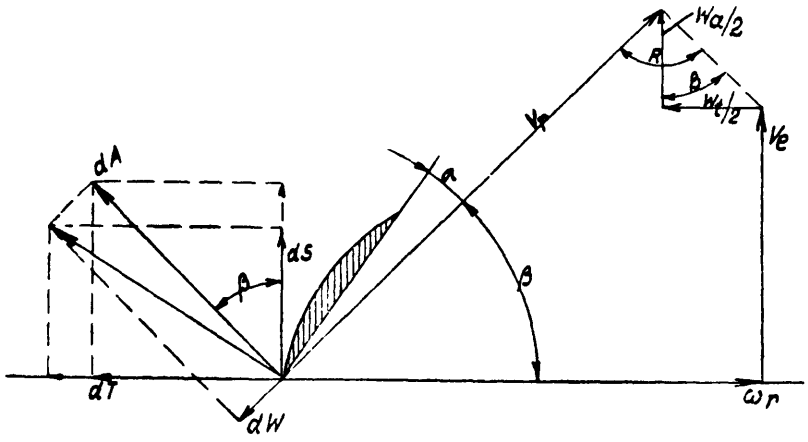
$W_a/2$
R
β
$W_t/2$
V_e
W
dA
dS
β
α
β
dT
dW
ωr

Fig. 33

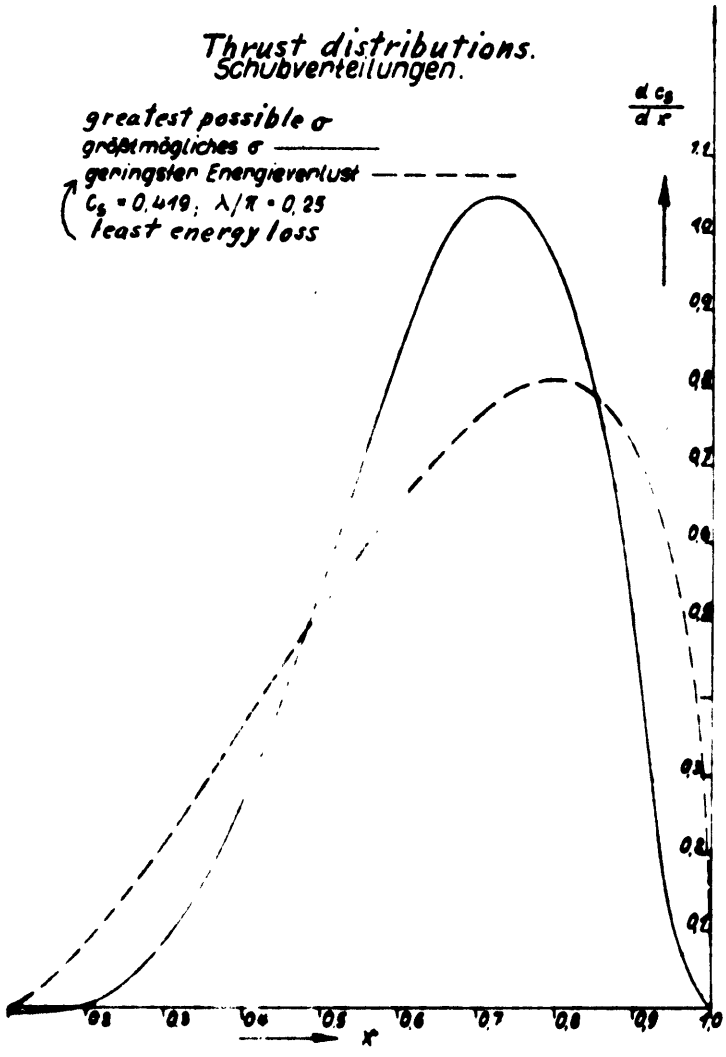
Thrust distributions.
Schubverteilungen.
greatest possible σ
größtmögliches σ
geringsten Energieverlust
$c_s = 0.419$; $\lambda/\pi = 0.25$
least energy loss
$\frac{d\,c_s}{d\,x}$
x

Fig. 33

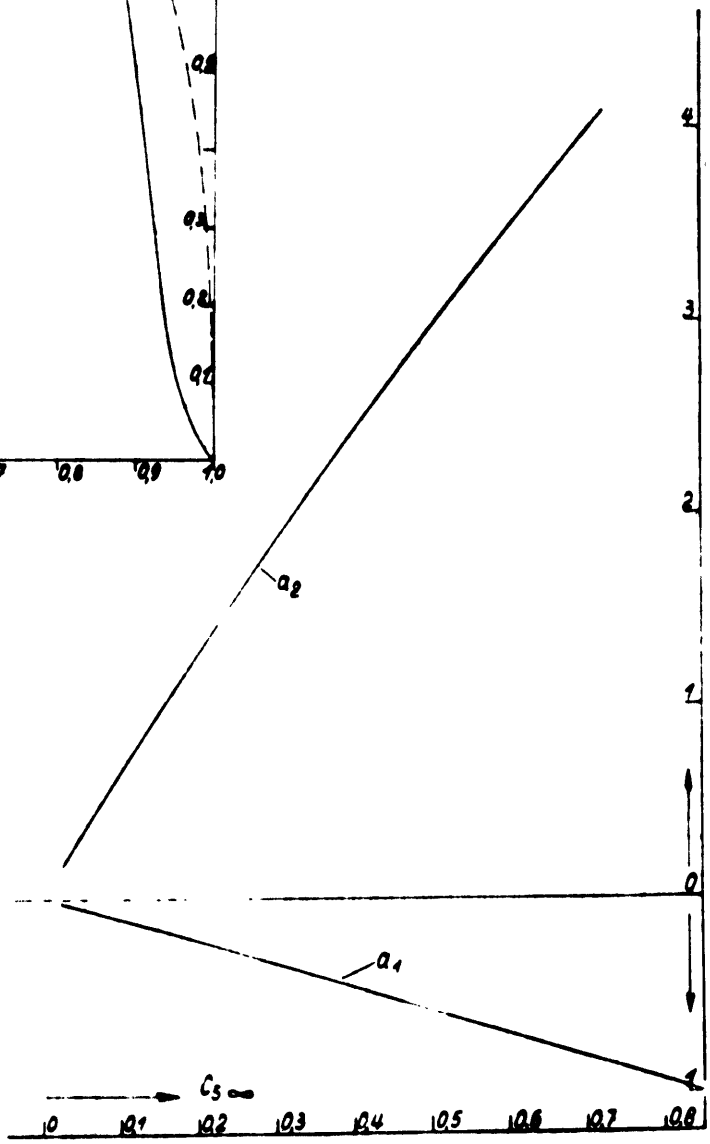
a_2
a_1
$c_s =$

Fig. 34

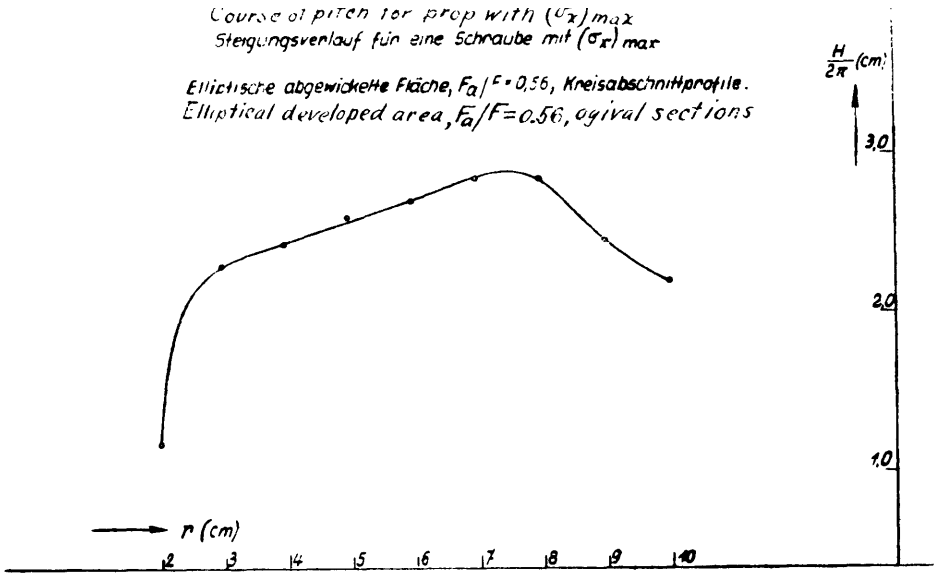

Fig. 36

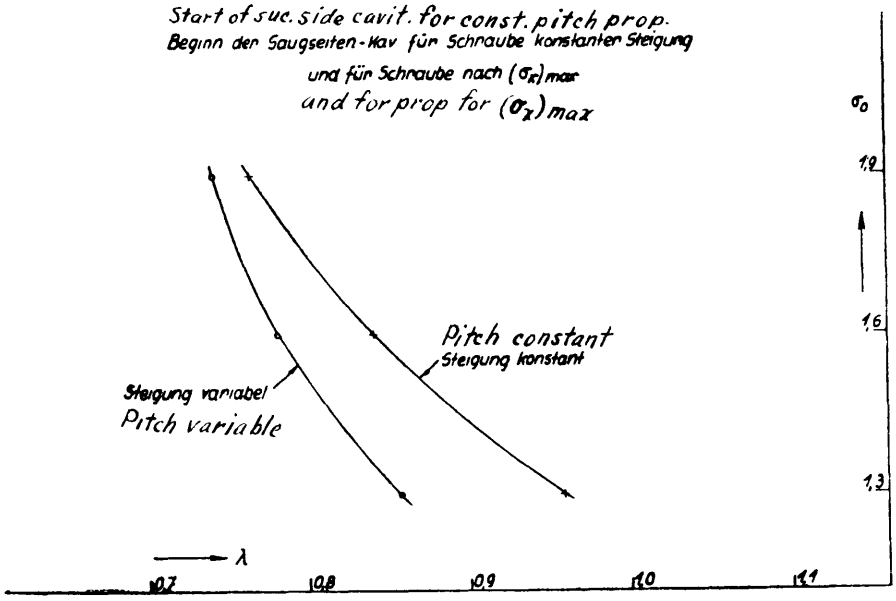

Fig. 37

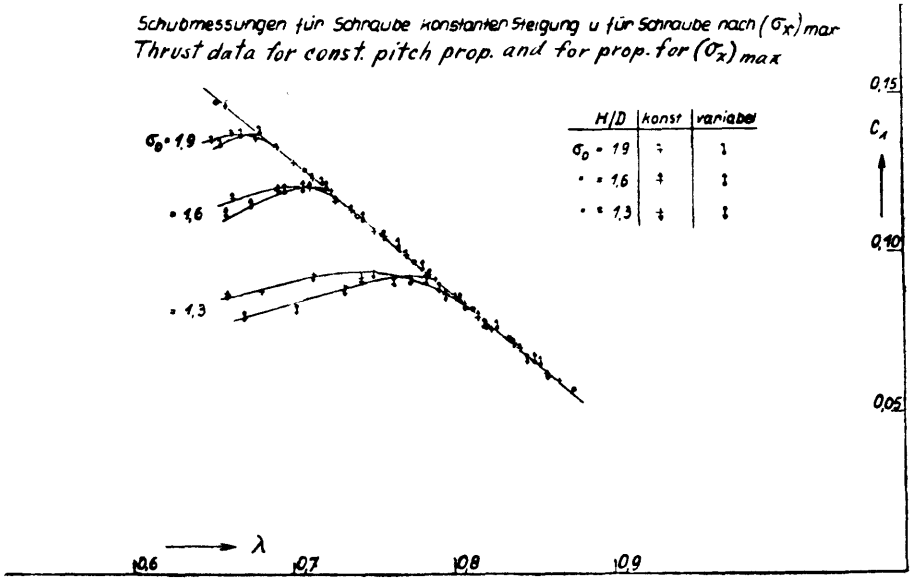

Fig. 38